Arch. Comput. Meth. Engng.
Vol. **13, 3,** 389-464 (2006)

**Archives of Computational Methods in Engineering**
*State of the art reviews*

# Recent Advances in Non-probabilistic Approaches for Non-deterministic Dynamic Finite Element Analysis

D. Moens and D. Vandepitte

K.U.Leuven, Department of Mechanical Engineering,
Celestijnenlaan 300 B, B-3001, Heverlee, Belgium
david.moens@mech.kuleuven.ac.be

## Summary

There is a growing awareness of the impact of non-deterministic model properties on the numerical simulation of physical phenomena. These non-deterministic aspects are of great importance when there is a large amount of information to be retrieved from the numerical analysis, as for instance in a numerical reliability study or reliability based optimisation during a design process. Therefore, the non-deterministic properties form a primordial part of a trustworthy virtual prototyping environment. The implementation of such a virtual prototyping environment requires the inclusion of non-deterministic properties in the numerical finite element framework. This articel gives an overview of the emerging non-probabilistic approaches for non-deterministic numerical analysis, and compares them to the classical probabilistic methodology. Their applicability in the context in engineering design is discussed. The typical implementation strategies applied in literature are reviewed. A new concept is introduced for the calculation of envelope frequency response functions. This method is explained in detail and illustrated on a numerical example.

## 1 INTRODUCTION

The finite element method nowadays has become an indispensable cornerstone of structural design in engineering. The ability to numerically predict the behaviour of a structure under static or dynamic loads is not only of great scientific value, it is also very useful from an economical point of view. During the design process, a reliable finite element analysis reduces the need for prototype production and, therefore, significantly reduces the associated design validation cost. Furthermore, it enables a reliability driven optimisation already in an early stage of the design process. It as such embodies the core of the evolution towards a virtual prototyping environment. Such a numerical environment which provides all necessary tools to reliably model, optimise and verify a design is the ultimate exponent of numerical structural analysis.

There is, however, a general scepticism towards pure numerical design validation through deterministic methods. A natural sense in the rational mind of any designer tells that a single deterministic beneficial result provided by a numerical analysis does not suffice to declare a design reliable. The foundation of this natural sense, be it conscious or subconscious, lies in the presence of uncertainties in the numerical description of physical reality. In the field of numerical design validation, this scepticism has inspired an alternative employment of the ever growing computational capabilities of modern computers. Instead of spending the extra computation time creating extremely fine models of deterministic design details, it could be of much greater value when utilised for the inclusion of uncertainties in the numerical model. From the viewpoint of the reliability analyst, this substantially increases the credibility of the numerical analysis.

The non-deterministic approaches in numerical design validation have gained much popularity over the last decade. The aim of these analyses is to describe the behaviour of the design in its working conditions taking into account every possible variation or uncertainty

 ISSN: 1134–3060 Received: June 2005

that could be present in the model or its environment. Classically, this results in a quantification of the reliability of the design which expresses the presumed likelihood that the design will successfully accomplish its intended task. The application of these methods to dynamic finite element analyses of complex structures revealed the rather unpredictable nature of the propagation of variations in design properties to the analysis result. Furthermore, the numerical dynamic analyses often amplify rather small and, therefore, presumed harmless model variations to a non-negligible variation in the outcome of the analysis. Therefore, a representative numerical reliability analysis of a finite element model subject to uncertainties is of particular interest in the global context of a virtual prototyping environment for dynamic design optimisation and validation.

It is clear that a reliable identification and representative quantification of the sources of uncertainty in the analysis form the basis of a trustworthy numerical reliability study. The uncertainties present in the finite element procedure can be roughly divided in two basic forms:

- A typical source of uncertainty is located in the mathematical equations that are used to describe physical phenomena. Albert Einstein formulated his opinion on the limitations of mathematical models in the following way: *"As far as the laws of mathematics refer to reality, they are not certain, and as far as they are certain, they do not refer to reality"*. By this he meant that mathematical equations only to a certain degree reliably describe the relationship between structural properties and the physical behaviour of the structure. This type of uncertainty is also inherent to the finite element methodology. It requires the result of a finite element analysis always to be treated with a sufficient amount of criticism.

- The input data for the finite element model form the second important source of uncertainty in the finite element analysis. Many design properties that describe the geometry, materials and environmental effects on the design are subject to uncertainty. But even if the design and its environment are completely defined, production inaccuracy and design tolerances introduce variability which inevitably leads to a scatter on the nominal behaviour of the design. Guyader *et al.* [1] clearly illustrates this by analysing the vibro-acoustic behaviour of industrially identical cars.

This work focusses on this second source of uncertainty. In order to quantify these uncertainties, a number of possible numerical models have been developed throughout the last decades. In this field, the structural stochastic analysis was the first well established framework. Its popularity in the early days was mainly due to the relatively low computational effort involved in the manipulation of random variables when they are reduced to their main statistical properties. However, due to the exponential increase in computational capacities, the probabilistic simulation techniques recently have gained popularity. They are nowadays the basis of most commercially available uncertainty analysis software. Their popularity has initiated numerous research activities which focus mainly on an increase in the method's efficiency.

The validity of the result of a numerical procedure is always limited by the validity of the input data of the model. The probabilistic methods generally require much information about the input quantities. Therefore, they are limited in their applicability when little information is present on the non-deterministic quantities in the model. An increasing number of researchers nowadays acknowledges that this forms an important but often underestimated limitation of probabilistic analysis. The feeling grows that other, less information intensive non-deterministic concepts could give more valuable insight into the behaviour of a mechanical structure which is subject to uncertainties. This has given rise to the application of alternative uncertainty models in numerical analysis. Elishakoff

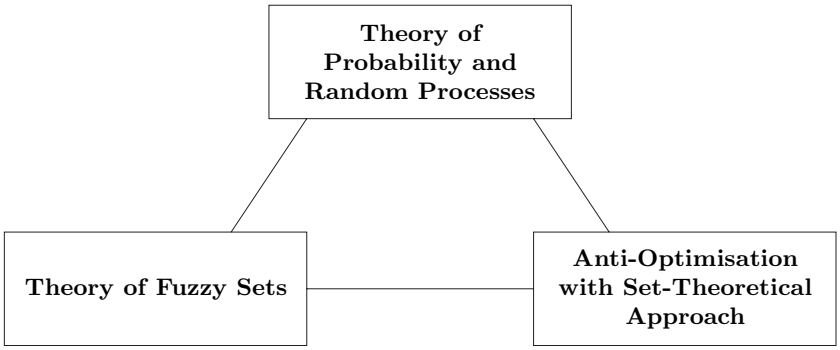


**Figure 1.** The uncertainty triangle as introduced by ELISHAKOFF in 1990

in [2] introduces a general classification of the principal different methodologies using the uncertainty triangle illustrated in Figure 1. Opposed to the universally accepted theory of probability and random processes, he distinguishes between two fundamentally different non-probabilistic concepts: fuzzy sets and the anti-optimisation approach. The latter is also referred to as interval analysis. The application of these non-probabilistic concepts for uncertainty description in numerical analysis is a rather recent evolution. It is the aim of this work to contribute to this evolution by studying the applicability of these non-probabilistic methods in the framework of dynamic finite element analysis.

As indicated by KLIR [3], the development of a numerical analysis tool which includes uncertainty consists of four major steps:

1. the selection of an appropriate mathematical representation of the uncertainty present in the simulated physical model
2. the development of a calculus to manipulate this numerical representation of the uncertainty properly
3. find a meaningful way to measure or quantify relevant uncertainty within the developed concept in any situation
4. the development of a methodology to perform a meaningful numerical simulation

Section 2 of this paper first focusses on the first two steps of this scheme in the context of finite element analysis. Since the intention of this work is not to develop new numerical uncertainty concepts, this section basically consists of a review of numerical concepts available from literature, and their application for non-deterministic finite element modelling. This literature study should give a clear and profound insight in the capabilities of the available concepts. In order to enable a critical assessment of the non-probabilistic concepts, the literature overview starts with a description of the probabilistic concept and its application in non-deterministic finite element analysis. In Section 3, the applicability of the non-deterministic approaches is discussed in the context of designing under uncertainty. This requires first a terminology definition in order to clearly distinguish between uncertainties, variabilities and errors. This section then describes how the available non-deterministic modelling tools fit in these definitions. Each of these numerical representations has its specific consequences for the interpretation of the non-deterministic analysis results in the context of design optimisation or reliability analysis.

The remainder of the paper concentrates on step four in the above procedure, i.e., the development of numerical methodologies to perform the analysis. Since the interval

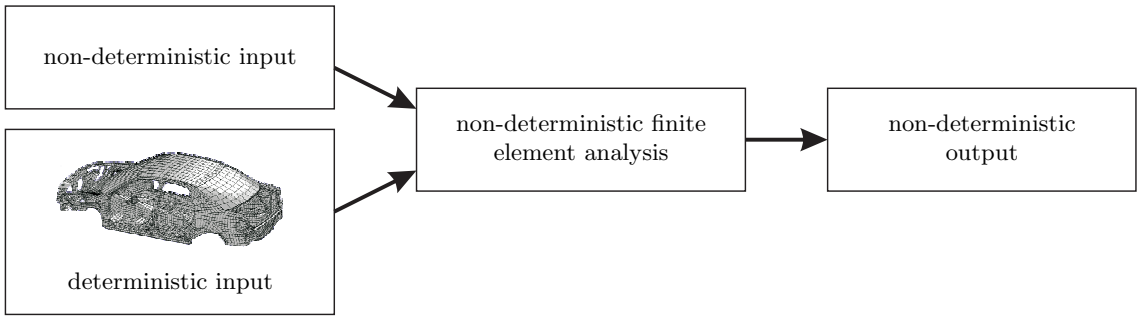


**Figure 2.** Non-deterministic finite element procedure

finite element analysis is the numerical core of the fuzzy analysis, the focus in entirely on the numerical aspects of implementing and using the interval technique for dynamic finite element analysis. The aim of Section 4 is to critically assess the state-of-the-art of the interval finite element solution techniques found in literature. Section 5 introduces a new hybrid methodology for the implementation of the interval finite element analysis, and than describes how this hybrid procedure can be usefully applied to implement the interval equivalent of the frequency response function analysis. Is is shown how this technique leads to a good approximation of the envelope on the response functions of finite element models with interval parameters. This technique is finally illustrated on a numerical example in Section 6.

## 2 NUMERICAL CONCEPTS FOR NON-DETERMINISTIC FINITE ELEMENT ANALYSIS

The aim of this section is to give a general survey of numerical concepts for non-deterministic finite element analysis. The generally accepted probabilistic approach is by far the most popular in this context. However, during the last decade, some non-probabilistic alternatives succeeded in arousing the interest of numerous researchers working in the field of non-deterministic finite element analysis. Lately, the interest has grown to a level which resulted in the development of practical implementations of non-probabilistic finite element analyses in various domains. The initial attempts to perform non-probabilistic finite element analyses clearly demonstrated the added value to the existing probabilistic methods, mainly manifested as a substantial reduction in computation time. This motivated further development towards generalisation and refinement of the initial numerical procedures. In order for this work to contribute to this development, this section first gives an overview of the applicability of both the probabilistic and the non-probabilistic concepts within the general framework of non-deterministic finite element analysis. The principal steps of the underlying procedure is conceptually illustrated in Figure 2. This procedure is identical for all non-deterministic numerical concepts discussed in this section. The deterministic input first is completed with the information on the non-deterministic model properties (e.g. material properties, element properties...) using a concept for the quantification of non-deterministic numerical data. In the next step, a non-deterministic finite element code solves the problem and produces the required non-deterministic output.

Sections 2.1, 2.2 and 2.3 give a description of the application of respectively the probabilistic, interval and fuzzy concept for non-deterministic finite element analysis. All three sections start from a brief description of the basic properties of the numerical concept, after which the basic numerical methodologies for the corresponding non-deterministic implementation of the finite element procedure are discussed.

## 2.1 Probabilistic Finite Element Methods

### *2.1.1 Basic properties of the probabilistic concept*

The goal of a probabilistic quantity description is to define a domain of possible values for the quantity, and to give information on the frequency of occurrence or likelihood of the quantity inside this domain. This is typically done by defining a probability density function $f_X(x)$ (PDF) for the probabilistic quantity $X$ over the domain of possible values. The probability that the quantity lies within the interval $[a, b]$, indicated by $P(a \leq X \leq b)$, is directly derived from this probability density function:

$$P(a \leq X \leq b) = \int_a^b f_X(x)\, dx \tag{1}$$

The expectation of a function $g(X)$ with respect to $f_X(x)$ is defined as:

$$E\{g(X)\} = \int_{-\infty}^{\infty} g(x) f_X(x) dx \tag{2}$$

The mean value or average of the distribution $f_X(x)$ equals $E\{X\}$. The other most dominant features of a probabilistic quantity are commonly described by the central moments associated with the probability density function. The $n^{th}$ central moment $m_n$ follows from the mean value using:

$$m_n = \int_{-\infty}^{\infty} (x - E\{X\})^n f_X(x)\, dx \tag{3}$$

The second order central moment is the most commonly used, and referred to as the variance of the distribution denoted by $var(X)$. The standard deviation is defined as $\sigma_X = \sqrt{var(X)}$. It is a common measure for the dispersion of the distribution about the mean value.

For multiple probabilistic quantities, the probability density function concept is extended to more dimensions using the joint probability density function $f_{X_1 \ldots X_n}(x_1, \ldots x_n)$. The expectation is defined in an analogous manner as for the univariate distributions. The covariance, the first order joint central moment, gives a measure of the interdependence between the quantities. It is commonly represented by the covariance matrix $\Gamma$ containing all individual variances and covariances:

$$\Gamma = \begin{bmatrix} var(X_1) & cov(X_1, X_2) & \ldots & cov(X_1, X_n) \\ cov(X_2, X_1) & var(X_2) & \ldots & cov(X_2, X_n) \\ \vdots & \vdots & \vdots & \vdots \\ cov(X_n, X_1) & cov(X_n, X_2) & \ldots & var(X_n) \end{bmatrix} \tag{4}$$

with

$$cov(X_i, X_j) = E\{(X_i - m_{X_i})(X_j - m_{X_j})\} \tag{5}$$

Extensive literature exists on the subject of probability theory, treating a vast variety of probability density function and their applicability for description of random quantities. An overview of these can be found in [4] and [5]. The remainder of this section now focusses on the application of the probabilistic concept for the non-deterministic quantity representation in a general non-deterministic finite element framework.

Two principally different probabilistic finite element techniques can be distinguished, depending on the type of the non-deterministic model properties that are described. The first type refers to a variation on the numerical quantification of model properties which

are considered to have a specific value in a single simulation of the physical behaviour of the model, but show a variation in time or from unit to unit over the actual realisations of the modelled product. Random variables are generally used to describe this first type of non-deterministic properties. The second type refers to a possible spatial variation on model properties inside a single simulation of the physical behaviour of the model. A typical example is the possible variation of some geometrical dimensions like plate thicknesses or material properties within the model. This type of non-determinism is generally modelled in a probabilistic concept using random fields. Sections 2.1.2 and 2.1.3 discuss some numerical procedures to process respectively random variables and random fields defined on a finite element model.

Up to now, nearly all procedures to include non-determinism into finite element analysis start a non-deterministic representation of physical parameters in the model. These parameters refer to actual unknowns or variations in the description of the finite element model, as for instance in the geometrical or in the material properties. Both the random variable and the random field approaches are based on this parametric approach. Recently, an alternative non-parametric approach has been proposed [6]. In this approach, the non-determinism is viewed as a global factor which influences the total model rather than an effect which can be localised in specific model parts. As such, it accounts for general modelling errors, as for instance errors in the used governing partial differential equations, or the fundamental discretisation error. The application of this non-parametric approach in a probabilistic context has been successfully illustrated. Still, it is unclear to what extent this approach can be of service for a design engineer who has to deal with variability or uncertainty on design properties which generally directly relate to model properties.

### *2.1.2 Random variables*

The approach for dealing with random variables in the context of finite element analysis has strongly evolved over the past decades. In the first publications on this subject, there was a general tendency towards the use of a perturbational approach. In this approach, result variations are expressed as a linear combination of input variations based on a Taylor series expansion. The sensitivities expressing the influence of the non-deterministic input properties on the analysed output quantity are used to calculate the variance on the result based on the known variances of the inputs. Generally, this approach only aims at the calculation of the first two statistical moments of the scatter on the result. Ibrahim [7] gives a comprehensive review of the first applications of random variables in structural dynamic analysis. Although other probabilistic methods are currently gaining popularity, the perturbational approach remains under continuous research (see e.g. Manohar *et al.* [8] for an overview of recent developments).

Although the perturbation analysis has proven its value in numerous applications, its validity is limited by the approximation used in the Taylor series expansion. Mainly the finite order of the expansion (generally limited to one) and the extrapolation of local sensitivities, both of which are intrinsic to this approach, narrows its area of application. Especially in designing for high reliability which is more and more demanded in modern design processes, the perturbational approach becomes less interesting because of its limited validity in predicting the tails of the output distribution. This has lead to a strong increase of the application of simulation methods for random variable analysis in the context of finite element modelling. The exponential growth of the capabilities of modern computers over the last decades has strongly stimulated this evolution.

The history of the Monte Carlo simulation approach starts with Buffon, who in 1768 conducted an experiment to determine a value of $\pi$ by casting needles on a ruled grid. Since the early 1930's, the method has become the basic tool for probabilistic numerical calculations both in science and more industrial applications. With the recent exponential

increase of computational capacities, Monte Carlo simulation is often seen as the ultimate probabilistic tool, capable of tackling all probabilistic computations of numerical analyses without nearly an exception. A comprehensive introduction to the Monte Carlo simulation methodology can be found in [9, 10].

The basic principle of Monte Carlo simulation is that the deterministic numerical analysis is performed repeatedly on a large number of samples of the input parameters. The desired statistics of the response quantities, such as the mean value, variance and specific event probabilities are then evaluated based on the generated output samples. The sampling on the input quantities is conducted in such a manner that the samples represent the probabilistic characteristic of each parameter. The sampling procedure is based on the numerical description of the input probability density function of each parameter, and is executed with the aid of a random number generator.

The most important aspect of a good Monte Carlo simulation is the availability of a trustworthy representation of the probabilistic input through probability density function. Whenever there exists correlation between the input quantities, ideally also the joint probability density function is required. In most cases, however, the interdependency between the inputs is unknown and, therefore, neglected by presuming all input quantities as independent. This assumption simplifies the simulation procedure. The availability of trustworthy data is an important prerequisite for performing a meaningful probabilistic analysis, which is gaining a lot of attention in recent literature. The effect of misjudging correlations on results of a Monte Carlo simulation should not be ignored. To the contrary, Annis in [11] shows that the standard deviation can be severely overestimated (up to 700% in his specific example) when correlations are neglected. The impact of assumptions in probabilistic input data specification is adressed more in detail in Section 3.3.2.

A number of enhancements and extensions of the initial Monte Carlo simulation have been proposed:

- **Importance sampling** [12]: This approach aims at generating more samples in the critical region in the design parameter space. To achieve this, samples are generated from an altered probability density function, centered in the critical region of the design parameter space. The sampling probability density function is afterwards compensated in the approximation of the failure probability. This procedure reduces the variance of the Monte Carlo simulation estimator.

- **Adaptive sampling** [13]: An initial sampling distribution is generated based on the statistical moments of the failure region. During each following simulation, the sampling distribution is adapted based on the result of all simulations thus far.

- **Directional sampling** [14]: In the normalised parameter space, sample direction vectors are generated with uniformly distributed direction. The estimation of the probability of failure then equals the average of the conditional probability of failure in each sampled direction. This method is advantageous when this conditional probability of failure has a closed-form expression. Directional sampling can be improved with importance and adaptive sampling applied on the vector direction distribution [15].

- **Latin hypercube sampling** [16]: In this method, the sampling space is divided into subsets of equal probability. The number of samples is reduced to represent each subset of each independent variable only once.

In order to use Monte Carlo simulation on finite element analyses, the different sampling methods have been implemented in software environments which provide the data management of the input and output samples of the simulation. On the one hand, they generate

the samples which serve as input for the finite element analysis, and on the other hand they perform the statistical analysis on the output samples. The core of the analysis is still the deterministic finite element code, which acts as a black box for the data management software.

Driven by its popularity, Monte Carlo simulation is still under continuous research, which nowadays is mainly focussed on the rationalisation of the computational cost of the procedure by problem reduction or advanced parallel processing techniques [17] and new methodologies to control the Monte Carlo simulation [18].

#### *2.1.3 Random fields*

The objective of a random field is to represent a spatial variation of a specific model property by a stochastic variable defined over the region on which the variation occurs. The underlying idea is that, although assumed to be constant over specific regions of a numerical model, physical properties are generally not expected to have a single deterministic value in an eventual realisation of the product. Random fields are the perfect tool to analyse the effect of these internal model variations. A comprehensive overview of random fields is given by VANMARCKE in [19]. In order to substantiate the discussion on the application of non-probabilistic concepts in the framework of non-deterministic field variables later in this work, the main principles of the probabilistic analysis of random fields are briefly summarised here.

The principle of the random field approach is to express the non-deterministic model property as a field variable $v(\{x\},\theta)$ in which $\{x\}$ represents the spatial variation and $\theta$ refers to its probabilistic behaviour. The specification of a random field generally comes down to the specification of the spatial evolution of the first two statistical moments of the field variable:

$$m_v(\{x\}) = E[v(\{x\},\theta)] \tag{6}$$

$$V(\{x\}) = var[v(\{x\},\theta)] \tag{7}$$

and a corresponding covariance function, expressing the spatial dependency of the field variable:

$$C(\{x_1\},\{x_2\}) = E[(v(\{x_1\},\theta) - m_v(\{x_1\}))(v(\{x_2\},\theta) - m_v(\{x_2\}))] \tag{8}$$

Different concepts have been proposed in literature to represent this spatial covariance kernel, most popular of which are the first- and second-order autoregressive fields.

The application of the concept of random fields in a numerical modelling framework requires some sort of discretisation of the spatially varying stochastic field over the defined geometry. This conversion has been studied extensively in literature (see e.g. [8] for an overview). All these discretisation techniques aim at a transformation of the continuous field to a finite discrete representation which is manageable in a numerical context. The discretisation technique based on the KARHUNEN-LOEVE expansion [20] has gained particular attention in literature. It consists of a decomposition of the initial field into a superposition of a finite number of orthogonal random variables which are weighted with deterministic spatial functions:

$$v(\{x\},\theta) \approx m_v(\{x\}) + \sum_{i=1}^{M} \sqrt{\lambda_i} f_i(\{x\})\xi_i(\theta) \tag{9}$$

with M the truncation order of the KARHUNEN-LOEVE decomposition, $\xi_i(\theta)$ an orthonormal normal random space, and $f_i(\{x\})$ and $\lambda_i$ the eigenfunctions and eigenvalues of the covariance kernel:

$$\int_\Omega C(\{x_1\},\{x_2\}) f_i(\{x_1\}) d\{x1\} = \lambda_i f_i(\{x_2\}) \tag{10}$$

It is clear from its definition in Eq. (8) that the covariance kernel determines the spatial aspect of the random field. It also strongly influences the numerical approximation incorporated in most discretisation techniques, as can be seen directly for the KARHUNEN-LOEVE expansion from Eq. (10). Therefore, it is very important to impose a realistic covariance function in order for the analysis to have a representative outcome. In order for the method to have a predictive value in a design process, a well-founded assessment of the spatial correlations intrinsically incorporated in the assumed covariance kernels is necessary. How this can be achieved based on the limited data a designer generally has available is rather unclear. On the other hand, if the assessment is impossible based on the limited available information, the impact of the assumed covariance function should be clearly identified.

The essence of the random field simulation, i.e., how to relate scatter on a numerical outcome of the analysis to the actually occurring spatial variation of model properties, is of very high value for a designer who is observing such model variations. However, it is the overall impression of the authors that the developments in the area of random fields are basically driven by mathematical assumptions, which are far from easy to verify in a practical engineering situation. The question on how to derive or approximate actual covariance functions in practical and realistic engineering applications seems far from answered, and deserves some attention in order for the method to attain a place among the non-deterministic virtual prototyping tools.

## 2.2 The Interval Finite Element Method

### *2.2.1 Basic properties of the interval concept*

A number of concepts have been developed in order to represent non-deterministic quantities with limited available information. These alternatives are generally lumped together as *non-probabilistic* methods. This section describes the most simple form of non-probabilistic numerical concepts: the interval model.

The history of interval analysis goes all the way back to ARCHIMEDES who defined the irrational number $\pi$ by an interval: $3\frac{10}{71} < \pi < 3\frac{1}{7}$. Recent developments in interval arithmetics are mainly based on the work of MOORE [21], who introduced interval vectors and matrices and the first non-trivial applications.

By definition, the range of an interval scalar consists of a single continuous domain in the domain of real numbers $\mathbb{R}$. This means that the range is bounded by a lower and an upper bound. If both the lower and upper bound are members of the interval scalar, the interval is *closed*. In this work, all interval objects are considered to be closed. The domain of interval scalars defined over $\mathbb{R}$ is denoted by $\mathbb{IR}$.

In order to facilitate the development of the mathematical background in the remainder of this work, this section introduces a generalised notation for intervals and sets. There exists no generally accepted convention concerning this notation. The proposed concept enhances the readability of equations involving sets of matrices, vectors and scalars.

A general *interval scalar* is denoted by a boldface variable $\mathbf{x}$. The lower and upper bound of an interval scalar $\mathbf{x}$ are denoted by $\underline{x}$ respectively $\overline{x}$. A real closed interval scalar is defined as:

$$\mathbf{x} = \left\{ x \mid (x \in \mathbb{R})\,(\underline{x} \leq x \leq \overline{x}) \right\} \tag{11}$$

An alternative notation for an interval $\mathbf{x}$ is $[\underline{x}, \overline{x}]$. The midpoint of the interval is defined as:

$$\check{\mathbf{x}} = \frac{\underline{x} + \overline{x}}{2} \tag{12}$$

The radius of an interval equals:

$$\bar{\mathbf{x}} = \frac{\overline{x} - \underline{x}}{2} \tag{13}$$

A straightforward extension of an interval scalar is a general *set scalar* denoted by $\langle x \rangle$. It consists of a number of disjoint interval scalars in $\mathbb{IR}$:

$$\langle x \rangle = \bigcup_{i=1\ldots n} \mathbf{x}_i \tag{14}$$

with:

$$\bigcap_{i=1\ldots n} \mathbf{x}_i = \emptyset \tag{15}$$

The *interval matrix* $[\mathbf{X}] \in \mathbb{IR}^{n \times m}$ describes the set of all matrices for which each matrix entry $x_{ij}$ is contained within its corresponding interval scalar $\mathbf{x_{ij}}$:

$$[\mathbf{X}] = \left\{ [X] \mid x_{ij} \in \mathbf{x_{ij}} \right\} \tag{16}$$

An *interval vector* similarly is denoted by $\{\mathbf{x}\} \in \mathbb{IR}^n$. The definitions of Eq. (12) and (13) are easily extended to interval matrices and vectors by applying them on each entry in the vector or matrix.

An interval matrix or vector requires that interval scalars are defined for each entry in the matrix or vector. According to the definition of Eq. (16), an interval matrix or vector includes any combination of the entries as long as they are within the bounds of their interval scalar. This means that they implicitly presume independence between all entries. Hence, an interval vector represents a hypercube in a general multidimensional space. It as such cannot be used to give a precise description of a general convex set in a multidimensional space.

The *set matrix* $\big\langle [X] \big\rangle$ describes the set of all possible matrices where each matrix entry $x_{ij}$ is contained within its corresponding set scalar $\langle x_{ij} \rangle$:

$$\big\langle [X] \big\rangle = \left\{ [X] \mid x_{ij} \in \langle x_{ij} \rangle \right\} \tag{17}$$

Again, the matrix elements are implicitly considered independent.

A conservative approximation of a general set object $\langle x \rangle$ is denoted by $\langle\!\langle x \rangle\!\rangle$. Similarly, $\left[\!\left[ \underline{\underline{x}}, \overline{\overline{x}} \right]\!\right]$ is a conservative approximation of the interval object $\mathbf{x}$, with $\underline{\underline{x}}$ and $\overline{\overline{x}}$ the respective conservative lower and upper bound approximation.

A final convention is introduced for the notation of the range of a general function $f(x_1, \ldots x_n)$ with reference to the set vector $\big\langle \{x\} \big\rangle$, which is defined as the set of all results of the function considering all possible combinations of the function's argument inside the defined vector $\big\langle \{x\} \big\rangle$:

$$\langle f(x_1, \ldots x_n) \rangle_{\big\langle \{x\} \big\rangle} = \left\{ f(x_1, \ldots x_n) \mid (x_i \in \langle x_i \rangle, i = 1 \ldots n) \right\} \tag{18}$$

This definition of the range of a function considers the argument sets mutually independent. This is of great importance when considering the conservatism of the resulting range of the function for specific applications. This will be addressed more in detail in Section 4.2.

#### *2.2.2 Extension to convex modelling*

The definition of the interval objects states that the uncertain values lie within a hypercube, the vertices of which are defined by the lower and upper bounds on each component of the object. For instance, if the object consists of two components $x_1$ and $x_2$, the possible values of $x_1$ and $x_2$ are represented by a rectangle in the $(x_1, x_2)$-space. If it is thought to

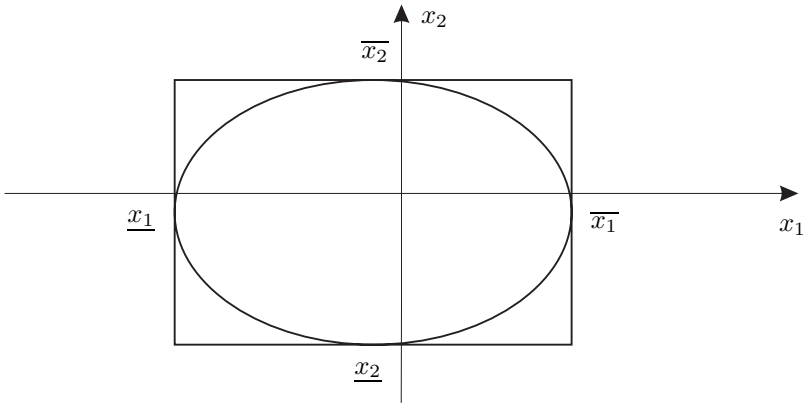


**Figure 3.** Comparison between the interval and general convex representation of an uncertain 2-dimensional object

be unlikely that the bounds on the components of the object are reached simultaneously, an alternative ellipsoidal description could be a more realistic representation of the uncertain object, as shown in Figure 3. More generally, any region could be defined within this $(x_1, x_2)$-space. When this region is convex for all uncertain objects, it is referred to as *convex modelling* [22] of uncertain objects.

A typical convex description of a set of uncertain parameters $\{x\}$ is the elliptical region defined by:

$$\{x\}^T \Omega \{x\} \leq a \tag{19}$$

with $\Omega$ a positive definite matrix and $a$ a positive constant.

More complex convex sets could be used to bound properties derived from the uncertain parameters rather than the parameters themselves. Ben-Haim *et al.* [23] for instance applies energy bounds on the inputs and bounds on the Fourier transform to describe the uncertain input of a seismic analysis by convex sets.

The added value of the convex model is that it enables the representation of correlations between interval values. This could be of great importance, but complicates strongly the analysis phase. The concept proves to be of great value for describing an uncertain excitation bounded in a convex set [23, 24], but also geometrical imperfections have been modelled successfully using this concept [25, 26]. However, only very few practical applications have been studied so far. Therefore, this work focusses on the basic interval concept

#### *2.2.3 Basic concept of the interval finite element analysis*

The finite element analysis at this point is considered in its most general form, i.e., a numerical procedure to simulate a physical phenomenon which is described by partial differential equations. The finite element procedure basically consists of the discretisation of the continuous domain in which the equations are defined, and the solution of a set of equations representing the partial differential equations of the original problem in this discretised space. Generally, a number of assumptions are necessary to obtain a numerically feasible solution strategy.

The goal of the interval finite element analysis is to obtain the maximal meaningful information on the simulated physical behaviour based on a given interval description of the uncertainty on some input parameters of the problem. Since the interval input uncertainty description gives no information on the frequency of occurrence of the uncertain parameters within the interval bounds, the problem reduces to finding the range of the analysis result.

Numerically, this means that the solution procedure should focus on finding the minimal and maximal deterministic analysis results taking all possible models into account that lie within the interval uncertainty description.

Considering the parameter vector $\{x\}$ defined to be contained within an interval vector $\{\mathbf{x}\}$ and the deterministic finite element analysis generally represented by the function $f(\{x\})$ applied on these parameters, the interval finite element procedure is numerically equivalent to finding the following solution set:

$$\langle\{y\}\rangle = \left\{ \{y\} \mid \Big(\{x\} \in \{\mathbf{x}\}\Big)\Big(\{y\} = f(\{x\})\Big) \right\} \tag{20}$$

with $\{y\}$ a general multidimensional result of the finite element analysis. The correct interpretation of this expression is that the set $\langle\{y\}\rangle$ contains all vectors $\{y\}$ which are obtained from applying the function $f(.)$ on all vectors within the interval vector $\{\mathbf{x}\}$. If an analytical expression of the analysis result is available and the interval vector of the input quantities is analytically expressed in a closed-form, this solution set can be derived through the use of the LAGRANGE multipliers [27]. This, however, does not apply for general finite element analysis.

There is only limited information on the output set of an interval finite element analysis, since there is generally no analytical expression of the input-output relation. Some basic observations are:

- If the output consists of physical quantities, all components of the output vector are generally continuous functions of the input. Consequently, an interval input will result in a continuous output domain.
- The components of the output vector are related through the design parameters. Therefore, the solution set can basically adopt any form in the output space.

From these observations it is clear that an exact description of the solution set is extremely difficult to find. Generally, however, only the individual ranges of some components of the result vector are really of interest. Therefore, most research focusses on calculating an interval vector which approximates the exact solution set $\langle\{y\}\rangle$, but neglects the interdependencies between the output vector components. This is referred to as a hypercubic approximation of the result. It describes a range for each vector component, but not all combinations of vector components within these ranges are part of the exact solution set. Ideally, the approximation should be the smallest hypercube around the exact solution set. If the result is used for reliability analysis, the hypercube should be conservative. This means that the hypercube should contain the complete exact solution set. Figure 4 gives a two-dimensional illustration of an exact solution set and the corresponding approximate hypercubes.

Research nowadays focusses on three different numerical solution strategies to calculate a hypercubic approximation of the exact solution set: the global optimisation approach, the interval arithmetic approach and the vertex approach, described respectively in Sections 4.1, 4.2 and 4.3. This work later introduces a new hybrid approach in Section 5.1.

## 2.3 The Fuzzy Finite Element Method

### *2.3.1 Basic properties of the fuzzy concept*

ZADEH [28] introduced the theory of fuzzy logic as a scientific concept for representing uncertainty. While the concept was invented in 1965, it resulted mainly in practical applications during the last two decades. The works of DUBOIS and PRADE [29, 30, 31] contributed to

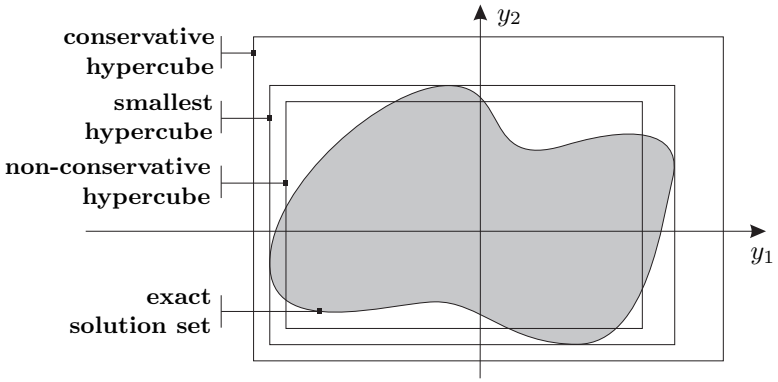


**Figure 4.** Hypercubic approximations of a continuous two-dimensional output set of an interval finite element analysis

a large extent to this evolution. The concept has been most successful in the application to controller design, known as *fuzzy control* [32]. In a fuzzy controller, the fuzzy concept is the basis for a human-like decision process for choosing an appropriate process control value based on fuzzily described state variables. This human-like concept does not require strict mathematical control rules, but is capable of handling linguistic rules often based on expert knowledge rather than strict objective data. The fact that the theory is capable of handling linguistic and, therefore, incomplete information, lately has inspired research activities in the field of numerical analysis. This section describes the most important aspects of the application of fuzzy numbers in such a numerical environment.

First, it is very important to understand what a fuzzy set exactly is. This is best explained by interpreting a fuzzy set as an extension of a classical set. A classical set clearly distinguishes between members and non-members of the set. The fuzzy set, on the other hand, introduces a degree of membership, represented by the *membership function*, which describes the grade of membership to the fuzzy set for each element in the domain. The difference with the classical (or also called *crisp*) set is that the fuzzy concept allows for membership values different from zero and one. This enables the representation of a value that is only to a certain degree member of the set. The membership function of a fuzzy set $\tilde{x}$ is defined as $\mu_{\tilde{x}}(x)$:

$$\tilde{x} = \left\{ \left(x, \mu_{\tilde{x}}(x)\right) \mid \left(x \in X\right)\left(\mu_{\tilde{x}}(x) \in [0,1]\right) \right\} \tag{21}$$

for all $x$ that belong to the domain $X$. If $\mu_{\tilde{x}}(x) = 1$, $x$ is definitely a member of the subset $\tilde{x}$. If $\mu_{\tilde{x}}(x) = 0$, $x$ is definitely not a member of the subset $\tilde{x}$. For every $x$ with $0 < \mu_{\tilde{x}}(x) < 1$, the membership is not certain. This concept softens the distinction between members to non-members in a classical set, and as such enables the definition of a zone in which there is a gradual transition of members to non-members. This gradual transition can be used to represent the uncertainty one would like to attach to parameters in a numerical analysis.

In the context of numerical analysis, a class called *normal fuzzy numbers* is generally used. For these fuzzy numbers, there is at least one point where the membership is equal to one, and the membership is strictly increasing and decreasing to the left respectively the right of this point. The most frequently applied shapes for the membership functions are the triangular and Gaussian shape. Figure 5 illustrates the concept of fuzzy numbers on an uncertain Young's modulus . In this figure, $\tilde{E}_1$ is a fuzzy representation of a classical interval defined as a five percent error margin on the nominal value of 2.1 GPa. The membership function of $\tilde{E}_2$ introduces uncertainty on the bounds on the interval, whereas

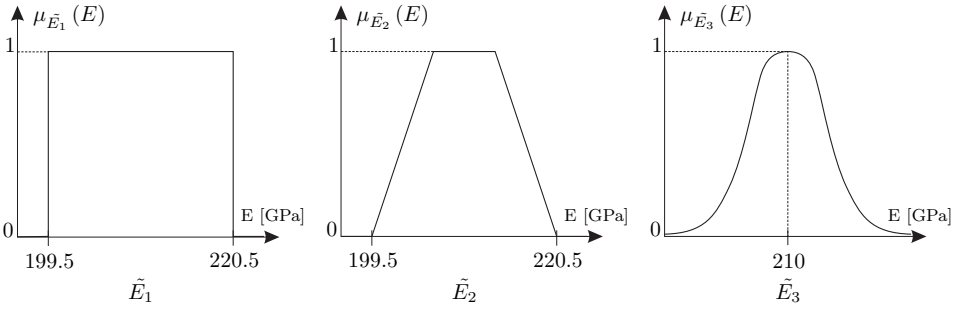


**Figure 5.** Some typical membership functions that describe linguistic variables

$\tilde{E}_3$ demonstrates a Gaussian membership function.

In his later work, ZADEH [33] extended the theory of fuzzy sets to a basis for reasoning with possibility. In this interpretation, the membership function is considered as a possibility distribution function, providing information on the values that the described quantity can adopt. More generally, the possibility is defined as *a subjective measure that expresses the degree to which the analyst considers that an event can occur*. It provides in a system of defining intermediate possibilities between strictly impossible and strictly possible events. Through this interpretation, the fuzzy concept has become a tool to model subjective knowledge numerically in a non-probabilistic concept. This has drawn the attention of the numerical community, since knowledge of uncertainties in a numerical model is commonly based on expert opinion. This has lead to applications of the fuzzy concept in miscellaneous numerical physical process simulations, ranging from multi-body kinematics [34] over uncertainty modelling of imprecise parameters in water flow simulations [35] to fuzzy modelling of powder snow avalanches [36]. Of particular interest is the application of the fuzzy concept in a non-deterministic finite element framework for numerical analysis of non-deterministic models. Section 2.3.2 now focusses on the general principle and some numerical aspects of this fuzzy finite element method.

### *2.3.2 Basic concept of the fuzzy finite element analysis*

The goal of the fuzzy finite element analysis [37, 38] is to obtain a fuzzy description of some output quantities of a finite element analysis in which the non-deterministic input is modelled using the fuzzy set model. It consequently aims at the derivation of the membership function of the output quantities given the membership functions of all input quantities:

$$\{\tilde{y}\} = f(\tilde{x}_1, \tilde{x}_2, \ldots \tilde{x}_n) \tag{22}$$

The fuzzy finite element analysis requires first of all a concept to handle the combination of the input sets, i.e., a definition of a Cartesian product combining different fuzzy sets. The membership function of a Cartesian product of variables described by individual membership functions has been defined in literature [39]:

$$\mu_{\tilde{x}_1 \times \ldots \times \tilde{x}_n}(x_1, \ldots x_n) = \min\left(\mu_{\tilde{x}_1}(x_1), \ldots \mu_{\tilde{x}_n}(x_n)\right) \tag{23}$$

This definition states that the possibility of a combination of fuzzy events equals the minimum of the possibilities of all individual events.

Next to the Cartesian product, the fuzzy finite element analysis also requires an arithmetic which handles the numerical evaluation of functions of fuzzy sets. A general concept follows directly from ZADEH's extension principle [40], which is one of the most basic ideas of fuzzy set theory. It provides a general method for extending crisp mathematical concepts

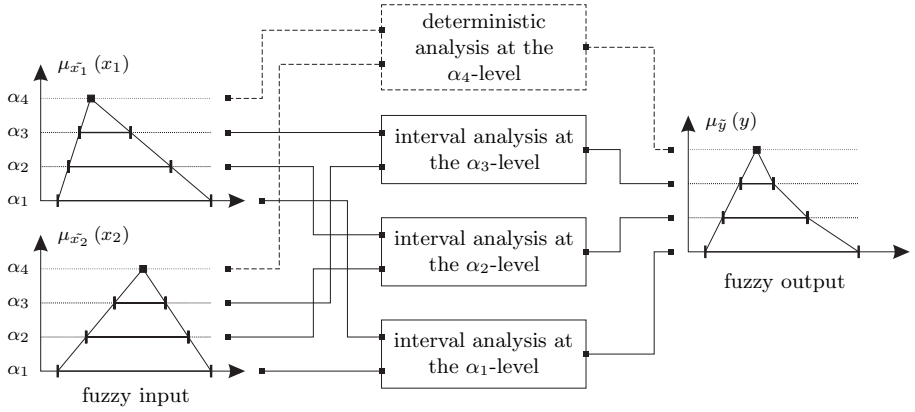


**Figure 6.** Scheme of the numerical procedure to perform a fuzzy finite element analysis by discretisation of the range of the membership function using 4 $\alpha$-sublevels

in order to deal with fuzzy quantities. It allows to calculate the fuzzy output $\tilde{y}$ of the crisp function $f(x_1, x_2, \ldots, x_n)$ applied to $n$ fuzzy numbers $\tilde{x}_i$:

$$\begin{cases} \mu_{\tilde{y}}(y) = \sup\limits_{\substack{x_1,\ldots x_n \\ y=f(x_1,\ldots x_n)}} \Big(\min\big(\mu_{\tilde{x}_1}(x_1), \ldots \mu_{\tilde{x}_n}(x_n)\big)\Big) \\ \\ \mu_{\tilde{y}}(y) = \quad 0 \quad \text{if} \quad f^{-1}(y) = \emptyset \end{cases} \tag{24}$$

This means that the membership value of the fuzzy result $\tilde{y}$ for a specific value $y^*$ equals the largest among the membership values $\mu_{\tilde{x}_1 \times \ldots \tilde{x}_n}$ of all input combinations $(x_1, \ldots x_n)$ resulting in $y^*$. The input combinations which result in $y^*$ are referred to as realisations of $y^*$. The possibilistic interpretation of the extension principle is that if a value $y^*$ can be achieved for different combinations of the input quantities, it will adopt its degree of possibility from the realisation with the highest degree of possibility.

A major drawback of the extension principle as defined in Eq. (24) is that it is not readily implementable in a numerical context. For each value $y$ of the observed output domain, it requires the complete set of realisations in the input domain to derive the membership value. An alternative approach consists of searching in the output domain for sets which have an equal degree of membership. This is achieved by analysing the input domain on a specific level of membership $\alpha$. At this level, the $\alpha$-cuts of the input quantities are defined as:

$$\mathbf{x_{i}}_{\alpha} = \big\{x_i \in X_i, \mu_{\tilde{x}_i}(x_i) \geq \alpha\big\} \tag{25}$$

This means that an $\alpha$-cut is the interval resulting from intersecting the membership function at $\mu_{\tilde{x}_i}(x_i) = \alpha$ (see Figure 6). After deriving the $\alpha$-cuts of all input quantities at a specific level, a general interval analysis as described in section 2.2.3 is performed on these intervals:

$$\mathbf{y}_{\alpha} = \left\{ y \mid \Big(x_i \in \mathbf{x_{i}}_{\alpha}, \forall i\Big)\Big(y = f\big(\{x\}\big)\Big) \right\} \tag{26}$$

It can be proven [41] that the obtained output interval is an intersection of the output membership function at the $\alpha$-level, and consequently represents an $\alpha$-cut of the output. This means that a discretised approximation of the output membership function can be obtained from repeating the $\alpha$-level procedure at a number of levels, as shown in Figure 6.

Based on this $\alpha$-cut strategy strategy, a number of fuzzy finite element applications have been published in specific research domains: static structural analysis [38, 42, 43], dynamic analysis [44, 45], geotechnical engineering [37, 46, 47], solid mechanics [48] and analysis of smart structures [49]. Recently, the fuzzy finite element approach has also been applied to non-linear analysis for fatigue life predictions based on the modelling of interlaminar cracks [50]. Since, through the $\alpha$-cut strategy, the interval finite element analysis forms the corner stone of the fuzzy finite element method, this work will focus on the implementation of the interval finite element analysis in sections 4 and 5.

At this point, it is important to note that the definition of the Cartesian product as in Eq. 23 does not provide a concept for dealing with mutual relationships that might exist between the fuzzy input properties. In fact, the fuzzy concept totally lacks a way of dealing with correlation. It is clear that this has a major impact on its application in numerical analysis, especially when spatially varying fields are to be taken into account. As discussed in section 2.1.3, the spatial correlation of the random field variable has a very high impact on the analysis. This explains why there currently is no research activity that the authors know of on the application of non-probabilistic concepts for random field analysis. However, as discussed above, the importance of the assumed correlation of the field necessitates trustworthy data to derive the spatial correlation kernel. If the information is rather limited, a less data-intensive but conservative approach as presented by the non-probabilistic concepts could be a valuable alternative, even for random field analysis.

## 3 APPLICATION OF THE NON-DETERMINISTIC FINITE ELEMENT ANALYSIS IN DESIGN

The introduction of the non-probabilistic approaches for non-deterministic numerical analysis has initiated a profound discussion in literature. On one side, some claim that the probabilistic approach is only a subcategory of the more universal fuzzy concept (see e.g. [51]). Therefore, the latter would represent a more unified approach for non-deterministic analysis. On the other side, some argue that probabilistic methods are able to model anything the non-probabilistic approach can. The goal of this section is not to choose either side in this discussion, but merely to review the applicability of the non-probabilistic concepts from an objective viewpoint. This is done based on a definition of different classes of non-determinism typically occurring in a finite element problem, described in section 3.1.1. Then, for each non-deterministic numerical modelling concept, its compatibility with the non-deterministic classes is discussed in section 3.2. This discussion focusses on the ability to objectively represent the available information. Finally, section 3.3 gives an overview of possible applications of the non-probabilistic approaches in a typical design process.

### 3.1 Sources of Non-Determinism in General Finite Element Modelling

#### *3.1.1 A classification of non-determinism in numerical analysis*

In literature treating non-deterministic numerical analysis, different researchers apply the same terminology in a rather inconsistent manner. This work applies the definitions of *error*, *uncertainty* and *variability* as proposed by Oberkampf *et al.* in [52], which enable a clear classification of non-deterministic aspects in numerical analysis. Section 3.1.2 gives some additional nuances which are necessary to enable a profound discussion of the applicability of the probabilistic and non-probabilistic concepts in non-deterministic finite element analysis in sections 3.2 and 3.3.

*Variability* is defined as *the variation which is inherent to the modelled physical system or the environment under consideration.* Referring to numerical analysis, a variability is generally described by a distributed quantity defined over a range of possible values. The

exact numerical value attached to the representation of the variable model property is assumed to be within this range, but it will vary from unit to unit or from time to time. Ideally, objective information on both the range and the likelihood of the quantity within this range is available. Others in literature refer to this variability as *aleatory uncertainty* or *irreducible uncertainty*. The term irreducible refers to the fact that even when all information on the particular property is available, the quantity cannot be deterministically determined. Typical examples of variability are manufacturing variability, environmental effects (temperature, humidity, ...), properties of non-uniform materials, ...

*Uncertainty* is defined as *a potential deficiency in any phase or activity of the modelling process that is due to lack of knowledge*. The word *potential* stresses that the deficiency may or may not occur. This means that there may be no deficiency even though there is some lack of knowledge, i.e., when the numerical model of the phenomenon happens to be correct rather by chance than due to exact knowledge. This definition basically states that uncertainty is caused by incomplete information resulting from either vagueness, nonspecificity or dissonance [53]. Vagueness characterises information which is imprecisely defined, unclear or indistinct. It is typically the result of human opinion on unknown quantities ("*the density of this material is around x*"). Nonspecificity refers to the availability of a number of different models that describe the same phenomenon. The larger the number of alternatives, the larger the nonspecificity. Dissonance refers to the existence of conflicting evidence of the described phenomenon, for instance when there is evidence that a quantity belongs to disjoint sets. Possibly, limited objective information is available, for instance when a range of possible values is known. In most cases, however, information on uncertainties is subjective and based on some expert opinion. Others in literature refer to this uncertainty as *reducible*, *epistemic* or *subjective uncertainty*. In a finite element context, uncertainties typically exist in the parts which are difficult to model, like non-rigid boundary conditions, joints, material damping. But also other unpredictable model changes over time can belong to this category, like ageing, loading, ...

Finally, an *error* is defined as *a recognisable deficiency in any phase of modelling or simulation that is not due to lack of knowledge*. The fact that the error is recognisable states that it should be identifiable through examination, and as such is not caused by lack of knowledge. This means that the error could be avoided by an alternative approach which is known to be more accurate, but which is possibly limited in practical applicability by computational cost or other practical considerations. A further distinction between *acknowledged* and *unacknowledged* errors is possible. Unacknowledged errors are blunders or mistakes, for instance where the analyst tries to model one phenomenon but as a result of human error, applied the wrong governing equations. These unacknowledged errors cannot be corrected. An example of an acknowledged error is the error associated with the conversion of partial differential equations into discrete equations using the finite element methodology. Other typical examples of acknowledged errors in finite element modelling are the use of linear models, the use of partial differential equations for the description of the analysed phenomenon, the representation of the displacement inside an element by a polynomial shape function, ... It is clear that the acknowledged errors are all inherent to the finite element analysis methodology as for any numerical analysis tool which tries to describe physical reality. This means that remedying these errors implies an alternative approach to the classical finite element principles. This, however, lies not within the scope of this paper.

Figure 7 summarises the definitions in this section with their main characteristics in the context of the finite element methodology.

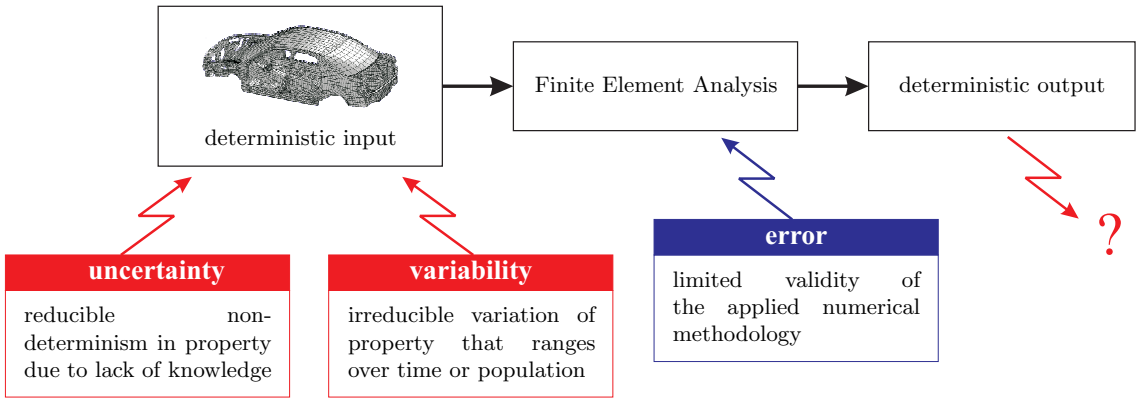


**Figure 7.** Occurrence of variabilities, uncertainties and errors in the finite element procedure

### *3.1.2 Discussion and extension of the definitions*

The definitions of uncertainty and variability above are not mutually exclusive, since a variability could be subject to lack of knowledge when information on its range or likelihood within the range is missing. This is for instance the case for every design dimension subject to tolerances, but without further specification of manufacturing process or supplier. The tolerances represent the bounds on the feasible domain, but there is no information on the likelihood of the possible values within these bounds. Consequently, because there is a lack of knowledge, such a variability is also an uncertainty. It is referred to here as an *uncertain variability*. Some vague knowledge may be available ("*the mean value is approximately* $x$") but also nonspecificity may play an important role in the uncertainty, for instance in choosing an appropriate model to describe a random quantity. Opposed to the uncertain variability, a *certain variability* refers to a variability the range and likelihood of which are exactly known.

Also, it appears logical to state that every property in a numerical model corresponding to a physical quantity is a variability, since it will eventually have a range of possible values and a likelihood inside this range in the physical realisation of the model. This argumentation implies that all uncertainties are also variabilities. In practice, however, the majority of model properties are implemented as constant deterministic values in the numerical model. Though they are subject to variation, the influence of their variability on the analysis result is considered to be negligible. Often, uncertainties refer to a possible lack of knowledge in these deterministic properties. This type of uncertainty is referred to as *invariable uncertainty*. Note that *invariable* in this case does not mean that the property cannot change over different analyses. According to the definition of uncertainty, it will change when information that decreases the amount of uncertainty is acquired. The invariable uncertainties typically occur in model properties for model parts that are difficult to describe numerically, but considered constant in the final physical product (connections, damping, ...). Other examples are design properties which have negligible variability but which are not defined exactly in an early design stage. Figure 8 gives a graphical illustration of the proposed subdivision of the definitions for uncertainty and variability.

### *3.1.3 Example*

The above definitions give a clear distinction between the different classes of non-deterministic model properties. In order to do a meaningful analysis, it is very important to determine the right class of the non-deterministic properties present in the treated problem. The

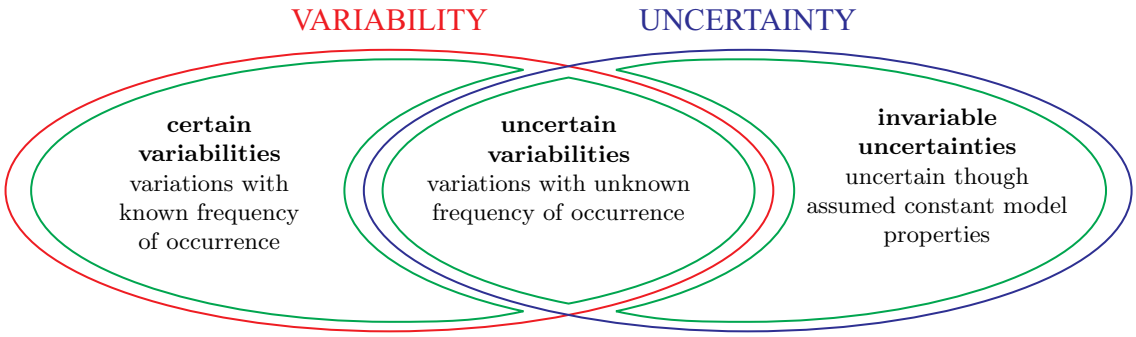


**Figure 8.** Classification of variabilities and uncertainties in numerical modelling

following small example illustrates that this classification is not always obvious, and can be influenced by the intention of the non-deterministic analysis.

Consider of a tank design, which is designed to carry a prescribed amount of fuel. Suppose that we want to assess the structural design of this tank through numerical analysis, using the amount of fuel in the tank as a non-deterministic parameter. In other words, we want to analyse the effect of the amount of fuel in the tank on its structural behaviour. In the most conventional interpretation of this problem, the purpose is to account for all possible uses of the tank, from being empty to completely filled. In that case, the mass of the fuel in the tank can be interpreted as a variability, since there clearly will be a variation over time or from unit to unit in the amount of fuel the tank contains. This means that the analysis indeed should focus on the effect of this variation in fuel mass between the absolute minimum and the absolute maximum.

On the other hand, the problem is totally different when we want to analyse the same tank when it is designed for a single mission, e.g., as a fuel supply tank in a space mission. In that case, the difference between the actual carried amount of mass and the amount the tank is designed for can be expected to be very small. The amount of fuel now no longer represents a variability. It could however be useful to analyse its influence on the design, for instance to assess the robustness of the design, or to determine the range of allowable usage. In that case, the fuel mass becomes an invariable uncertainty, the range of which can be chosen by the analyst according to his own expert knowledge or preference.

## 3.2 Numerical Representation of Non-Determinism

### *3.2.1 Probabilistic variability and uncertainty representation*

In most available non-deterministic finite element software codes, the probabilistic concept is applied to describe both variabilities and uncertainties in a model. This is mainly due to the fact that there exists a large number of numerical analysis procedures based exclusively on probabilistic input quantities. Therefore, every non-deterministic quantity in a model is readily replaced by a probabilistic quantity by introducing an appropriate probability density function. However, the probabilistic concept does not necessarily represent the available objective information. For the study of the applicability of the probabilistic concept, distinction between certain variabilities, uncertain variabilities and invariable uncertainties is necessary.

It is clear that the probabilistic concept is most appropriate to represent *certain variabilities*, since in the frequentist interpretation, the probabilistic description using a probability density function is completely consistent with the definition of a variability as in section 3.1.1. The information on the range and the likelihood of a certain variability can be unambiguously incorporated in the probability density function. Furthermore, the prob-

abilistic outcome of the analysis will give an indication of the actual expected frequency of occurrence of the analysed phenomenon. It is, however, important that all information is available in order for the model to realistically represent the variability. For instance, if more than one variable property is present in the model, the correlation between the different variabilities might play an important role in the probabilistic analysis. Ideally, the joint probability density function describing the likelihood and interdependence of all non-deterministic model properties is available. Since this is almost never the case, the probabilistic description of variability interdependence is generally limited to some moments of low order. Often, when cross correlations are unknown, the variabilities are assumed to be independent of one another.

For *uncertain variabilities*, a representation by a single random quantity is generally not sufficient. Engineering scientist FREUDENTHAL [54] who was one of the pioneers of probabilistic methods in engineering states that *" . . . ignorance of the cause of variation does not make such variation random."*. By this, he means that when crucial information on a variability is missing, it is not good practice to model it as a probabilistic quantity represented by a single random probability density function. On the contrary, in this case it is mandatory to apply a number of different probabilistic models to examine the effect of the chosen probability density function on the result. For instance, when the range of the variability is known but the information on the likelihood is missing, all possible probability density function over the range should be taken into consideration in the analysis. The analyst will generally select only a few probabilistic models which he considers consistent with the limited available information or most appropriate to obtain as much knowledge as possible on the result.

Most often, *invariable uncertainties* are represented by random quantities in probabilistic analysis. As such, the analyst tries to express his lack of knowledge of the property. This means that some probability density function is chosen which to the knowledge of the analyst represents best the uncertain nature of the quantity, but which is not based on available objective information. It is clear that in this case, the information contained in the random quantity does not represent the actual variation of the quantity in the final product, since by definition, the invariable uncertainties are considered to be constant. The random quantity in this case merely represents the presumed likelihood that a model parameter will adopt a value. As such, the lack of knowledge is filled by subjective information provided by the analyst, expressed in the form of a probability density function. This is sometimes referred to as a subjective probability density function. In this context, Bayesian methods are becoming increasingly popular for the modelling of subjective uncertainty. The main advantage of using the probabilistic approach for subjective uncertainty modelling is that the available probabilistic procedures can be readily applied for the analysis. It should be kept in mind, however, that the main strength of the Bayesian approach is its capability of incorporating objective information that becomes gradually available. When this is not the case, the Bayesian approach remains a fully subjective representation of reality.

At this point, it is very important to emphasize the consequences of the difference in the use of the probabilistic concept for variabilities on the one hand, and invariable uncertainties on the other hand. The former represents variability defined as a variation from unit to unit or in time for the final product, while the latter clearly may not be interpreted in this sense. Consequently, when interpreting the results of a probabilistic analysis based on both uncertainties and variabilities, it is imperative to distinguish between the different meanings attached to both. Though this seems straightforward, neglecting this distinction is a very common mistake in probabilistic uncertainty analysis. Section 3.3.2 elaborates further on the implications of this problem for probabilistic reliability analysis.

Recently, some criticism on the general application of probabilistic methods is arising. A first argument concerns the necessity of the probabilistic analysis. In some cases,

non-deterministic analysis is merely a tool to enhance or optimise the expected physical behaviour of a design based on (limited) knowledge of external non-deterministic influences. While probabilistic analyses are applicable for this purpose, probabilistic information on the behaviour of a design is not always primordial. Especially when subjective information is present in the analysis, other non-probabilistic techniques could give a valuable, maybe even additional insight into the non-deterministic nature of the simulated behaviour. Whether or not these techniques are valuable alternatives depends on the added value of the results. A second often heard argument against probabilistic analysis relates to its computational time-efficiency. This refers to the popular implementation using a Monte Carlo simulation, which is a rather time consuming technique, as it uses a high number of deterministic calculations to simulate the probabilistic process. Therefore, its computational efficiency will always lag behind the efficiency of the corresponding deterministic analysis.

Combining both arguments above, the criticism comes down to the fact that for some cases, the added value of the results of a probabilistic analysis does not justify the computational effort required to obtain them. In order to objectively assess this criticism as an argumentation in favour of non-probabilistic concepts, a clear insight in the added value of the alternative techniques is necessary. Therefore, the next sections describe the applicability of the interval and the fuzzy concept for variability and uncertainty representation. Section 3.3 will then discuss their added value for engineering design purposes.

#### *3.2.2 Interval variability and uncertainty representation*

The information represented by an interval object depends on the type of modelled non-deterministic quantity. Also here, distinction between certain variabilities, uncertain variabilities and invariable uncertainties is necessary.

For *certain variabilities*, the input interval objects are derived from the support of the corresponding input probability density function. Consequently, the result of an interval analysis only represents the actual range of the variable outcome of the analysis. The available information on the likelihood inside the range is lost, which is an important disadvantage. Especially for a variability with a justifiable probability density function support that is very large, using the support as input for the interval analysis will generally result in an extremely wide output interval. While it is theoretically correct to state that the final result will range over this output interval, disregarding the probability of the probability density function tails in this case clearly strongly devaluates the interval analysis.

When the upper and lower bounds of a non-deterministic property are well-defined but information on the type of the distribution is missing, it belongs to the class of *uncertain variabilities*. In this case, the interval model represents perfectly the available information. However, especially for variabilities with a very large probability density function support, the determination of the corresponding interval bounds is not always unambiguous, since the probability of the values that are located in the tails of the commonly applied probability density function with large support is typically very low. If these tails cannot be justified adequately with experimental data, there is no reason to unconditionally use the probability density function support for the interval analysis. In this case, the analyst should implement the bounds which he considers realistic with respect to the available experimental data. Often, the $3\sigma$-bounds are assumed to be realistic interval bounds. This conversion does not necessarily reduce the truthfulness of the uncertainty representation when there is little information on the actual tails of the probability density function. Still, if the tails of the probability density function are expected to have little probability, the impact of the subjective interval bounds on the interval analysis result is much larger than the impact of subjective probability density function support limits on the probabilistic analysis result. Therefore, variabilities with unknown probability density function support but a well-known normal-like behaviour near the center of the probability density function are best modelled

probabilistically.

For *invariable uncertainties*, generally a subjective interval is required. In this case, care should be taken not to interpret the interval quantity as the actual range in the physical product. It merely represents the values the analyst considers possible at the time the analysis is performed. Therefore, similar to the application of the probabilistic concept for invariable uncertainties, it is important to acknowledge the subjectivity in the result of the analysis. However, since the interval concept requires less subjective information to be added to the problem description, there is less room for misinterpretation of the results.

To conclude, we can state that the probabilistic concept remains the most valuable for the representation of certain variabilities and uncertain variabilities with unknown support but known normal-like behaviour. The omission of a known probability density function through the interval concept can only be justifiable when probabilistic information is not required, or the computational cost of the interval analysis is significantly lower. The interval concept is most valuable when dealing with uncertain variabilities with known support but unknown distribution, or invariable uncertainties.

#### *3.2.3 Fuzzy variability and uncertainty representation*

The application of the fuzzy concept for non-deterministic numerical modelling is not straightforward. The main problem of the representation of a model property through a fuzzy set, is that the membership function does not relate to an objective measurable quantity. The level of membership that is assigned to different members of a fuzzy set is completely based on the subjective beliefs of the analyst. Therefore, also the fuzzy results obtained from the analysis will be biased with the subjective input. Hence, these results may only be interpreted in reference to the assumed fuzzy input. This poses an important restriction on the use of the fuzzy approach for numerical design validation purposes. The practical consequences of this restriction will be further addressed in section 3.3. First, the applicability of the fuzzy concept for variability and uncertainty representation is discussed.

For a fuzzy representation of *certain variabilities*, the known probability density function has to be converted to a compatible membership function. A number of methods have been developed for this purpose [31, 55]. The basic law for the conversion follows from the consistency principle, which states that the degree of possibility of an event is greater than or equal to its degree of probability. This principle implies the following rule for conversion of probabilistic into possibilistic distributions:

$$\int_B f_X(x)\, dx \;\leq\; \max_{x \in B} \left( \frac{\mu_{\tilde{x}}(x)}{\max \mu_{\tilde{x}}(x)} \right) \tag{27}$$

for any set B in the feasible domain. This means that even a completely known probabilistic quantity has an infinite number of possibilistic representations. Therefore, these conversion techniques always rely on some sort of subjective judgement. Still, it is the author's opinion that forcing the application of fuzzy sets into the domain of certain variabilities through a conversion of probability density function as described above is rather irrational. Available objective probabilistic data is replaced by a subjective description, resulting in the loss of very valuable information. This loss is generally unjustifiable. Therefore, the conversion of a probability density function to a membership function should not be done.

For *uncertain variabilities*, the fuzzy concept can be used for a hybrid uncertainty model. It stems from an alternative interpretation of a possibility distribution introduced by Dubois and Prade [56] based on the *Evidence Theory* [57]. In this approach, a fuzzy number is used to represent a class of probability random quantities that have a cumulative distribution function in between boundaries derived directly from the possibility distribution. The left boundary on the compatible cumulative density functions coincides with the

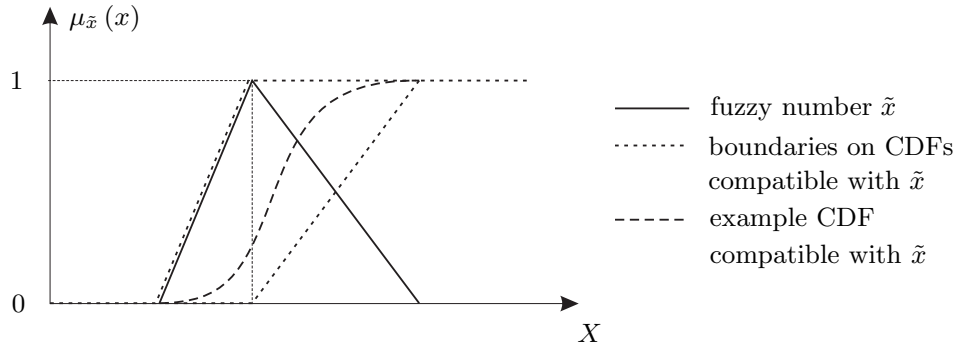


**Figure 9.** Possibility distribution of a fuzzy number and corresponding lower and upper boundaries for a cumulative density function compatible with the fuzzy number

increasing branch of the fuzzy number. The right boundary coincides with the complement of the decreasing branch of the fuzzy number. Figure 9 clarifies this approach. In this concept, the possibilistic approach becomes a tool to simultaneously examine the effect of a set of different probability density function in a single analysis. While the ability of this concept to model classes of probabilistic data seems extremely powerful, it has only been applied very rarely in uncertainty analysis.

Finally, an *invariable uncertainty* requires a fuzzy set that represents the subjective expectation of the analyst. When the invariable uncertainty represents an open design decision subject to optimisation, the analyst can express his preference of the quantity through the possibility distribution. Still, when interpreting the results, reference to the chosen input membership functions is imperative.

Considering the explicit subjective nature of a fuzzy set, it is concluded that it is most useful to describe uncertainties. The more objective information becomes available on a non-deterministic model property, the less the fuzzy concept is appropriate to describe it.

## 3.3 Application of Non-Deterministic Finite Element Analysis in Design

From the discussion above, it is clear that non-deterministic approaches can be very valuable to model non-deterministic properties in a finite element model in absence of crucial probabilistic information. Still, the decision on which non-deterministic concept to use should not be based exclusively on the available information at the analysis input. As shown in the example in Section 3.1.3, the clear definition of the objective of the analysis is at least equally important in the determination of the most appropriate non-deterministic analysis tool. Therefore, this section now focusses on a number of practical non-deterministic analysis types that concern a design engineer. Again, in order to evaluate the possibilities of the non-probabilistic approaches in specific applications, references will be made to the corresponding probabilistic treatment of the non-determinism.

### *3.3.1 Numerical non-determinism in a design process*

The main objective of the application of numerical tools in a design process is to assess the product quality at a specific design stage by simulation of its realistic physical behaviour. Still, an exact quantification of the design quality based on the numerical predictions is not always straightforward. This is mainly due to the non-determinism implicitly contained in the numerical analysis results. Analysing the design quality over time, very often an evolution as illustrated in Figure 10 is observed [58].

The design quality is expected to increases over time. Still, there always is a scatter on the predicted design quality, represented by the grey area in the figure. This scatter tends

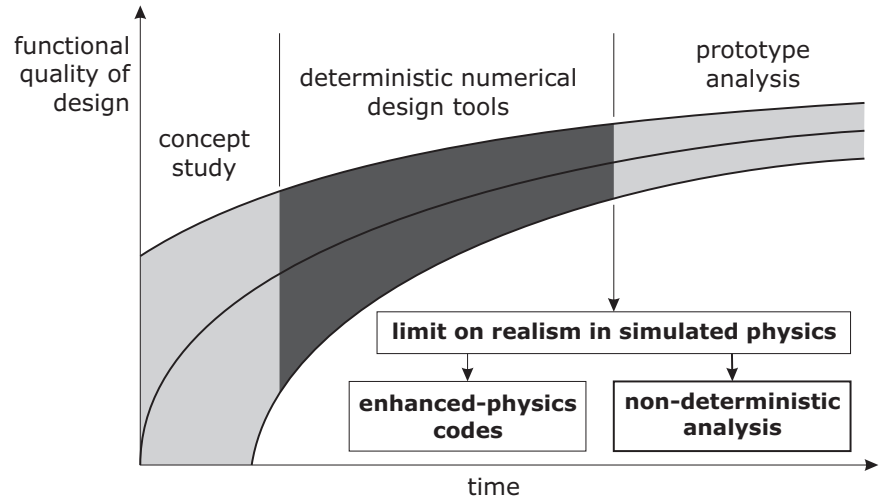


**Figure 10.** Limits on the application of numerical analysis in design

to decreased over the process, since additional information acquired over time will decrease the amount of uncertainty. On the other hand, the scatter will generally not disappear because of the presence of irreducible variability. Figure 10 indicates the evolution of the applicability of design analysis tools over time. The upper bound on the useful range of numerical methods is induced by the limit on the realism in numerical simulation of physics. There are currently two fundamentally different approaches that aim at moving this upper bound forward into the design process. On the one hand, there is a tendency towards integrated numerical analysis, aiming mainly at multi-physics simulations that incorporate all physics relevant for the design into a single simulation. On the other hand, it is more and more acknowledged that the introduction of non-determinism in the numerical analysis is equally, if not more important in influencing this upper bound. Therefore, it is imperative to have insight in the numerical analysis tools that can be of use to incorporate non-determinism in the analysis during design. This will not only extend the useful range of numerical methods, but should simultaneous lead to a better understanding of the sources of the scatter on the predicted behaviour. This information on its turn can be extremely important to improve the design quality obtained after the numerical design cycle. Figure 11 summarises these envisaged effects of numerical analysis of non-determinism in a design process.

Generally, there is an evolution of the type of non-determinism encountered during a typical design process, or as formulated by Ross *et al.* [59]: *As more information about a problem becomes available, the mathematical description of non-determinism can transform from one theory to the next in the characterization of the uncertainty as the uncertainty diminishes or, alternatively, as the information granularity increases and becomes specific.* In an early stage, objective information on model properties is often difficult to obtain, since a large number of model properties have yet to be defined. Some design decisions are even intentionally postponed in order to be able to study their effect on the design quality. Furthermore, early design improvements are commonly the result of expert knowledge rather than detailed numerical procedures. This means that the amount of objective information on average is low, and therefore subjectiveness is substantially present in the analysis. This leads to the conclusion that in early design stages, most non-determinism belongs to the uncertainty class. Through the course of a design process, the amount of information generally increases. In some cases, the non-deterministic properties can be more objectively

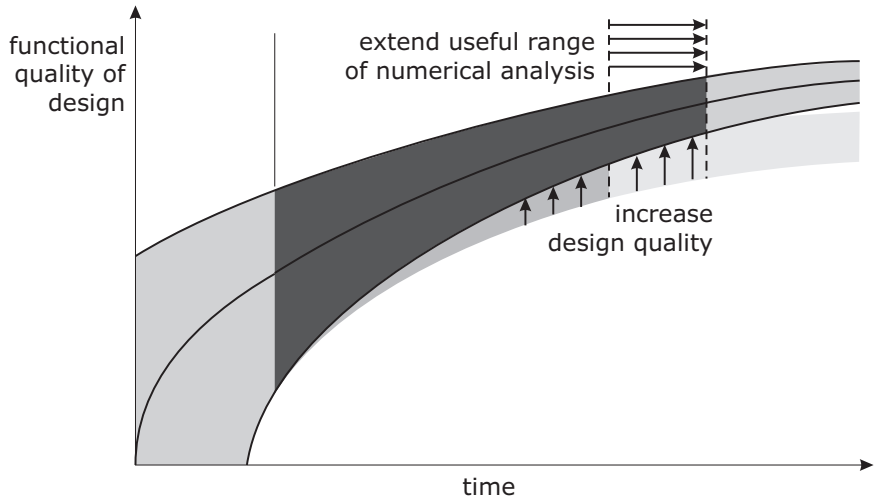


**Figure 11.** Extending the applicability of numerical methods and improving design quality through the application of non-deterministic analysis techniques in the numerical design cycle

described, e.g., when certain design aspects are fixed, or component manufacturers are chosen. The classification of the remaining non-determinism gradually moves towards to what has been defined as model variability, i.e., design independent variations in the product or its environment.

The evolution of non-determinism in a typical design process as described above is illustrated in Figure 12. This figure also indicates the evolution of the numerical concepts that are most appropriate for the dominant class of the occurring non-determinism. In the early stages, the non-determinism in the numerically predicted design quality is mainly driven by model uncertainties, which leads to the conclusion that non-probabilistic concepts are most appropriate in these early stages. Later in the design process, variability becomes more important, leading to a more prominent application of the typical variability modelling tool, i.e., the probabilistic concept.

The evolution of a property from one class of non-determinism to another can be clarified using a simple example. Take for instance the design of a new car body. The start point of the structural design is generally a conceptual design inspired esthetically rather than mechanically. In this initial design, there is a lot of non-determinism on the dimensions of structural components, such as for instance plate thickness. Since there is no information whatsoever on the exact plates that will be used, numerical analysis in this phase can only incorporate subjective knowledge based on other designs. Alternatively, a designer could be interested in the impact of a certain plate thickness on the behaviour of the design. In that case, a preferred range could be defined for the thickness in order to identify the most appropriate value. In either case, there is no clear objective information on the actual property in the final product. Hence, if non-determinism on this property is to be taken into account, this can only be achieved through modelling of subjective knowledge. Later, at a certain point in the design process, a specific reference value will be chosen for the thickness of the plates in the car body structure. Tolerances are chosen, which define the allowable region for these properties in the actual product. At this point, the range of the thickness in the actual product is known, but there's no information on the likelihood inside the range. The property is clearly evolved to an interval. Finally, when the design is finalised up to the detailed description of the manufacturing process, information on the

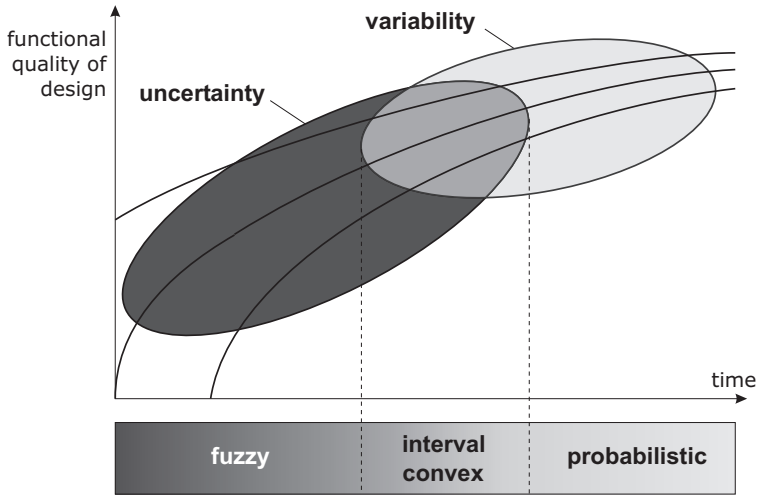


**Figure 12.** Typical occurrence of non-determinism in the product quality predictions during a design process

variation of the plate thickness within the bounds of the tolerances could become available. The value for the thickness then becomes a variability.

### *3.3.2 Probabilistic reliability analysis*

The reliability of a product is defined as the likelihood that it will successfully fulfil its intended task over a predefined period in time under specific environmental conditions. Numerical reliability analysis is very popular in a structural design context because it can provide a designer with crucial information on the likelihood of failure of the analysed design. As such, it can be usefully applied in an economical product analysis taking into account the cost associated with failure.

Reliability analysis of non-deterministic structures using the probabilistic concept has been studied extensively in literature. Very powerful software codes exist supplying the analyst with a vast arsenal of probabilistic reliability analysis procedures. See Casciati *et al.* [60] for a comprehensive overview of probabilistic reliability methods. Most commonly, the probabilistic reliability analysis results in a *probability of failure*, defined as *the likelihood that the structure will successfully fulfil its intended task over a predefined period in time under specified environmental conditions*. This probabilistic reliability analysis is broadly applied and already incorporated in generally accepted design specifications in civil engineering. However, its application in mechanical engineering is far less standardised. This is mainly due to the plentitude of different mechanical products, which all require a different amount of reliability under very different environmental and loading conditions. Hence, there are very few standards for reliability in mechanical design. Each product designer applies rules which are based on experience rather than on general engineering standards.

Mathematically, the probabilistic reliability analysis requires the definition of a performance criterion based on the relevant load and resistance parameters. This performance function generally is referred to as the *limit state* function and is described as:

$$Z = g(X_1, X_2, \ldots, X_n) \tag{28}$$

The *failure surface* is then defined as $Z = 0$. It represents the boundary between what are considered to be unsafe and safe design regions in the parameter space. The limit state can

be an explicit or implicit function of the parameters. This characteristic has an important influence on the analysis procedure.

Using the definition of Eq. (28) the probability of failure $P_f$ equals:

$$P_f = \int \dots \int_{g(X_1,X_2,\dots,X_n)<0} f_X(x_1, x_2, \dots, x_n)\, dx_1 dx_2 \dots dx_n \tag{29}$$

with $f_X(x_1, x_2, \dots, x_n)$ the joint probability density function for the considered parameters. This equation forms the basis of probabilistic reliability analysis. However, it is in most cases impossible to solve because the necessary information to describe the joint probability density function is missing. But even if it was available, evaluating the multiple integral is extremely difficult. In this context, approximation methods have been developed. Each of these methods has its own requirements concerning the performance function. Only the most common are listed here:

- **First Order Reliability Methods (FORM)**: After transformation to a standard normal parameter space, each limit state function is replaced with a first-order polynomial approximation at a specific point in the parameter space. This point is usually the point on the failure surface nearest to the origin, and is generally referred to as the *design point* or *most probable point*. The probability of failure follows directly from the distance from the origin to the design point.
- **Second Order Reliability Methods (SORM)**: This method is completely similar to FORM, with the exception that a second-order polynomial is used for the limit state function approximation. (see [61] for a general introduction to FORM and SORM)
- **Mean Value Based Methods (MVBM)**: This method constructs a first-order Taylor series expansion of the limit state functions around the mean values of the random variables.
- **Simulation Methods (SM)**: The approximation of the probability of failure results directly from a series of analysis runs using samples of each variable.

The FORM, SORM and MVBM require information on the derivatives of the limit state function to the parameters. Therefore, they are most appropriate when an analytical closed-form expression of the limit state function is available. This is generally not the case for reliability assessment based on finite element analysis, where the relation between the model parameters and the limit state function is implicit. This has led to the development of specific algorithms for sensitivity analysis which directly aim at the calculation of these derivatives, either analytically or based on numerical approximations. This is already provided in a number of commercial finite element codes nowadays. When there is no explicit relation between design parameters and the limit state, response surface methods are commonly applied to approximate the limit state function in the design space. With these, a limited number of analysis runs is performed at several points in the design space based on a design of experiments strategy. The approximation of the true limit state function then generally results from a second-order polynomial fitted through the resulting points. These developments induced implementations of FORM, SORM and MVBM around a finite element code. The computational burden for these implementations, however, remains large. Furthermore, the exactness of these methods decreases rapidly when the range of the parameter variabilities increases because the approximations are based on local information.

Currently, the simulation methods are by far the most popular numerical tool to predict the probability of failure of a given design. This is mainly due to the fact that they are

easy to use, straightforward, and require little background in probability theory. Their main disadvantage is that they are computational expensive. However, in combination with a response surface approximation of the limit state, their efficiency can be increased. Simulation methods are described more in detail in section 2.1.2. The probability of failure can be derived numerically based on a Monte Carlo simulation by rewriting Eq. (29) to:

$$P_f = \int_{-\infty}^{\infty} I\left(g\left(x\right)\right) f_X(x) dx = E\left\{I\left(g\left(x\right)\right)\right\} \tag{30}$$

with:

$$I\left(g\left(x\right)\right) = \begin{cases} 1 \text{ if } g(x) \leq 0 \\ 0 \text{ if } g(x) > 0 \end{cases} \tag{31}$$

Therefore, it can be estimated from $N$ Monte Carlo samples using:

$$P_f \approx \frac{1}{N} \sum_{i=1}^{N} I\left(g\left(X_i\right)\right) \tag{32}$$

with $X_i$ the numerical value of the samples. From this approximation it is also clear how a good preceding response surface procedure could greatly improve the efficiency of Monte Carlo simulation. Recently , Schuëller *et al.* [62] give a clear overview of the recent advances in Monte Carlo based simulation procedures for application in reliability analysis of high dimensional problems.

According to its definition, reliability belongs clearly to the probabilistic framework in the frequentist context. On the one hand, this complicates probabilistic analysis of designs intended for limited production, since the fact that the product is only produced in limited quantity strongly complicates a decent aposterior verification of the non-deterministic numerical predictions. Furthermore, for most designs intended for limited production nowadays, an unverifiably high reliability is requested (e.g. spacecraft). The current tendency towards designing for 6-$\sigma$ clearly illustrates this evolution. However, such specifications require an extremely high accuracy of the predicted probabilistic behaviour, especially in the tails of the obtained probability density functions. This is extremely difficult to achieve. Furthermore, even if a mass production is envisaged, such high reliability requirements can never be verified. Therefore, it is the authors opinion that it is rather irrational to attach any objective meaning to reliability values of $1 - 10^{-9}$ or more. The reliability specification in this case comes down to requiring an extremely reliable product, which is a clear step towards treating reliability in a subjective non-deterministic context.

As discussed in section 2.1.1, while applying the probabilistic concept for the representation of subjective information is possible, results from such an analysis should definitely not be interpreted as indication for an absolute frequency of occurrence. This means that the subjectiveness devaluates the use of the probabilistic results in a reliability context. It is important to note that the subjectiveness incorporated in the information on which the analysis is based is not always detected. For instance, neglecting unknown correlation between properties by assuming them as independent is a common simplification that is sometimes implicitly made, but that can have important consequences. This implicit assumption of independence between probabilistic quantities was one of the important errors that were the source of the Challenger space shuttle disaster [63]. In this case, the impact of different extreme weather conditions on the launch was analysed for each condition individually beforehand. The impact of a combination of more than one of these events, however, was never checked. Although each of the events had a very low probability of occurring, the probability of their combination proved to be not simply a multiplication of

the probabilities of the single events. The correlation between the conditions was clearly misjudged, leading to a plausible but unaccounted for weather situation with disastrous consequences.

The lack of credibility of numerical predictions of reliability is generally compensated by safety factors. However, one could argue that using these safety factors after applying sophisticated and computationally expensive numerical procedures is not a really economical situation. Much effort is spent on a numerical prediction, which, in the end, still has to be corrected based on practical experience. In this context, the non-probabilistic approaches could prove their value. The remainder of this section briefly discusses possible applications of the non-probabilistic concepts for numerical reliability analysis.

#### *3.3.3 Non-probabilistic reliability analysis*

The application of the interval concept in numerical reliability studies is often referred to as *anti-optimisation*. This name stems from the fact that from all numerical models within the interval input boundaries, the one with the least favourable analysis result is the most interesting from reliability point of view. Finding this least favourable result is mathematically equivalent to performing a numerical optimisation aimed at the worst case result with respect to the input intervals.

The concept of anti-optimisation has been introduced as the basis for a non-probabilistic reliability framework [64]. This requires an evolution from a reliability concept as *probability of failure* towards *range of acceptable behaviour*. This means that the design must assure that the performance remains within an acceptable domain, without specifying a likelihood of failure. Reliability then becomes a crisp criterion distinguishing between either acceptable or unacceptable designs. The most important benefit of the anti-optimisation concept is that it broadens the objectivity of reliability studies to uncertain variabilities with known range, because the interval model perfectly represents these uncertainties without the need for subjective input. For instance, this enables a fast assessment of dimension tolerances on a design, without knowing the actual distribution of the dimension within the bounds of the prescribed tolerance. For some cases, it can be shown that the anti-optimisation procedure results in the same choice of design parameters as a probabilistic analysis if the required reliability tends to one [65]. The anti-optimisation in this case proves to be far less expensive in computation time.

The numerical implementation of the anti-optimisation approach is subject to an important requirement. Since the result of the analysis is the source of a crisp decision between acceptable and unacceptable designs, approximate results should always be kept on the safe side of the exact result. This means that if approximate solution procedures are used in the numerical implementation, they should guarantee conservatism in their result. On the other hand, this conservatism should not be excessively high in order for the result to be of any practical value.

Also the fuzzy concept has been introduced as a numerical reliability assessment tool [66] . In the interpretation of the membership function as a degree of possibility, the fuzzy outcome of an analysis could be used to define a possibility of failure. This possibility is clearly influenced by the subjectiveness that is implicitly incorporated in the fuzzy input of the analysis. This means that for the same problem, different analysts can and generally will end up with different possibilities of failure. This could be compensated by defining a personal threshold value for the allowed possibility of failure in the final decision on acceptable or unacceptable designs. However, due to the necessary amount of personal interpretation of the analyst, possibility of failure only has a relative value. Therefore, this approach is extremely difficult to standardise in a general reliability framework.

Still, based on the $\alpha$-sublevel technique as described in Section 2.3.2, the fuzzy approach becomes very useful when the effect of interval bounds on the anti-optimisation result has

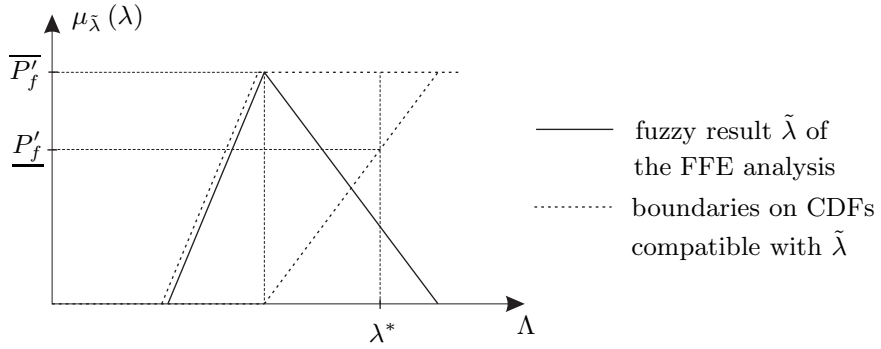


**Figure 13.** Example of the application of the fuzzy outcome of a fuzzy finite element analysis to predict bounds on the probability of failure

to be analysed. In this context, the fuzzy analysis can serve as a tool to derive the $\alpha$-level on which the required safety margins are reached on the crisp failure modes. The input intervals derived from the input membership functions intersected at this $\alpha$-level then define the allowable range for the non-deterministic input properties. The fuzzy reliability analysis as proposed by Biondini *et al.* [67] is based on this principle. The same approach was applied by Catallo [68] for reliability assessment based on a fuzzy analysis of limit state load multipliers of a precast concrete structure.

A different application of the fuzzy concept in reliability analysis is based on the use of the membership function as limit cumulative density functions as explained in Section 3.2.3. It was shown by Ferrari *et al.* [69] that if the input membership functions represent boundaries on the cumulative density functions of the input parameters, the membership function resulting from fuzzy analysis on this input forms reliable boundaries on the actual cumulative density function of the result. Therefore, the fuzzy result of a fuzzy finite element analysis can be used to derive bounds on the probability of failure. A simple example illustrates this. Suppose that a fuzzy finite element analysis results in a membership function $\mu_{\tilde{\lambda}}(\lambda)$ representing a crucial eigenfrequency of a design as illustrated in Figure 13. Suppose furthermore that a crisp criterion states that the design is acceptable if this eigenfrequency is kept below the value $\lambda^*$. The fuzzy result envelopes the exact cumulative density function of the eigenfrequency. This means that the bounds on the probability that the eigenfrequency of the design lies below $\lambda^*$ can be derived from the fuzzy result. The probability interval is obtained from taking the value of the envelope curves at $\lambda^*$ as indicated in the figure by $\underline{P'_f}$ and $\overline{P'_f}$. The most conservative statement resulting from the analysis is that the probability of failure equals $(1 - \underline{P'_f})$ in the worst case.

It is clear that also the above non-probabilistic reliability methods are subject to the limitation that whenever there is subjective information involved in the problem definition, the results can not be interpreted as absolute measures of design quality. In an absolute reliability context, the amount of expert knowledge required in the distinction between a good or bad design is proportional to the amount of subjectiveness incorporated in the description of the non-determinism. Still, subjective analysis can be of great value when used in a relative framework, as for instance a design optimisation procedure. This will be discussed in the next section.

### *3.3.4 Numerical design optimisation*

The principal goal of design optimisation is to define the best possible product under certain restrictions. These restrictions can be anything from manufacturing cost to limitations

placed on physical properties of the design. The ingredients of the goal function and their relative weights determine the final result of the optimisation. Reliability can be used as an indication for the design quality, and therefore can be an important part of the goal function. Classically, this is approached from a probabilistic view point, and referred to as *reliability based design optimisation*. YOUN *et al.* [70] gives an overview of different approaches that aim at an increase in design quality or robustness through an optimisation based on numerical reliability predictions.

Still, when reliability is used as a design quality indicator in an iterative design optimisation process, the demands on the objectivity are much lower than when it is used for absolute design assessment. A relative reliability improvement during an optimisation process can already be very valuable, even though the absolute reliability is only roughly approximated. This means that also subjective analysis can be usefully applied in a design optimisation context. While applying subjective probability for this purpose is possible, it is not always the most advisable approach. In some cases, especially in design optimisation, a probabilistic reliability measure is not required. For instance, if the range on some parameters is all information that is available, placing subjective probability density function on these ranges only complicates the numerical problem, while it doesn't necessarily add any valuable meaning to the analysis. In that case, it doesn't really make sense to transform the problem to the probabilistic concept. Or as formulated by ROSS *et al.* [71]: *Sometimes, striving for precision can be expensive, or adds little or no useful information, or both.* This indeed holds for the application of reliability calculations in an iterative optimisation procedure, where the numerical efficiency becomes very important. It is now discussed to what extend the non-probabilistic approaches can be considered as valuable alternatives for design analysis in an optimisation framework.

For the interval concept, the most useful application lies in modelling invariable uncertainties. Though they are assumed to be constant, they could play an important role during design optimisation. The analyst may ask the question whether the defined ranges for the invariable uncertainties result in an allowable range for the behaviour, without really being interested in the likelihood of occurrence within the defined interval bounds. Or, alternatively, the invariable uncertainty represents an open design decision, i.e., a model property that has yet to be quantified, and the value of which will be optimised. Pure probabilistic analysis in both cases seems like an unnatural thing to do, since it requires information that is not available (probabilistic input) to produce information that is not requested (probabilistic output). The interval procedure is limited to the definition of the intervals on the uncertainties the analyst would like to take into account. Subsequently, the design can be assessed from an interval analysis by reassuring that the worst case output is still within the range of acceptable physical behaviour. This comes down to a worst-case oriented design optimisation.

A commonly formulated criticism on this approach is that the worst-case behaviour generally results from the combination of extremely rare events. Taking these combinations into account in a design assessment procedure could lead to severe over dimensioning. This criticism only holds if you can objectively verify the actual probability of occurrence of the model properties which are considered to be extreme events. But even more important, if you want to give a realistic weight to the actual occurrence of such an extreme combination of events, it is imperative to incorporate the exact mutual interdependence between these extreme events in the procedure, as discussed for the Challenger case in section 3.3.2. In such cases, worst case analysis could be a tool for identification of extreme events which lead to failure, without the need for a prediction of the actual probability of this extreme event. This identification should not necessarily lead to adapted designs and the generally associated over dimensioning. In the Challenger case, accustomed launch protocols incorporating identification of possible disastrous extreme weather conditions would already have

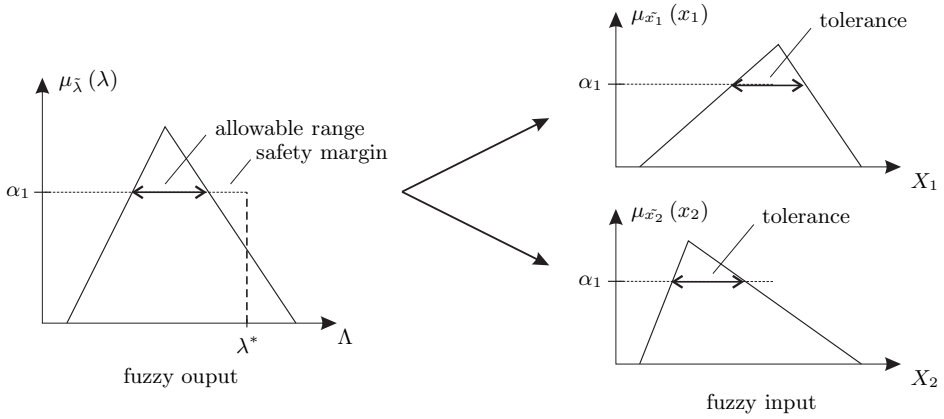


**Figure 14.** Illustration of the application of fuzzy concept for design tolerance analysis

been of great value.

As discussed in the previous section, due to its implicit subjective nature, the value of fuzzy finite element analysis as an absolute reliability analysis tool is rather limited. In an optimisation procedure, however, the complete process is generally conducted or followed up by one and the same analyst. This means that the subjective possibility measure can be interpreted in a consistent manner throughout the optimisation procedure. Therefore, the possibility of failure can be used as a quality measure in an optimisation procedure. In this context, Choi *et al.* [72] recently introduced a possibility-based design optimisation procedure based on a fuzzy representation of the uncertain design aspects.

Apart from reliability optimisation, an important aspect of designing under uncertainty is to define a robust design, i.e., a design whose critical properties have a minor sensitivity to changes in the uncertain influences like for instance external loading. Also in this context, the fuzzy approach can be of value. By placing fuzzy membership functions as loading factors on the crucial loading components, the sensitivity of some design quality indicators to these external influences can be analysed. Using this approach, the robustness of the design can be assessed by measuring the width of the resulting membership function on the critical design quality indicators.

Another practical approach of the fuzzy analysis is in the study and choice of tolerances placed on design dimensions. From the $\alpha$-cut strategy, it is clear that the fuzzy finite element analysis is actually a large-scale sensitivity analysis of the combined effect of the bounds defined on some interval design variables on critical design properties. By placing membership functions on the design properties subject to tolerances, the effect of their range on the design behaviour can be analysed. This can be helpful in defining tolerance intervals in the model. For instance, at a certain $\alpha$-level, an allowable range could be identified in the fuzzy outcome of the analysis. The corresponding input intervals at this $\alpha$-level can then be chosen as the set of tolerances on the analysed design properties. This procedure is clarified in Figure 14, where the design specification is assumed to be an upper bound $\lambda^*$ on an eigenfrequency. The analyst can control the analysis by defining the possibility distributions on the input according to personal preference or practical limitations. A different possibility distribution for the design variables will yield a different possibility distribution of the analysis result, and consequently also different tolerances for the design variables. The design based on these alternative allowable ranges, however, is equally safe. In this context, again, the possibility distribution is rather a useful tool to control the allowable range for the uncertainties than an absolute quality measure.

### 3.4 How are probabilistic, interval and possibilistic analyses related?

Elishakoff [73] compares the concepts of probabilistic analysis, fuzzy sets and anti-optimisation applied on finite element analysis. He concludes that each of the methods has its own advantages and could be preferred above the others under specific circumstances. De Lima *et al.* [74] compared the result of a probabilistic finite element analysis and an equivalent fuzzy finite element analysis analysis on a simple example. He concludes that the fuzzy method leads to less expensive qualitative results which are adequate for practical engineering purposes.

To compare the applicability of the different methods, it is of interest to study the performance of each of the different concepts when applied to the same design problem. After all, they are all aimed at providing the analyst with enough information on the influence of the non-deterministic input on the numerical analysis to draw conclusions regarding the performance of the design. Maglaras *et al.* [75] compares experimentally the designs resulting from optimising reliability in both a probabilistic and possibilistic framework. He concludes that the design acquired through probabilistic analysis is better when there is enough information to describe the probabilistic data realistically. Another comparison of probabilistic and possibilistic design under uncertainty by Nikolaidis *et al.* [76] demonstrates that a fuzzy set method yields safer designs than probabilistic design methods when very limited information is available. Both these conclusions confirm the main drawback of probabilistic analysis, i.e., the fast devaluation of its result with increasing lack of information on the non-deterministic input.

It could be useful to do an analysis using a mixture of different uncertainty models, for instance when there is sufficient statistical data to describe some variabilities, but also uncertainties are present in the model. For this purpose, a hybrid finite element analysis has been developed by Langley [77]. It consists of a single mathematical algorithm to analyse all three models of non-deterministic quantities simultaneously, based on a SORM or FORM approach for reliability. A different approach for combined uncertainty and variability analysis was proposed by Rao *et al.* [78]. It is based on a separate probabilistic and non-probabilistic analysis run, after which both results are unified to a hybrid-uncertainty mean value and variance.

Based on the discussion in Sections 3.1, 3.2 and 3.3, it is concluded that the mutual relationship between the probabilistic and the non-probabilistic approaches is rather weak. While both can be put to use in a numerical design procedure, their application field is strongly dependent on the available information and the intention of the numerical analysis. Considering a design process as given in Figure 12, this leads to the conclusion that the non-probabilistic approaches should be regarded as complementary rather than competitive to the probabilistic approach.

## 4 NUMERICAL IMPLEMENTATION OF THE INTERVAL FINITE ELEMENT METHOD

The previous section clearly shows that the interval and fuzzy approach can be very valuable concepts for modelling incomplete information under specific circumstances. It is clear that, using the $\alpha$-level strategy as described in Section 2.3, the interval analysis forms the numerical backbone of the fuzzy implementation. This section now focusses exclusively on the implementation of the interval finite element methodology. Sections 4.1, 4.2 and 4.3 describe three principle strategies to tackle the general problem as defined in Eq. (20) in Section 2.2. Section 4.4 then gives an overview of the application of these strategies for selected finite element analysis types.

### 4.1 The Global Optimisation Approach

In essence, calculating the smallest hypercube around the solution set expressed in Eq. (20) is equivalent to performing a global optimisation, aimed at the minimisation and maximisation of the components of the deterministic analysis results $\{y\}$. The deterministic finite element analysis is the goal function of the optimisation and the uncertain parameters are the design variables. The interval vector in which the uncertain parameters are contained defines the constraints for the variables. The optimisation is performed independently on every element of the result vector $\{y\}$. Therefore, the solution set of Eq. (20) becomes an interval vector $\{\mathbf{y}\}$ describing the hypercube around the exact solution:

$$\{\mathbf{y}\} = \left\{ \begin{array}{c} \mathbf{y_1} \\ \mathbf{y_2} \\ \vdots \\ \mathbf{y_n} \end{array} \right\} \tag{33}$$

with:

$$\underline{y}_i = \min_{\{x\}\in\{\mathbf{x}\}} f_i\big(\{x\}\big),\ i = 1 \ldots n \tag{34}$$

$$\overline{y}_i = \max_{\{x\}\in\{\mathbf{x}\}} f_i\big(\{x\}\big),\ i = 1 \ldots n \tag{35}$$

An efficient and robust optimisation algorithm is primordial for this solution strategy. Rao *et al.* [38] applied Powell's method to tackle the optimisation. Köylüoğlu *et al.* [79] defined a linear programming solution for this purpose. Möller *et al.* [80] introduces a genetic approach to perform the global optimisation efficiently on every $\alpha$-level. The input interval vector defines the number of constraints and, therefore, strongly influences the performance of the procedure. Also, because of the required execution of the deterministic finite element analysis in each goal function evaluation, the optimisation approach is numerically expensive. Therefore, this approach is best suited for rather small finite element models with a limited number of input uncertainties.

### 4.2 The Interval Arithmetic Approach

The interval arithmetic approach consists of translating the complete deterministic numerical finite element procedure to an equivalent interval procedure. This translation is based on the interval arithmetic operations for addition, subtraction, multiplication and division of interval scalars:

$$\mathbf{a} + \mathbf{b} = \left[\underline{a} + \underline{b}, \overline{a} + \overline{b}\right] \tag{36}$$

$$\mathbf{a} - \mathbf{b} = \left[\underline{a} - \overline{b}, \overline{a} - \underline{b}\right] \tag{37}$$

$$\mathbf{a} \times \mathbf{b} = [\min(\underline{a}\times\underline{b}, \underline{a}\times\overline{b}, \overline{a}\times\underline{b}, \overline{a}\times\overline{b}) \quad \max(\underline{a}\times\underline{b}, \underline{a}\times\overline{b}, \overline{a}\times\underline{b}, \overline{a}\times\overline{b})] \tag{38}$$

$$\mathbf{a}/\mathbf{b} = \mathbf{a} \times \left[\tfrac{1}{\overline{b}}, \tfrac{1}{\underline{b}}\right],\ \text{if } 0 \notin \mathbf{b} \tag{39}$$

By replacing each of the basic operations in a deterministic code with its interval arithmetic counterpart, the corresponding interval code is generated. This means that the outline of the interval procedure corresponds completely to the deterministic procedure. The main difference is that each substep of the interval algorithm calculates the range of the intermediate subfunction instead of the deterministic result. Application of this principle on the complete algorithm results in the range of the output of the analysis.

There is an important drawback for this method. The inclusion property for ranges of nested functions states that an arithmetic interval operation introduces conservatism in its result if it neglects correlation that exists between the operands. A simple example illustrates this. Consider the function:

$$f(\{x\}) = \left((x_1 + x_2)\,(x_1 - x_2)\right)^2 \tag{40}$$

applied on the intervals:

$$\{\mathbf{x}\} = \left\{ \begin{array}{c} \mathbf{x1} \\ \mathbf{x2} \end{array} \right\} = \left\{ \begin{array}{c} [-1, 2] \\ [-2, 3] \end{array} \right\} \tag{41}$$

Using the global optimisation approach, it is easily checked that the exact range of the above function equals:

$$\langle f \rangle_{\{\mathbf{x}\}} = [0, 81] \tag{42}$$

The interval arithmetic approach now consists of the translation of all operations in the function as defined in Eq. (40) to their interval arithmetic counterparts. By rewriting Eq. (40) as $f(\{x\}) = z_2^2$ with:

$$z_2 = z_{11} \times z_{12} \tag{43}$$
$$z_{11} = x_1 + x_2 \tag{44}$$
$$z_{12} = x_1 - x_2 \tag{45}$$

and translating these subfunctions, we obtain:

$$\langle z_{11} \rangle_{\{\mathbf{x}\}} = [-3, 5] \tag{46}$$
$$\langle z_{12} \rangle_{\{\mathbf{x}\}} = [-4, 4] \tag{47}$$
$$\langle\langle z_2 \rangle\rangle_{\{\mathbf{x}\}} = [-20, 20] \tag{48}$$
$$\langle\langle y \rangle\rangle_{\{\mathbf{x}\}} = [-400, 400] \tag{49}$$

It is immediately observed that although this is a very easy implementable procedure, the final result is subject to a very large amount of conservatism, caused by the artificial independence between the operands $x_1$ and $x_2$ of the subfunctions. In an automatic computer procedure, this phenomenon cannot be avoided because it is impossible to keep track of the relationships between all intermediate results of the algorithm. Consequently, each interval substep results in an enclosure of the exact substep range. Therefore, also the final result is a conservative approximation of the exact range. Generally, the degree of conservatism is unknown. It possibly can be too high to be useful for practical applications. In order to be of any practical use, it is imperative that any newly developed interval procedure based on the interval arithmetic approach is thoroughly checked on its vulnerability to artificial conservatism in its results.

The implementation of the interval finite element approach based on this interval arithmetic approach consists of two parts:

1. The translation of the input intervals $\{\mathbf{x}\}$ to an interval system description in the form of interval system matrices. These are obtained by translating the deterministic assembly procedure to interval analysis. In a first step, the element interval matrices are obtained. For instance, for undamped structural dynamic analysis, these are denoted by $[\mathbf{K}^{\mathbf{e_i}}]$ and $[\mathbf{M}^{\mathbf{e_i}}]$. The interval arithmetic equivalent of the assembly phase then results in the interval system matrices $[\mathbf{K}]$ and $[\mathbf{M}]$.

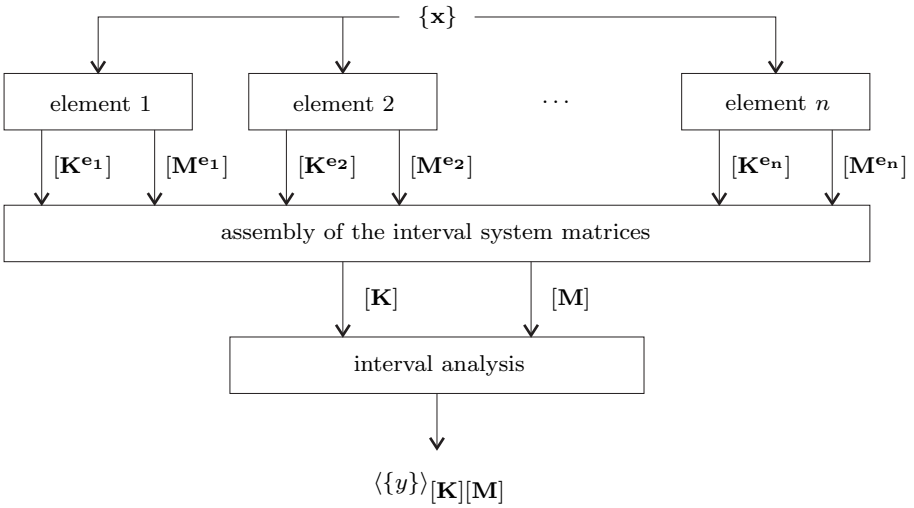


**Figure 15.** Scheme of the interval arithmetic implementation of an undamped structural dynamic interval finite element analysis

2. The approximation of the solution of the analysis expressed as an interval problem using the interval system matrices. . The exact solution set then becomes:

$$\langle\{y\}\rangle_{[\mathbf{K}][\mathbf{M}]} = \left\{ \{y\} \mid \Big([K] \in [\mathbf{K}]\Big)\Big([M] \in [\mathbf{M}]\Big)\Big(\{y\} = f\big([K],[M]\big)\Big) \right\} \tag{50}$$

with $f$ the function representing the calculation of the analysis result based on the system matrices.

The interval arithmetic finite element procedure is graphically summarised in Figure 15.

It is clear that through the numerous basic operations that are required in a general finite element solution procedure, the amount of conservatism introduced by the inclusion property can be substantial. The interval matrix assembly phase was shown to have a very important contribution to this conservatism in the final analysis results [41]. So far, there is very little effort in literature to remedy, study or even acknowledge the sources of conservatism inherent to the interval arithmetic procedure. Nearly all current research in this area starts from the interval system matrix formulation of the problem, totally disregarding the interval matrix assembly phase. One fact remains too often covered in silence: even if the exact interval solution of the interval arithmetic equivalent of the deterministic analysis can be obtained, there remains a substantial amount of conservatism with respect to the original problem due to the conservatism in the matrix assembly phase. In order to realistically assess any interval finite element implementation based on the interval arithmetic approach, it is imperative to analyses all sources of uncertainty, including those resulting from the assembly phase.

From a numerical point of view, the applicability of the interval arithmetic strategy mainly depends on the availability of a calculation procedure for the hypercubic approximation of the solution set of Eq. (50). This procedure strongly depends on the numerical properties of the intended finite element analysis, as will be discussed in Section 4.4.

### 4.3 The Vertex Method

Dong *et al.* [81] introduced the vertex method as a tool for the approximation of the bounds on the exact set resulting from a general operation on one or multiple interval numbers. The

approximation results from introducing all possible combinations of the boundary values of the input intervals into the analysis. For $N$ input intervals, there are $2^N$ vertices for which the analysis has to be performed. These vertices are denoted by $\{c_j\}, j = 1, \ldots 2^N$. Each of these represents one unique combination of lower and upper bounds on the $N$ input intervals. The approximate analysis range of a function $f(.)$ applied on these intervals is deduced from the extreme values of the set of results for these vertices:

$$\{\mathbf{y}\} \approx \left[\min_j f\big(\{c_j\}\big), \max_j f\big(\{c_j\}\big)\right] \tag{51}$$

In literature, the vertex method is by far the most applied numerical procedure to calculate output sets of interval and fuzzy finite element analyses. Hanss *et al.* [82] formulates a transformation method in order to organise the vertex method such that the fuzzy solution can be efficiently calculated. Despite its simplicity, this method has some disadvantages. It is clear from Eq. (51) that the computational cost increases exponentially with the number of input intervals. This limits the applicability of the vertex method to rather small systems, or systems with few interval uncertainties. The main disadvantage of this method is that it cannot identify local optima of the analysis function which are not on the vertex of the input space. To illustrate this, the vertex method is now applied on the problem stated in Eq. (40) and (41). By substituting the four vertex combinations into the function, we obtain the solutions $\{0, 9, 25, 64\}$, and therefore:

$$\langle y \rangle_{\{\mathbf{x}\}} \approx [0, 64] \tag{52}$$

This means that in this case, the vertex solution is an inner approximation of the actual range of the function as given by the global optimisation solution of Eq. (42). More generally, we can state that the vertex method only results in the smallest hypercube if the analysis function is monotonic over the considered input range. This is a strong condition that is difficult to verify for finite element analysis because of the complicated relation of analysis output to physical input uncertainties. The approximation obtained when monotonicity is not guaranteed is not necessarily conservative. This fact reduces the validity of this method for design validation purposes. Recently, Hanss [83] suggested an extension of the classical vertex procedure in order to deal with this problem of non-monotonicity.

## 4.4 Implementation of the Interval Methodology for Selected Finite Element Analysis Types

### *4.4.1 Static finite element analysis*

In the case of static finite element analysis, the second phase of the interval analysis consists of an equilibrium or steady-state problem. This is numerically equivalent to a matrix equation which requires the solution of a system of equations. Historically, this problem has been addressed most frequently in its interval arithmetic formulation. Using the interval arithmetic approach, the interval matrix problem yields:

$$\big\langle \{y\} \big\rangle = \left\{ \{y\} \mid \Big([A] \in [\mathbf{A}]\Big)\Big(\{b\} \in \{\mathbf{b}\}\Big)\Big([A]\,\{y\} = \{b\}\Big) \right\} \tag{53}$$

with $\{\mathbf{b}\}$ the interval vector representing the uncertain generalised loading of the considered model. This solution set contains all vectors $\{y\}$ which are a solution of the matrix equation $[A]\,\{y\} = \{b\}$ with $[A]$ and $\{b\}$ ranging respectively over the interval objects $[\mathbf{A}]$ and $\{\mathbf{b}\}$. From the world of interval arithmetic, this solution set is referred to as the *united solution set* [84] and denoted by $\Sigma_{\exists\exists}\big([\mathbf{A}], \{\mathbf{b}\}\big)$. In general, the components of this united solution

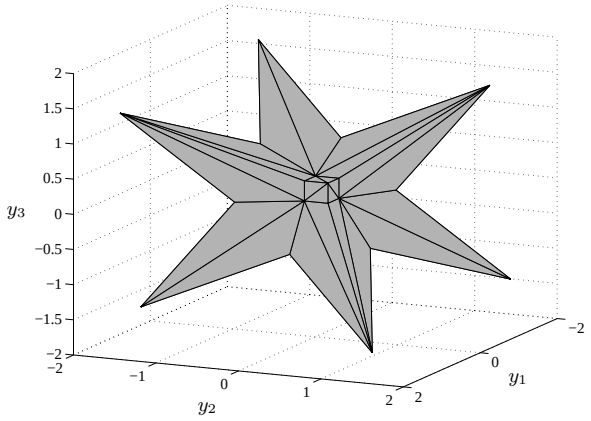


**Figure 16.** Exact output set of a 3D static interval finite element problem

set are related because they result from common interval coefficients in the equations. The exact solution set is described analytically by the Oettli-Prager lemma [85]:

$$\{y\} \in \Sigma_{\exists\exists}\Big([\mathbf{A}], \{\mathbf{b}\}\Big) \Leftrightarrow \Big|\big[\check{\mathbf{A}}\big]\,\{y\} - \big\{\check{\mathbf{b}}\big\}\Big| \leq \big[\bar{\mathbf{A}}\big]\Big|\{y\}\Big| + \big\{\bar{\mathbf{b}}\big\} \tag{54}$$

In order to illustrate the complex form of the united solution set, a simple example is analysed. Consider the following interval system of equations:

$$\begin{bmatrix} 3.5 & [0,2] & [0,2] \\ [0,2] & 3.5 & [0,2] \\ [0,2] & [0,2] & 3.5 \end{bmatrix} \begin{Bmatrix} y_1 \\ y_2 \\ y_3 \end{Bmatrix} = \begin{Bmatrix} [-1,1] \\ [-1,1] \\ [-1,1] \end{Bmatrix} \tag{55}$$

For this problem, the description of the exact united solution set as defined in Eq. (53) is possible using the Oettli-Prager lemma. The inequality in the right-hand side of Eq. (54) defines a polyhedron in the output space. Figure 16 illustrates this polyhedron for this specific case. This figure clearly illustrates the complex nature of the united solution set. This complexity further increases for systems of a higher order. Neumaier [86] shows that the Oettli-Prager lemma is of little use for numerical implementation of a solution procedure for physical relevant structures. Furthermore, it has been shown in literature that any iterative solution scheme which pursues this exact solution set is extremely hard even for small academic problems. Consequently, there is no generally applicable procedure for the exact calculation of the united solution set. Therefore, current research in this domain focusses on the development of efficient calculation procedures of hypercubic approximations of the exact solution set.

Based on the interval arithmetic approach as described in Section 4.2, basically any deterministic procedure that solves the system of equations is a possible candidate for step-by-step translation to an interval procedure. One of the first efforts to give a hypercubic approximation of the united solution set is given by Alefeld *et al.* [87], who derived the interval equivalent of the standard Gaussian elimination scheme. Neumaier [86] formalises and extends the Gaussian approach by preconditioning the interval matrices. However, due to the large number of required interval operations, this method is subject to extreme conservatism as far as realistic finite element models are concerned. More recently, Shary [88, 84] introduced an algebraic approach for the problem. His approach, however, poses strong restrictions on the properties of the interval matrix. These properties are seldom met by a generalised stiffness matrix resulting from a finite element model description.

Rao *et al.* [89] proposes a strategy to limit the large amount of conservatism introduced by the Gaussian approach. It consists of placing a maximum on the width of the intervals in each substep of the algorithm. The truncation threshold is determined based on the width of the input variables. While this is a simple approach, it is a rather artificial and unsafe method to reduce conservatism. Many other approaches have been proposed to approximate the exact united solution set, among which a Taguchi design of experiments based approach [90], an iterative solution based on inclusion method of Rump [91] and interval perturbation analysis [92]. See also Rao *et al.* [89] and McWilliam [93] for an elaborated comparison and numerical examples of some strategies.

Still, as mentioned above, it is imperative to check the conservatism introduced by any method that is based on the interval arithmetic approach. One has to keep in mind that the conservatism of the solution increases with every interval operation. Therefore, the amount of conservatism depends strongly on the chosen algorithm, as clearly demonstrated by Hanss *et al.* [82] comparing the result of the interval equivalent of a finite element analysis using the direct matrix inversion and decomposition technique. Furthermore, it was shown that, even if the smallest hypercube surrounding the united solution set can be calculated, there remains a substantial amount of conservatism due to the matrix assembly phase [94]. This is caused by neglecting the correlation between the entries of the finite element matrices which is generally very high. For instance, an interval on a geometrical uncertainty will affect all matrix entries that relate to this property. Although it is clear that the different matrix entries that are related to a single uncertain model property are strongly coupled, the interval arithmetic approach totally disregards this correlation by posing independent intervals in the matrix. This means that the problem stated in Eq. (53) already incorporates a high amount of conservatism. The only possible remedy for this is to shortcut the matrix assembly by inserting the interval quantities directly as physical properties into the analysis. This can be achieved using either the vertex or the global optimisation approach.

The global optimisation approach requires a solution of the full system for each iteration within the optimisation procedure. This can become an extremely expensive task, especially for large models. Furthermore, the optimisation has to be repeated for each individual output quantity (nodal displacement, reaction force) the analyst is interested in. Therefore, the vertex analysis is far more popular in current literature on interval finite element solution strategies. However, it is important to stress that the validity of the vertex analysis results relies entirely on the response quantity having a monotonic relationship with respect to the input uncertainties. This is very hard to check, and certainly not generally true for static analysis. Therefore, vertex results of static interval finite element problems should always be interpreted with caution.

#### *4.4.2 Eigenvalue analysis*

The deterministic procedure of the finite element eigenvalue analysis consists of the assembly of the system stiffness and mass matrices $[K]$ and $[M]$, after which the deterministic eigenvalue $\lambda_i$ satisfies the equation:

$$[K]\{\phi_i\} = \lambda_i [M]\{\phi_i\} \tag{56}$$

with $\{\phi_i\}$ the corresponding eigenvector. In the corresponding interval procedure, the aim is to calculate the bounds on specific eigenfrequencies, given that the uncertain parameters are within their defined ranges $\{\mathbf{x}\}$. Using the function $\Lambda_i^x$:

$$\lambda_i = \Lambda_i^x(\{x\}) \tag{57}$$

which explicitly relates the eigenvalue to the uncertain input parameters, the solution set of the interval problem can be written as $\langle \Lambda_i^x \rangle_{\{\mathbf{x}\}}$.

The equivalent interval arithmetic interval finite element procedure requires the calculation of the solution set:

$$\left\{\lambda_i \mid \Big([K] \in [\mathbf{K}]\Big)\Big([M] \in [\mathbf{M}]\Big)\Big([K]\{\phi_i\} = \lambda_i [M]\{\phi_i\}\Big)\right\} \tag{58}$$

with $[K]$ and $[M]$ incorporating implicitly the dependency of the system matrices on the input parameters. Condensing Eq. (56) to an explicit function of the system matrices:

$$\lambda_i = \Lambda_i^{KM}([K], [M]) \tag{59}$$

the solution set of Eq. (58) is rewritten as:

$$\left\langle \Lambda_i^{KM} \right\rangle_{[\mathbf{K}][\mathbf{M}]} \tag{60}$$

It can be shown that, assuming independent interval system matrices, the exact bounds of this solution set are achieved for vertex matrix combinations [95]. This means that, based on the assumption that all interval entries appearing in the system matrices are independent, the exact solution of the interval eigenvalue problem can be found. Some algorithms have been developed which efficiently calculate this exact vertex solution of the interval eigenvalue problem. Chen *et al.* [95] introduced a non-iterative procedure based on the Rayleigh quotient, which states that the lower and upper bound on the $i^{th}$ eigenvalue follow directly from two deterministic eigenvalue problems:

$$\left(\left[\check{\mathbf{K}}\right] + \left[S^i\right]\left[\bar{\mathbf{K}}\right]\left[S^i\right]\right)\{\overline{\phi_i}\} = \overline{\lambda_i}\left(\left[\check{\mathbf{M}}\right] - \left[S^i\right]\left[\bar{\mathbf{M}}\right]\left[S^i\right]\right)\{\overline{\phi_i}\} \tag{61}$$

$$\left(\left[\check{\mathbf{K}}\right] - \left[S^i\right]\left[\bar{\mathbf{K}}\right]\left[S^i\right]\right)\{\underline{\phi_i}\} = \underline{\lambda_i}\left(\left[\check{\mathbf{M}}\right] + \left[S^i\right]\left[\bar{\mathbf{M}}\right]\left[S^i\right]\right)\{\underline{\phi_i}\} \tag{62}$$

with $\left[S^i\right] = \mathrm{diag}\left(\mathrm{sgn}(\phi_i^1), \ldots \mathrm{sgn}(\phi_i^n)\right)$ and $\{\phi_i\}$ the $i^{th}$ eigenvector from the deterministic analysis at the midpoints of the matrices. This method requires all the components of the eigenvector to have a constant sign over the considered domain and does not allow the occurrence of an eigenfrequency cross-over in the input parameter space. An enhanced methodology was developed by El-Gebeily *et al.* [96]. It provides a solution for the original problem with an extra restriction of symmetry on the considered system matrices:

$$\left\{\lambda_i \mid \Big([K_s] \in [\mathbf{K}]\Big)\Big([M_s] \in [\mathbf{M}]\Big)\Big([K_s]\{\phi_i\} = \lambda_i [M_s]\{\phi_i\}\Big)\right\} \tag{63}$$

with $K_s$ and $M_s$ symmetric. The most important effect of this extra restriction is that it intrinsically removes the conservatism resulting from allowing artificial non-symmetric system matrices. The numerical procedure is based on the interval translation of the deterministic Sturm sequence. It proves to be an efficient iterative algorithm. Unfortunately, it is limited to tridiagonal system matrices. This makes it only applicable for specific cases.

Currently, a number of research activities aiming at approximating the solution of the problem stated in Eq.(58) are still ongoing. Chen *et al.* [97] proposed a method based on an interval perturbation strategy. More recently, Qiu *et al.* [98] introduced a procedure for the calculation of interval eigenvalues based on a non-negative decomposition of the stiffness and mass matrices. However, similar as for the interval arithmetic approach for static problems discussed in Section 4.4.1, also here there is a substantial amount of conservatism incorporated in the interval matrix problem stated in Eq.(58) since the entries of the system matrices are implicitly decoupled. Furthermore, in this case, there is an additional source of conservatism due to the independent treatment of the mass and stiffness matrices.

These matrices indeed could be strongly mutually related, for instance when geometrical uncertainties are considered. Again, neglecting this coupling can introduce a severe overestimation in the obtained interval eigenvalue results, as also illustrated in [94]. Therefore, we have:

$$\langle \Lambda_i^x \rangle_{\{\mathbf{x}\}} \subseteq \langle \Lambda_i^{KM} \rangle_{[\mathbf{K}][\mathbf{M}]} \tag{64}$$

The exact amount of this conservatism is strongly problem-dependent. Therefore, it is very difficult to assess the results obtained from the interval matrix problem, no matter how close the exact solution set is approximated.

When applying the vertex approach to remedy the conservatism, again it should be verified whether the eigenvalues have a monotonic behaviour over the interval input space. Although this is generally the case, it is very hard to check this condition. The global optimisation approach on the other hand comes down to a minimisation and maximisation for each considered eigenfrequency:

$$\langle \Lambda_i^x \rangle_{\{\mathbf{x}\}} = \left[ \min_{\{x\} \in \{\mathbf{x}\}} \left( \Lambda_i^x(\{x\}) \right), \max_{\{x\} \in \{\mathbf{x}\}} \left( \Lambda_i^x(\{x\}) \right) \right] \tag{65}$$

The main advantage of the optimisation strategy is that it returns the exact range of the eigenvalues without any conservatism if performed successfully. Any numerical optimisation algorithm can be used to do this optimisation. The performance of most optimisation algorithms increases substantially when analytical expressions are available for the derivatives of the goal function to the design parameters. For the eigenvalue optimisation, these derivatives can be calculated analytically based on the system matrices derivatives [99]:

$$\frac{\partial \lambda_i}{\partial x_j} = \frac{\{\phi_i\}^T \left( \frac{\partial [K]}{\partial x_j} - \lambda_i \frac{\partial [M]}{\partial x_j} \right) \{\phi_i\}}{\{\phi_i\}^T M \{\phi_i\}} \tag{66}$$

Accordingly, the optimisation approach for interval eigenvalue analysis generally is not computationally expensive when the system matrices derivatives are known. But also when the derivatives have to be approximated numerically, generally a good convergence is observed. The numerical efficiency combined with the total absence of conservatism in the obtained results make the optimisation approach by far the most interesting for interval eigenvalue analysis.

## 5 A NOVEL APPROACH FOR INTERVAL FREQUENCY RESPONSE FUNCTION ANALYSIS

Different experimental studies show that the variability of physical properties of nominally identical structures can cause a large variability in the frequency response function [100, 101]. This substantially influences the predictive quality of deterministic numerical frequency response function analyses of these structures. There have been some attempts to study the scatter on the frequency response function in a probabilistic way. Worden [102] derives confidence bounds on the response function using a Monte Carlo simulation approach. Next to the fact that this procedure is computationally very expensive, the calculated probabilistic characteristics of the response proves to be very sensitive to variations in the probabilistic data used at the input of the problem. This stresses the necessity of the use of trustworthy probabilistic input data and encourages the use of alternative uncertainty models when incomplete knowledge is present. Therefore, the development of an alternative non-deterministic frequency response function analysis method based on the interval uncertainty representation embodies a very useful extension of the interval finite element analysis capabilities.

In order to achieve this, a new hybrid solution strategy is first introduced. This strategy combines the global optimisation approach with the interval arithmetic approach. The basic principle of this procedure is described and illustrated on an example in Section 5.1. Section 5.2 then shows how this hybrid strategy can be usefully applied to calculate the envelope frequency response function of an interval finite element model through the modal superposition principle.

### 5.1 A Hybrid Approach for the Interval Finite Element Implementation

In limited cases, a possible remedy to the conservatism in an interval arithmetic procedure is to perform as much as possible of the deterministic procedure analytically. The goal is to obtain an analytical description of some intermediate result in the algorithm, expressing the parametric dependency of this intermediate result to the uncertain model properties. By substituting the intervals in the obtained parametric expression, all sources of conservatism which occur before the point in the algorithm where the intermediate result occurs will be neutralised. Computing local element matrices of simple elements based on the analytical description rather than a numerical integration is an elementary illustration of this principle in the framework of the interval finite element analysis. For instance, for a bar element in a two-dimensional finite element analysis, the analytical description of the stiffness matrix in the local coordinate system yields:

$$[K^e_{local}] = \frac{EI}{L^3} \begin{bmatrix} 12 & 6L & -12 & 6L \\ 6L & 4L^2 & -6L & 2L^2 \\ -12 & -6L & 12 & -6L \\ 6L & 2L^2 & -6L & 4L^2 \end{bmatrix} \tag{67}$$

Interval uncertainties defined on the element properties appearing in this matrix now can be directly substituted in this analytic expression. The main advantage of this approach is that intervals on properties that are brought outside the matrix now no longer introduce conservatism through a decoupling of the matrix entries.

A possible extension of this strategy is to perform both the deterministic element matrix calculation and the total system matrix assembly analytically. This enables a similar procedure as described on the element level for global properties which can be brought outside the total system matrices. This approach was introduced by Enling [103] and later used by Dessombz *et al.* [91] to decrease the conservatism resulting from a globally defined uncertain Young's modulus. Mullen *et al.* [42] used a method based on an analytical description to introduce uncertainty on the load vector in the final step of an algorithm. While it is theoretically exact, this parametric approach is limited to small models with uncertain parameters that allow for a parametrical expression of the system matrix.

In order to extend the applicability of the interval finite element method, a more generally applicable remedy to excessive conservatism is derived from this principle. Instead of a partial analytical procedure, it consists of a partial optimisation in the first part of the analysis. This means that an optimisation is applied to calculate the interval result at some intermediate step of the total algorithm. In the second part, the interval analysis is performed on these intermediate results.

This method has two major advantages:

- because of the global optimisation, all conservatism prior to the optimised intermediate result is neutralised
- the performance of the optimisation step is controllable by adequately choosing the level on which to perform it

| **deterministic algorithm** | **interval arithmetic algorithm** | **hybrid algorithm** |
|---|---|---|
| $z_{11} = x_1 + x_2$<br>$z_{12} = x_1 - x_2$ | $\langle z_{11} \rangle_{\{\mathbf{x}\}} = [-3, 5]$<br>$\langle z_{12} \rangle_{\{\mathbf{x}\}} = [-4, 4]$ | |
| $z_2 = z_{11} \times z_{12}$ | $\langle\!\langle z_2 \rangle\!\rangle_{\{\mathbf{x}\}} = [-20, 20]$ | $\langle z_2 \rangle_{\{\mathbf{x}\}} = [-9, 4]$ |
| $y = z_2 \times z_2$ | $\langle\!\langle y \rangle\!\rangle_{\{\mathbf{x}\}} = [-400, 400]$ | $\langle\!\langle y \rangle\!\rangle_{\{\mathbf{x}\}} = [-36, 81]$ |

**Figure 17.** Comparison of the interval arithmetic and hybrid approach for the approximation of the result of an interval problem

The effect of the hybrid approach can be illustrated using the simple numerical example of Eq. (40) and (41). Figure 17 gives the deterministic algorithm and the pure interval arithmetic solution sequence as discussed in Section 4.2. It also describes the solution of the same problem using the hybrid procedure with an optimisation performed on the result $z_2$ of the second substep of the deterministic algorithm. This optimisation is mathematically expressed as:

$$\langle z_2 \rangle_{\{\mathbf{x}\}} = \left[ \min_{\{x\} \in \{\mathbf{x}\}} \left( x_1^2 - x_2^2 \right), \max_{\{x\} \in \{\mathbf{x}\}} \left( x_1^2 - x_2^2 \right) \right] \tag{68}$$

The hybrid approach clearly results in a substantial improvement of the conservative result approximation compared to the pure interval arithmetic approach.

Section 5.2 now illustrates how this hybrid procedure can be of use in the context of an interval finite element frequency response function analysis. In the first part of this procedure, the optimisation is used to translate the interval input parameter space to the exact ranges of the modal stiffness and mass parameters of the structure. The calculation of the envelope frequency response functions in the second part is done by applying the interval arithmetic equivalent of the modal superposition procedure on these interval modal parameters. This procedure neutralises all conservatism in the matrix assembly phase, since it directly uses the modal parameters as goal functions in the optimisation part.

### 5.2 Hybrid Envelope Frequency Response Function Calculation

The frequency response function between DOF $j$ and DOF $k$ of a finite element model is obtained taking the $j^{th}$ component of $\{X\}$ satisfying the dynamic equilibrium equation of undamped structures:

$$\left( [K] - \omega^2 [M] \right) \{X\} = \left\{ F^k \right\} \tag{69}$$

with

$$F_i^k = \begin{cases} 1 \text{ for } i = k \\ 0 \; \forall \, i \neq k \end{cases} \tag{70}$$

The basic problem of the envelope frequency response function procedure is the calculation of the range of the $j^{th}$ component of the response vector taking into account the interval ranges of the non-deterministic model properties in the interval vector $\{\mathbf{x}\}$:

$$\langle X_j \rangle = \left\{ X_j \mid \Big( \{x\} \in \{\mathbf{x}\} \Big) \Big( \left( [K] - \omega^2 [M] \right) \{X\} = \left\{ F^k \right\} \Big) \right\} \tag{71}$$

with $[K]$ and $[M]$ incorporating implicitly the dependency of the system matrices to the input parameters. Although this solution set consists of only one component of the response vector, its exact calculation is not straightforward. The solution set is clearly a function of the frequency $\omega$. Therefore, the most straightforward solution strategy is to calculate this set at a large number of discrete frequency lines in the considered frequency domain. The corresponding algorithm consists of a sequence of interval finite element problems defined on the deterministic linear systems of equations resulting from substituting discrete values for the frequency $\omega$ in Eq. (69).

The translation of the deterministic frequency response function procedure to interval arithmetics requires the solution of a sequence of interval systems of equations. As discussed in Section 4.4.1, there exists no generally applicable exact solution procedure for this problem. Furthermore, the approximate solution procedures are all computationally expensive and certainly not suited for application in a procedure that requires an iteration of interval solutions at a large number of discrete frequencies. On the other hand, also the application of the global optimisation strategy in this case is not advisable, since it requires two global optimisations at a high number of discrete frequencies in order to have a global view on the total envelope function. Clearly, the optimisation procedure for this analysis becomes excessively expensive. Finally, also the vertex approach is not very appropriate in this case. Since the response result generally is a highly non-linear function of the input parameters, the response limits taken from the set of vertex results will generally not coincide with the global interval bounds. Furthermore, the error on the vertex approximation is very difficult to estimate. To conclude, neither the vertex, nor the optimisation nor the interval arithmetic approach appear to be suited to solve the envelope frequency response function problem. All are computationally expensive and in the end they do not guarantee a useful result.

This conclusion leads to the application of the hybrid approach described in Section 5.1. In order to apply this principle, a suitable algorithm has to be selected, i.e., an algorithm exhibiting intermediate analysis results that are appropriate for a global optimisation procedure. The modal superposition procedure has been selected for this purpose. Section 5.2.1 first briefly summarises the classical deterministic form of this algorithm, after which Section 5.2.2 describes how it is translated to an interval procedure for the analysis of undamped structures. Sections 5.2.3 and 5.2.4 give two enhancements of the basic algorithm, both aiming at a reduction of the conservatism. Finally, Section 5.2.5 describes how the method can be extended to damped response analysis.

#### *5.2.1 The deterministic modal superposition procedure*

The modal superposition principle is easily derived from the basic dynamic equilibrium Eq. (69) using the eigenvectors resulting from a preliminary eigenvalue analysis on the system. The eigenvectors are assembled in a matrix $[\Phi] = [\{\phi_1\}, \{\phi_2\}, \ldots \{\phi_n\}]$. After premultiplying both the left- and right-hand side of Eq. (69) with $[\Phi]^T$ and substituting $\{X\}$ with $[\Phi]\{Y\}$, the equation becomes:

$$[\Phi]^T \left( [K] - \omega^2 [M] \right) [\Phi] \ \{Y\} = [\Phi]^T \left\{ F^k \right\} \tag{72}$$

Due to the orthogonality of the eigenvectors, the matrix on the left-hand side is a diagonal matrix for every frequency value. Using the definition of Eq. (70) for $\left\{F^k\right\}$ in the right-hand side of this equation, the components of the vector $\{Y\}$ yield:

$$Y_i = \frac{\phi_{ik}}{\{\phi_i\}^T [K] \{\phi_i\} - \omega^2 \{\phi_i\}^T [M] \{\phi_i\}} \tag{73}$$

with $\phi_{ik}$ the $k^{th}$ component of the $i^{th}$ eigenvector. Introducing these components of $\{Y\}$ in $\{X\} = [\Phi]\{Y\}$, the $j^{th}$ component of the vector $\{X\}$ equals:

$$X_j = \sum_{i=1}^{n} \frac{\phi_{ij}\ \phi_{ik}}{\{\phi_i\}^T [K] \{\phi_i\} - \omega^2 \{\phi_i\}^T [M] \{\phi_i\}} \tag{74}$$

According to the definition, this last expression equals the frequency response function between DOFs $j$ and $k$ of the model. It is a function of $\omega$ and will be referred to as $FRF_{jk}$. Equation (74) is easily rewritten as:

$$FRF_{jk} = \sum_{i=1}^{n} \frac{1}{\hat{k}_i - \omega^2 \hat{m}_i} \tag{75}$$

$$= \sum_{i=1}^{n} FRF_{jk}^{i} \tag{76}$$

with $FRF_{jk}^{i}$ the $i^{th}$ modal frequency response function and $\hat{k}_i$ and $\hat{m}_i$ the normalised modal parameters:

$$\hat{k}_i = \frac{\{\phi_i\}^T [K] \{\phi_i\}}{\phi_{ij}\ \phi_{ik}} \tag{77}$$

$$\hat{m}_i = \frac{\{\phi_i\}^T [M] \{\phi_i\}}{\phi_{ij}\ \phi_{ik}} \tag{78}$$

The main advantages of this approach over the direct formulation as in Eq. (69) are that the complete frequency domain is processed simultaneously, and that the computational effort can be limited by only incorporating the modes within the frequency domain of interest. Furthermore, the appearance of the modal mass and stiffness parameters as intermediate results in the analysis makes this algorithm very appropriate for the application of the hybrid approach.

#### *5.2.2 Hybrid implementation of the envelope frequency response function analysis*

The modal superposition procedure as described above can be divided in three consecutive steps:

1. the calculation of the modal mass and stiffness parameters $\hat{k}_i$ en $\hat{m}_i$ for each mode taken into consideration
2. the calculation of the modal response contributions $FRF_{jk}^{i}$
3. the summation of all considered modal contributions

The hybrid approach now is applied on this procedure, taking the modal parameters as intermediate results. This means that the exact ranges of the modal parameters of each mode will be calculated using a global optimisation approach, resulting in:

$$\left\langle \hat{k}_i \right\rangle_{\{\mathbf{x}\}} = \left\{ \hat{k}_i \mid \Big( \{x\} \in \{\mathbf{x}\} \Big) \left( \hat{k}_i = \frac{\{\phi_i\}^T [K] \{\phi_i\}}{\phi_{ij}\ \phi_{ik}} \right) \right\} \tag{79}$$

$$\langle \hat{m}_i \rangle_{\{\mathbf{x}\}} = \left\{ \hat{m}_i \mid \Big( \{x\} \in \{\mathbf{x}\} \Big) \left( \hat{m}_i = \frac{\{\phi_i\}^T [M] \{\phi_i\}}{\phi_{ij}\ \phi_{ik}} \right) \right\} \tag{80}$$

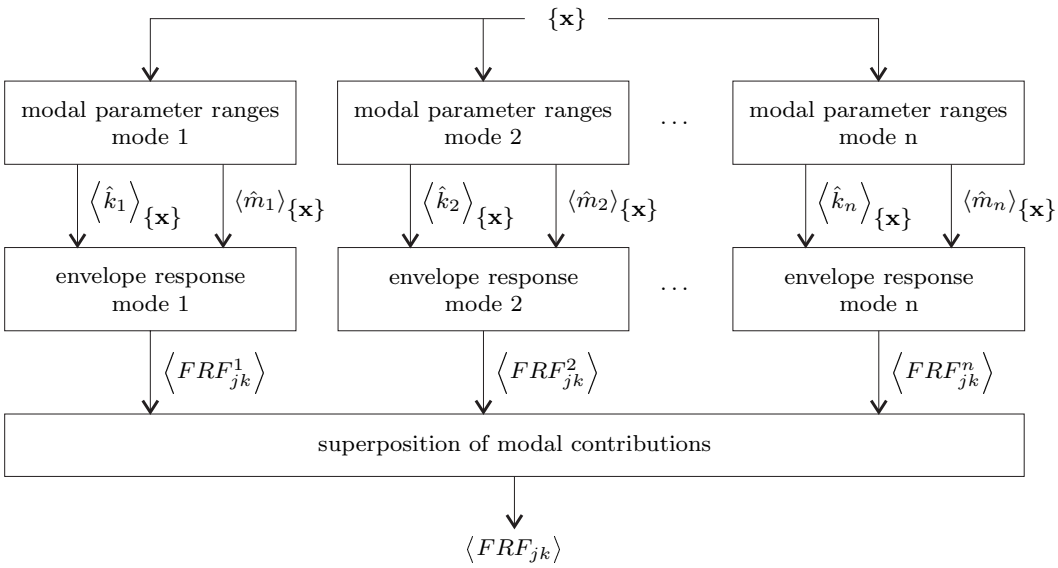


**Figure 18.** Scheme of the interval procedure resulting from applying the hybrid approach to the modal superposition algorithm

The modal parameters ranges then are used to calculate the response ranges of the modal contributions based on an interval arithmetic procedure. Finally, also the superposition is performed using an interval arithmetic summation of the modal envelope response functions from the previous step. Figure 18 summarises this procedure.

Since the optimisation is performed on the modal parameters, all sources of conservatism that would appear prior to this point are neutralised. This includes the generally non-negligible conservatism implicitly contained in the interval system matrices assembly phase. On the other side, this means that the system matrices will have to be assembled for each goal function evaluation. The remainder of this section now briefly summarises the most important aspects of the three consecutive steps of this procedure.

### Step 1: Modal parameter ranges

The first step of the procedure consists of the calculation of the modal parameter ranges $\left\langle \hat{k}_i \right\rangle_{\{\mathbf{x}\}}$ and $\langle \hat{m}_i \rangle_{\{\mathbf{x}\}}$. An optimisation directly on the modal parameters, however, is not possible because the expressions for the modal parameters given in Eq. (77) and Eq. (78) can become singular if one of the modal vector components $\phi_{ij}$ or $\phi_{ik}$ equals zero within the optimisation domain. However, based on their definitions of Eq. (77) and Eq. (78), it is easily shown that the inverse of the modal parameters will always have a continuous behaviour with respect to physical model parameters. Therefore, the optimisation will be performed on the inverted modal parameters. Using the mass and stiffness normalised modal vectors, this yields:

$$\hat{\mathbf{k}}_{\mathbf{i}}^{-\mathbf{1}} = \left[ \min_{\{x\} \in \{\mathbf{x}\}} \left( \phi_{ij}^K \phi_{ik}^K \right), \max_{\{x\} \in \{\mathbf{x}\}} \left( \phi_{ij}^K \phi_{ik}^K \right) \right] \tag{81}$$

$$\hat{\mathbf{m}}_{\mathbf{i}}^{-\mathbf{1}} = \left[ \min_{\{x\} \in \{\mathbf{x}\}} \left( \phi_{ij}^M \phi_{ik}^M \right), \max_{\{x\} \in \{\mathbf{x}\}} \left( \phi_{ij}^M \phi_{ik}^M \right) \right] \tag{82}$$

with

$$\left\{\phi_i^K\right\}^T [K] \left\{\phi_i^K\right\} = 1 \tag{83}$$

$$\left\{\phi_i^M\right\}^T [M] \left\{\phi_i^M\right\} = 1 \tag{84}$$

The result of the optimisation could be a completely positive or completely negative interval, or an interval ranging over zero if one of the eigenvector components reaches zero inside the parameter space. Because of the possible inclusion of zero in the optimisation result, the modal parameter range is obtained using the KAHAN inversion [104]:

$$\left\langle \hat{k}_i \right\rangle_{\{\mathbf{x}\}} = K^{-1}\left(\hat{\mathbf{k}}_\mathbf{i}^{-\mathbf{1}}\right) \tag{85}$$

$$\langle \hat{m}_i \rangle_{\{\mathbf{x}\}} = K^{-1}\left(\hat{\mathbf{m}}_\mathbf{i}^{-\mathbf{1}}\right) \tag{86}$$

The result of this KAHAN inversion is either a single interval with a constant sign or the union of a positive and negative interval including respectively plus and minus infinity. A mode for which the range of both normalised modal parameters $\hat{k}_i$ and $\hat{m}_i$ is entirely positive or negative is referred to as a *positive* respectively *negative* mode. A mode the modal parameters of which range over infinity is referred to as a *switch* mode. The result of this part of the total algorithm is summarised as follows:

$$\left\langle \hat{k}_i \right\rangle_{\{\mathbf{x}\}} = \left[ \frac{1}{\overline{\hat{k}_i^{-1}}}, \frac{1}{\underline{\hat{k}_i^{-1}}} \right] \tag{87}$$

$$\langle \hat{m}_i \rangle_{\{\mathbf{x}\}} = \left[ \frac{1}{\overline{\hat{m}_i^{-1}}}, \frac{1}{\underline{\hat{m}_i^{-1}}} \right] \tag{88}$$

for positive and negative modes, and:

$$\begin{aligned} \left\langle \hat{k}_i \right\rangle_{\{\mathbf{x}\}} &= \left[ -\infty, \frac{1}{\underline{\hat{k}_i^{-1}}} \right] \cup \left[ \frac{1}{\overline{\hat{k}_i^{-1}}}, +\infty \right] \\ &= \left\langle \hat{k}_i \right\rangle_{\{\mathbf{x}\}}^{-} \cup \left\langle \hat{k}_i \right\rangle_{\{\mathbf{x}\}}^{+} \end{aligned} \tag{89}$$

$$\begin{aligned} \langle \hat{m}_i \rangle_{\{\mathbf{x}\}} &= \left[ -\infty, \frac{1}{\underline{\hat{m}_i^{-1}}} \right] \cup \left[ \frac{1}{\overline{\hat{m}_i^{-1}}}, +\infty \right] \\ &= \langle \hat{m}_i \rangle_{\{\mathbf{x}\}}^{-} \cup \langle \hat{m}_i \rangle_{\{\mathbf{x}\}}^{+} \end{aligned} \tag{90}$$

for switch modes.

For the further development of the algorithm, the modal parameter ranges are combined in a set vector for each mode:

$$\left\langle \{\hat{p}_i\} \right\rangle = \left\{ \begin{array}{c} \left\langle \hat{k}_i \right\rangle_{\{\mathbf{x}\}} \\ \langle \hat{m}_i \rangle_{\{\mathbf{x}\}} \end{array} \right\} \tag{91}$$

For a positive or negative mode, this is an interval vector which represents a rectangle in the $\left(\hat{k}_i, \hat{m}_i\right)$-space. Therefore, this algorithm is referred to as the *Modal Rectangle* method (MR).

**Step 2: Modal envelope frequency response function**

The requested output of this step of the algorithm is the range of the modal response function $FRF^i_{jk}$ taking into account the range of the modal parameters in the vector $\langle\{\hat{p}_i\}\rangle$:

$$\left\langle FRF^i_{jk}\right\rangle_{\langle\{\hat{p}_i\}\rangle} = \left\{ \frac{1}{\hat{k}_i - \omega^2 \hat{m}_i} \mid \left(\hat{k}_i \in \left\langle \hat{k}_i \right\rangle_{\{\mathbf{x}\}}\right)\left(\hat{m}_i \in \langle \hat{m}_i \rangle_{\{\mathbf{x}\}}\right) \right\} \tag{92}$$

This step of the algorithm aims at the calculation of the modal envelope response function in a continuous frequency domain. This means that it does not consider discrete frequency values, but calculates the function range for the complete frequency range in one step. The procedure consists of the calculation of the function range of the denominator of the modal response contribution:

$$\mathcal{D}(\omega) = (\hat{k}_i - \omega^2 \hat{m}_i) \tag{93}$$

The range of this function then is inverted in order to obtain the actual modal envelope response function. The procedure differs for switch modes and positive or negative modes.

For switch modes, it is immediately clear that any value can be obtained in the denominator function using only the positive modal parameter ranges $\left\langle \hat{k}_i \right\rangle^+_{\{\mathbf{x}\}}$ and $\langle \hat{m}_i \rangle^+_{\{\mathbf{x}\}}$ since both vary from a finite value to infinity. In other words, the modal response denominator function range equals $[-\infty, +\infty]$ over the entire frequency domain. Therefore, also after inversion of the denominator, a switch mode's response function ranges over the entire domain of real values.

For positive and negative modes, the modal parameter ranges form an interval, and, therefore, the modal response denominator function range is easily derived from the bounds on these intervals. For the entire frequency domain, the range of the denominator $\mathcal{D}(\omega)$ equals:

$$\langle \mathcal{D}(\omega) \rangle_{\langle\{\hat{p}_i\}\rangle} = \left[ \underline{\hat{k}_i} - \omega^2 \overline{\hat{m}_i},\ \overline{\hat{k}_i} - \omega^2 \underline{\hat{m}_i} \right] \tag{94}$$

This modal response denominator function range is an interval for every frequency in the frequency domain. This interval contains zero for frequencies within the interval $\boldsymbol{\omega_0}$ with:

$$\boldsymbol{\omega_0} = \begin{cases} \left[ \sqrt{\underline{\hat{k}_i}/\overline{\hat{m}_i}},\ \sqrt{\overline{\hat{k}_i}/\underline{\hat{m}_i}} \right] & \text{for positive modes} \\ \left[ \sqrt{\overline{\hat{k}_i}/\underline{\hat{m}_i}},\ \sqrt{\underline{\hat{k}_i}/\overline{\hat{m}_i}} \right] & \text{for negative modes} \end{cases} \tag{95}$$

This means that the KAHAN inversion is required to invert the modal response denominator function range of Eq. (94):

$$\left\langle FRF^i_{jk}\right\rangle_{\langle\{\hat{p}_i\}\rangle} = \begin{cases} \left[ \underline{\underline{FRF^i_{jk}}}, \overline{\overline{FRF^i_{jk}}} \right] & \forall\, \omega \notin \boldsymbol{\omega_0} \\ \left[ -\infty, \overline{\overline{FRF^i_{jk}}} \right] \cup \left[ \underline{\underline{FRF^i_{jk}}}, +\infty \right] & \forall\, \omega \in \boldsymbol{\omega_0} \end{cases} \tag{96}$$

with

$$\underline{\underline{FRF^i_{jk}}} = \frac{1}{\overline{\hat{k}_i} - \omega^2 \underline{\hat{m}_i}} \tag{97}$$

$$\overline{\overline{FRF^i_{jk}}} = \frac{1}{\underline{\hat{k}_i} - \omega^2 \overline{\hat{m}_i}} \tag{98}$$

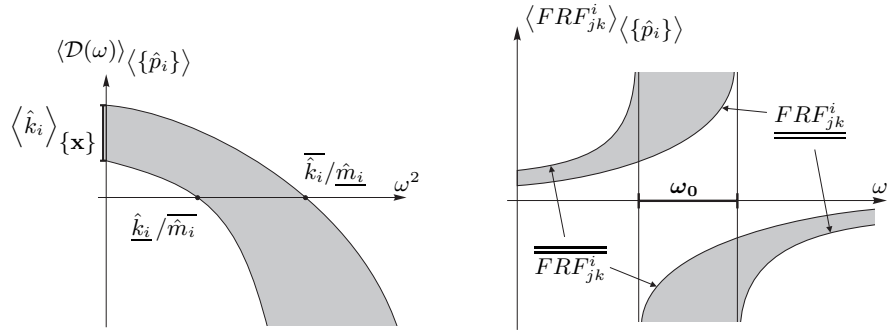


(a) Denominator function range (b) Modal envelope FRF

**Figure 19.** Modal denominator function range and response function envelope using the MR strategy

The double under and over score indicate that the modal envelope response functions constructed in this step are conservative approximations of the actual modal envelope response functions with respect to the input parameters. Figure 19 illustrates the result of the denominator inversion in the frequency domain. This figure demonstrates that the obtained modal envelope response function has the basic form of a deterministic modal frequency response function with some scatter added to the response value at every frequency. From this observation it is also clear that the interval $\boldsymbol{\omega_0}$ contains the eigenfrequencies which correspond to all modal response functions which compose the obtained modal envelope response function. Consequently, the $\boldsymbol{\omega_0}$ intervals obtained through this procedure are conservative approximations of the actual eigenfrequency ranges with respect to the model parameter input space.

**Step 3: Total envelope frequency response function**

The final step for the computation of the total envelope frequency response function consists of the summation of all modal envelope frequency response functions resulting from the previous step. The required result is formulated as:

$$\langle FRF_{jk} \rangle_{\left\langle \left\{ FRF^i_{jk} \right\} \right\rangle} = \left\{ \sum_{i=1}^{n} FRF^i_{jk} \mid \left( FRF^i_{jk} \in \left\langle FRF^i_{jk} \right\rangle_{\langle \{\hat{p}_i\} \rangle}, \forall i \right) \right\} \tag{99}$$

The range of the modal envelope frequency response function of switch modes is the entire domain of real values. This means that including a switch mode's contribution in the summation causes the total envelope frequency response function to range over the entire domain of real values at every frequency, which of course renders the result useless. Therefore, an important restriction of the modal rectangle method is that no switch modes should appear within the model input parameter space. This fairly strong restriction will be addressed in Section 5.2.3.

For positive and negative modes, the response range differs for frequencies within and outside $\boldsymbol{\omega_0}$ as indicated in Eq. (96). Therefore, the summation distinguishes between three subcases:

- for frequencies outside the $\boldsymbol{\omega_0}$ interval of every mode, the range of all terms in the summation is an interval:

$$\langle FRF_{jk} \rangle_{\left\langle \left\{ FRF^i_{jk} \right\} \right\rangle} = \left[ \sum_{i=1}^{n} \underline{\underline{FRF^i_{jk}}}, \sum_{i=1}^{n} \overline{\overline{FRF^i_{jk}}} \right] \tag{100}$$

- for frequencies inside exactly one $\boldsymbol{\omega_0}$ interval, one term in the summation is the union of two disjoint intervals over infinity:

$$\langle FRF_{jk} \rangle \left\langle \left\{ FRF^i_{jk} \right\} \right\rangle = \left[ -\infty, \sum_{i=1}^{n} \overline{\overline{FRF^i_{jk}}} \right] \cup \left[ \sum_{i=1}^{n} \underline{\underline{FRF^i_{jk}}}, +\infty \right] \tag{101}$$

- for frequencies inside more than one $\boldsymbol{\omega_0}$ interval, two or more terms are the union of two disjoint intervals over infinity:

$$\langle FRF_{jk} \rangle \left\langle \left\{ FRF^i_{jk} \right\} \right\rangle = [-\infty, +\infty] \tag{102}$$

#### *5.2.3 The modal rectangle method with eigenvalue interval correction*

The main shortcomings of the modal rectangle method are:

- the real eigenfrequency intervals do not show up in the final envelope frequency response function result
- switch modes are not allowed, which is equivalent to stating that none of the mode shapes of the modes used in the superposition is allowed to have a node in the input or output DOF of the considered frequency response function somewhere in the input parameter space
- the conservatism on the modal parameter level is high when there is a high correlation between the modal parameters through the input parameters

This section shows how the modal rectangle methodology can be enhanced in order to cope with these shortcomings.

A first enhancement is accomplished by the introduction of the exact eigenvalue bounds in the modal rectangle method. The effect of adding these eigenvalue bounds to the procedure is best illustrated by considering the two-dimensional modal space of each mode. In this $\left(\hat{k}_i, \hat{m}_i\right)$-space of each mode, the model interval uncertainties $\{\mathbf{x}\}$ define a domain of feasible modal parameter combinations:

$$\langle \hat{k}_i, \hat{m}_i \rangle = \left\{ \left( \hat{k}_i, \hat{m}_i \right) \mid \left( \{x\} \in \{\mathbf{x}\} \right) \right\} \tag{103}$$

This exact domain, however, is not known. The modal rectangle method as described in Section 5.2.2 computes the modal parameter ranges independently, resulting in an approximate rectangle for the $\langle \hat{k}_i, \hat{m}_i \rangle$-domain, as illustrated in Figure 20.

The bounds on the eigenvalues $\underline{\lambda_i}$ and $\overline{\lambda_i}$ now introduce additional mathematical limits for the modal parameters, since they state:

$$\underline{\lambda_i} \leq \frac{\hat{k}_i}{\hat{m}_i} \leq \overline{\lambda_i} \tag{104}$$

This inequality corresponds to two extra delimiters for the $\langle \hat{k}_i, \hat{m}_i \rangle$-domain approximation in the modal space, as illustrated in Figures 21.

This enhanced $\langle \hat{k}_i, \hat{m}_i \rangle$-approximation is referred to as the *Modal Rectangle with Eigenvalue interval correction* (MRE), and forms the basis of an enhanced modal envelope response function calculation. Figure 22 summarises the resulting algorithm.

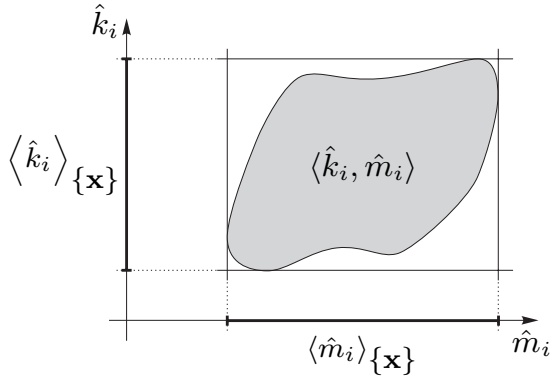


**Figure 20.** Illustration of the actual $\langle \hat{k}_i, \hat{m}_i \rangle$-domain (grey) and its rectangular approximation through independent optimisatoin of the modal stiffness and mass parameters

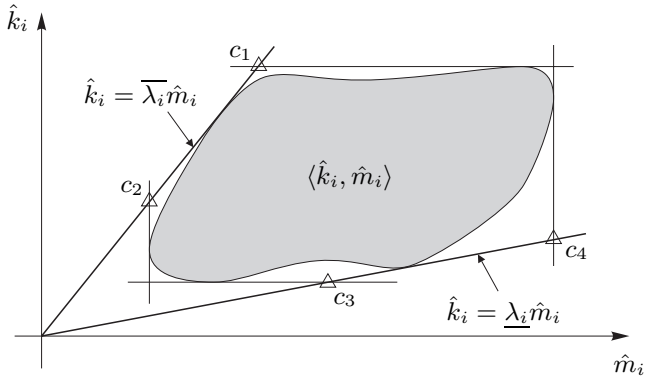


**Figure 21.** Effect of the addition of the exact eigenvalue bounds to the $\langle \hat{k}_i, \hat{m}_i \rangle$-domain approximation

The eigenvalue ranges can be obtained from an extra eigenvalue minimisation and maximisation for each mode. The crucial part in this algorithm, however, is in the next step, i.e., the calculation of the enhanced modal frequency response function contributions based on the MRE $\langle \hat{k}_i, \hat{m}_i \rangle$-domain approximation. The remainder of this section will focus entirely on this part of the algorithm. Since the final summation of the modal contributions to the total envelope frequency response function is completely similar to the procedure described in step 3 of the MR algorithm in Section 5.2.2, it is not repeated here.

In order to show how the conservatism in the modal frequency response function envelopes can be reduced, step two of the modal rectangle approach is first illustrated in the modal space. Graphically, the denominator function $\hat{k}_i - \omega^2 \hat{m}_i = \mathcal{D}^*$ represents a straight line in the $\left(\hat{k}_i, \hat{m}_i\right)$-space. All $\hat{k}_i, \hat{m}_i$-pairs on this line represent structures with equal values $\mathcal{D}^*$ for the modal frequency response denominator function. This value is graphically equivalent with the ordinate of the intersection of the line and the $\hat{k}_i$-axis. This is illustrated in Figure 23.

Using this graphical interpretation, the exact range of the modal response denominator function $\langle \mathcal{D} \rangle_{\{\mathbf{x}\}}$ follows from constructing both lines with a slope $\omega^2$ tangent to the exact $\langle \hat{k}_i, \hat{m}_i \rangle$-domain, as illustrated in Figure 24. However, since the exact $\langle \hat{k}_i, \hat{m}_i \rangle$-domain is unknown, the denominator function range has to be approximated using a $\langle \hat{k}_i, \hat{m}_i \rangle$-domain

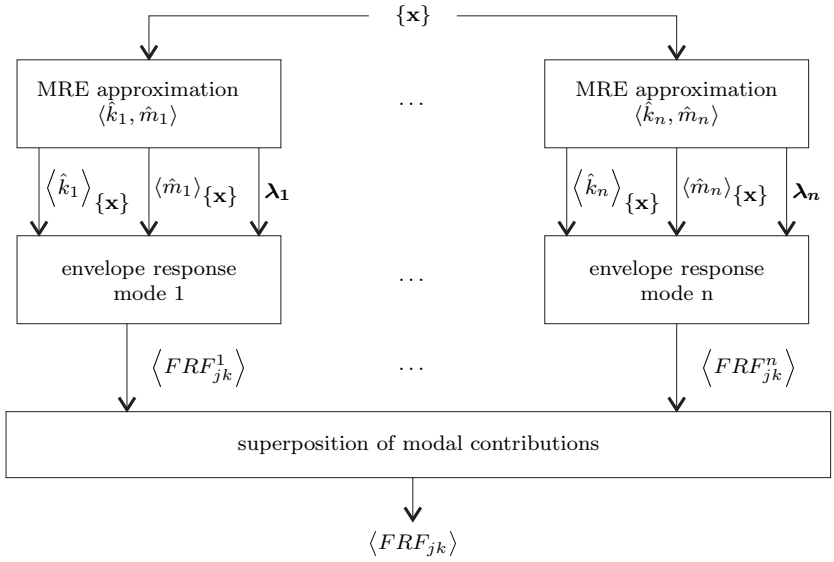


**Figure 22.** Scheme of the interval procedure resulting after the addition of the exact eigenvalue bounds

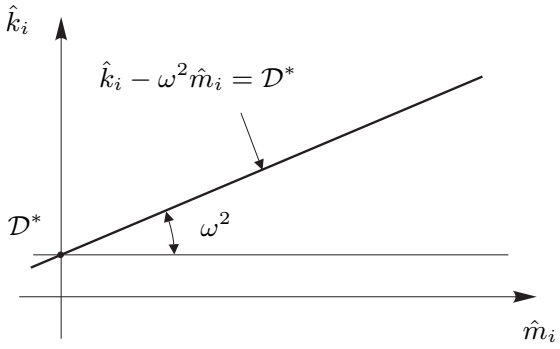


**Figure 23.** Graphical interpretation of the modal denominator function in the modal space

approximation. For the modal rectangle approach, this is done using the upper left and lower right corner of the rectangular approximation as also indicated in Figure 24.

Similarly, the range $\langle \mathcal{D} \rangle_{\{\mathbf{x}\}}$ can be derived for the MRE approach by constructing lines tangent to the new $\langle \hat{k}_i, \hat{m}_i \rangle$-domain approximation. In this case these lines pass through the corner points of the polygonal $\langle \hat{k}_i, \hat{m}_i \rangle$-domain approximation indicated with triangles in Figure 21. The approximation of the upper bound of the modal frequency response denominator function range uses $c_1$ for $\omega^2 \leq \overline{\lambda_i}$ and $c_2$ for $\omega^2 \geq \overline{\lambda_i}$, and the lower bound uses $c_3$ for $\omega^2 \leq \underline{\lambda_i}$ and $c_4$ for $\omega^2 \geq \underline{\lambda_i}$. For positive modes, this results in the following analytical description of the modal frequency response denominator function ranges:

$$\langle \mathcal{D}(\omega) \rangle_{\langle \{\hat{q}_i\} \rangle} = \begin{cases} \left[ \underline{\hat{k}_i} \left( 1 - \dfrac{\omega^2}{\underline{\lambda_i}} \right), \overline{\hat{k}_i} \left( 1 - \dfrac{\omega^2}{\overline{\lambda_i}} \right) \right] & \text{for } \omega^2 \leq \underline{\lambda_i} \\ \left[ \overline{\hat{m}_i} \left( \underline{\lambda_i} - \omega^2 \right), \overline{\hat{k}_i} \left( 1 - \dfrac{\omega^2}{\overline{\lambda_i}} \right) \right] & \text{for } \underline{\lambda_i} < \omega^2 < \overline{\lambda_i} \\ \left[ \overline{\hat{m}_i} \left( \underline{\lambda_i} - \omega^2 \right), \underline{\hat{m}_i} \left( \overline{\lambda_i} - \omega^2 \right) \right] & \text{for } \overline{\lambda_i} \leq \omega^2 \end{cases} \tag{105}$$

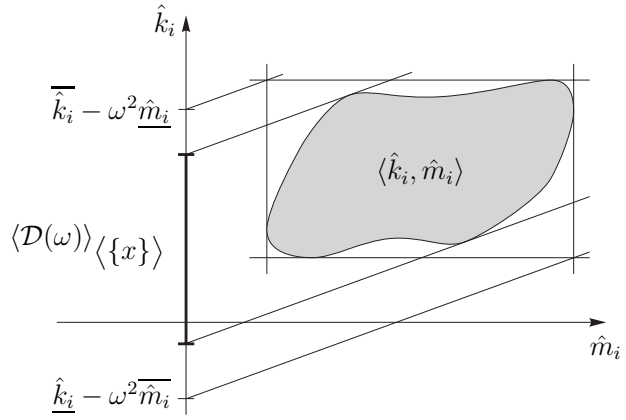


**Figure 24.** Conservatism in the modal frequency response denominator function range calculation using the modal rectangle method

with:

$$\left\langle \{\hat{q}_i\} \right\rangle = \left\{ \begin{array}{c} \left\langle \hat{k}_i \right\rangle_{\{\mathbf{x}\}} \\ \langle \hat{m}_i \rangle_{\{\mathbf{x}\}} \\ \langle \lambda_i \rangle_{\{\mathbf{x}\}} \end{array} \right\} \tag{106}$$

For negative modes, a similar derivation yields:

$$\langle \mathcal{D}(\omega) \rangle_{\left\langle \{\hat{q}_i\} \right\rangle} = \begin{cases} \left[ \underline{\hat{k}_i} \left( 1 - \dfrac{\omega^2}{\overline{\lambda_i}} \right), \overline{\hat{k}_i} \left( 1 - \dfrac{\omega^2}{\underline{\lambda_i}} \right) \right] & \text{for } \omega^2 \leq \underline{\lambda_i} \\ \left[ \underline{\hat{k}_i} \left( 1 - \dfrac{\omega^2}{\overline{\lambda_i}} \right), \underline{\hat{m}_i} \left( \underline{\lambda_i} - \omega^2 \right) \right] & \text{for } \underline{\lambda_i} < \omega^2 < \overline{\lambda_i} \\ \left[ \overline{\hat{m}_i} \left( \overline{\lambda_i} - \omega^2 \right), \underline{\hat{m}_i} \left( \underline{\lambda_i} - \omega^2 \right) \right] & \text{for } \overline{\lambda_i} \leq \omega^2 \end{cases} \tag{107}$$

In order to analyse the effect of the introduction of the eigenvalue intervals on the contribution of the switch modes to the total envelope frequency response function, the eigenvalue range is split in two parts similar to a switch mode's modal parameter range:

$$\langle \lambda_i \rangle_{\{\mathbf{x}\}} = \langle \lambda_i \rangle^-_{\{\mathbf{x}\}} \cup \langle \lambda_i \rangle^+_{\{\mathbf{x}\}} \tag{108}$$

with

$$\langle \lambda_i \rangle^-_{\{\mathbf{x}\}} = \left\{ \lambda_i \mid \Big( \{x\} \in \{\mathbf{x}\} \Big) \Big( \hat{k}_i < 0 \Big) \right\} \tag{109}$$

$$\langle \lambda_i \rangle^+_{\{\mathbf{x}\}} = \left\{ \lambda_i \mid \Big( \{x\} \in \{\mathbf{x}\} \Big) \Big( \hat{k}_i > 0 \Big) \right\} \tag{110}$$

These parts of the total eigenvalue range consist both of a positive interval. They are not disjoint since the eigenvalue range of a mode is always a single closed interval for physical input parameters. They can be calculated separately by introducing the sign of one of the modal parameters as extra constraint during the eigenvalue optimisation. Figure 25 illustrates the resulting approximation of the $\langle \hat{k}_i, \hat{m}_i \rangle$-domain in both the first and third quadrant.

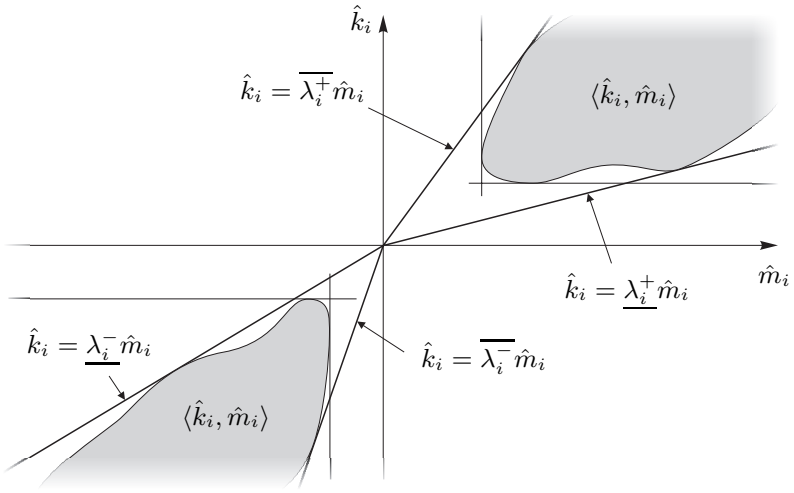


**Figure 25.** Effect of the exact eigenvalue interval introduction in the MRE method on the $\langle \hat{k}_i, \hat{m}_i \rangle$-domain approximation of a switch mode

The modal frequency response denominator function range is calculated for the first and third quadrant in the modal space separately, after which both are combined to obtain the total modal frequency response denominator range:

$$\langle \mathcal{D}(\omega) \rangle_{\langle \{\hat{q}_i\} \rangle} = \langle \mathcal{D}(\omega) \rangle_{\langle \{\hat{q}_i^-\} \rangle} \cup \langle \mathcal{D}(\omega) \rangle_{\langle \{\hat{q}_i^+\} \rangle} \tag{111}$$

with

$$\langle \{\hat{q}_i^-\} \rangle = \left\{ \begin{array}{c} \left\langle \hat{k}_i \right\rangle_{\{\mathbf{x}\}}^- \\ \langle \hat{m}_i \rangle_{\{\mathbf{x}\}}^- \\ \langle \lambda_i \rangle_{\{\mathbf{x}\}}^- \end{array} \right\} \tag{112}$$

and

$$\langle \{\hat{q}_i^+\} \rangle = \left\{ \begin{array}{c} \left\langle \hat{k}_i \right\rangle_{\{\mathbf{x}\}}^+ \\ \langle \hat{m}_i \rangle_{\{\mathbf{x}\}}^+ \\ \langle \lambda_i \rangle_{\{\mathbf{x}\}}^+ \end{array} \right\} \tag{113}$$

The advantage of this strategy is that the analytical descriptions of the modal frequency response denominator range for the positive and negative modes obtained in Eq. (105) and (107) are readily extended to the first respectively third quadrant contributions of a switch mode. This is achieved by substituting in Eq. (105) and (107) the upper bounds on the modal parameters by plus infinity in the first quadrant, the lower bounds by minus infinity in the third quadrant, and the eigenvalue bounds by the corresponding eigenvalue

bounds in the analysed quadrant. This results in:

$$\langle \mathcal{D}(\omega) \rangle_{\langle \{\hat{q}_i^+\} \rangle} = \begin{cases} \left[ \underline{\hat{k}_i^+} \left( 1 - \dfrac{\omega^2}{\underline{\lambda_i^+}} \right), +\infty \right] & \text{for } \omega^2 \leq \underline{\lambda_i^+} \\ [-\infty, +\infty] & \text{for } \underline{\lambda_i^+} < \omega^2 < \overline{\lambda_i^+} \\ \left[ -\infty, \underline{\hat{m}_i^+} \left( \overline{\lambda_i^+} - \omega^2 \right) \right] & \text{for } \overline{\lambda_i^+} \leq \omega^2 \end{cases} \tag{114}$$

for the first quadrant, and:

$$\langle \mathcal{D}(\omega) \rangle_{\langle \{\hat{q}_i^-\} \rangle} = \begin{cases} \left[ -\infty, \overline{\hat{k}_i^-} \left( 1 - \dfrac{\omega^2}{\underline{\lambda_i^-}} \right) \right] & \text{for } \omega^2 \leq \underline{\lambda_i^-} \\ [-\infty, +\infty] & \text{for } \underline{\lambda_i^-} < \omega^2 < \overline{\lambda_i^-} \\ \left[ \overline{\hat{m}_i^-} \left( \overline{\lambda_i^-} - \omega^2 \right), +\infty \right] & \text{for } \overline{\lambda_i^-} \leq \omega^2 \end{cases} \tag{115}$$

for the third quadrant. Both contributions yield disjoint intervals for frequencies outside the quadrant's eigenfrequency range, and the entire range of real values inside the eigenvalue range. Therefore, their union is straightforward.

The modal envelope frequency response function of a switch mode is finally obtained by inverting the modal frequency response denominator function range. Since the domain to be inverted for frequencies outside the total eigenfrequency range consists of a positive and negative interval over infinity, the inverse of the KAHAN inversion is applied. It yields a single interval ranging over zero. For frequencies inside the total eigenfrequency range, the result of the inversion is again the entire range of real values. The results are summarised as follows:

$$\left\langle FRF_{jk}^i \right\rangle_{\langle \{\hat{q}_i\} \rangle} = \begin{cases} \left[ \dfrac{\underline{\lambda_i^-}}{\overline{\hat{k}_i^-} \left( \underline{\lambda_i^-} - \omega^2 \right)}, \dfrac{\underline{\lambda_i^+}}{\underline{\hat{k}_i^+} \left( \underline{\lambda_i^+} - \omega^2 \right)} \right] & \text{for } \omega^2 \leq \underline{\lambda_i} \\ [-\infty, +\infty] & \text{for } \underline{\lambda_i} < \omega^2 < \overline{\lambda_i} \\ \left[ \dfrac{1}{\underline{\hat{m}_i^+} \left( \overline{\lambda_i^+} - \omega^2 \right)}, \dfrac{1}{\overline{\hat{m}_i^-} \left( \overline{\lambda_i^-} - \omega^2 \right)} \right] & \text{for } \overline{\lambda_i} \leq \omega^2 \end{cases} \tag{116}$$

Figure 26 illustrates the first and third quadrant's modal frequency response denominator function range contributions and the corresponding modal envelope frequency response function resulting from the inverse KAHAN inversion of this modal frequency response denominator function range. Clearly, switch modes are allowed in the MRE method because their modal frequency response function range has finite bounds outside the eigenfrequency range. This is a very important extra benefit from the introduction of the exact eigenvalue intervals.

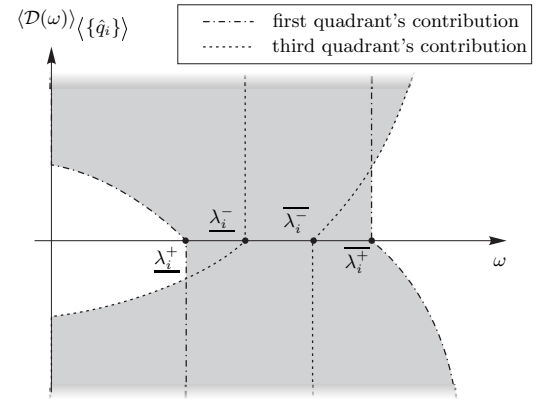


(a) Modal FRF denominator function range

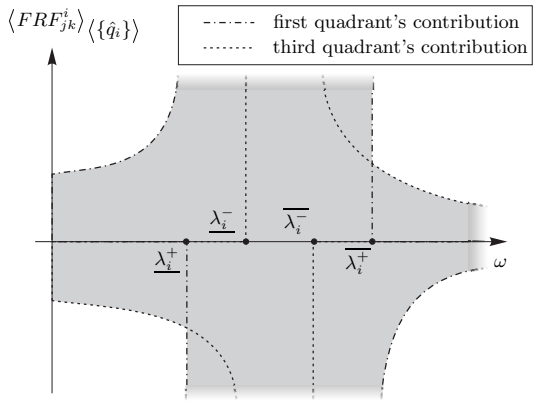


(b) Modal envelope FRF

**Figure 26.** Modal frequency response denominator function range and envelope frequency response function of a switch mode using the MRE method

### *5.2.4 The locally optimised modal rectangle method*

The *locally Optimised Modal Rectangle method (OMR)* aims at a decrease of the conservatism in the modal envelope frequency response function approximation through a tighter polygonal circumscription of the exact $\langle \hat{k}_i, \hat{m}_i \rangle$-domain. This is achieved by the addition of extra lines which delimit the $\langle \hat{k}_i, \hat{m}_i \rangle$-domain. The procedure distinguishes between switch and non-switch modes.

#### The OMR procedure for positive and negative modes

Using the graphical representation, adding delimiters to the $\langle \hat{k}_i, \hat{m}_i \rangle$-domain is equivalent to the minimisation and the maximisation of the modal frequency response denominator function in the input parameter space at a discrete frequency $\omega_\iota$. For a positive or negative mode, the required extra optimisation yields:

$$\langle \mathcal{D}(\omega_\iota) \rangle_{\{\mathbf{x}\}} = \left[ \min_{\{x\} \in \{\mathbf{x}\}} \left( \hat{k}_i - \omega_\iota^2 \hat{m}_i \right), \max_{\{x\} \in \{\mathbf{x}\}} \left( \hat{k}_i - \omega_\iota^2 \hat{m}_i \right) \right] \tag{117}$$

with the modal parameters depending on the input parameters through the eigenvalue analysis using their definitions of Eq. (77) and (78). The optimisation can be repeated for a

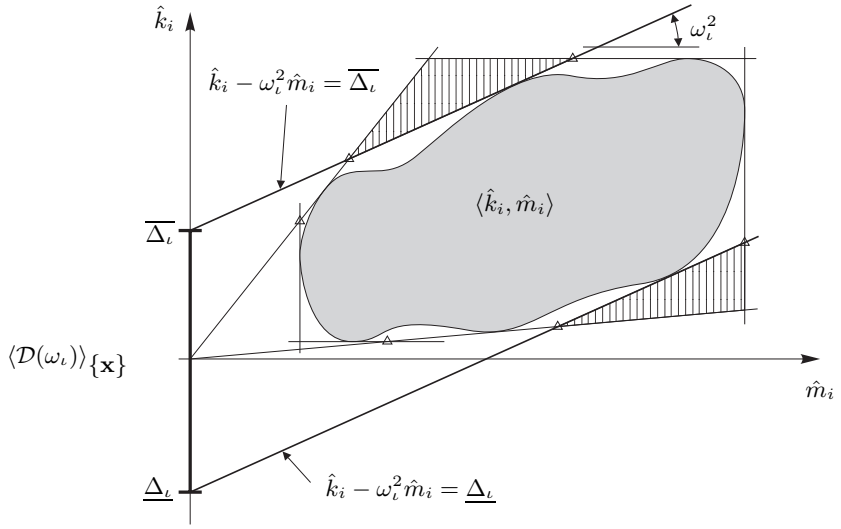


**Figure 27.** Effect of the extra global modal frequency response denominator optimisation at the frequency $\omega_\iota$ on the $\langle \hat{k}_i, \hat{m}_i \rangle$-domain approximation of a positive mode

number of discrete frequencies $\{\omega_1, \omega_2, \ldots \omega_\nu\}$ inside the considered frequency domain. The optimisation results in a set of exact denominator function ranges expressed as intervals at these frequencies, referred to as $\{\mathbf{\Delta_1}, \mathbf{\Delta_2}, \ldots \mathbf{\Delta_\nu}\}$. Figure 27 illustrates the lines representing the result of this extra optimisation step for one single optimisation at the discrete frequency $\omega_\iota$. The hatched area indicates the improvement of the polygonal circumscription compared to the MRE method.

The results of the optimisation have to be combined in a continuous analytical description of the modal frequency response denominator function range in order to obtain a conservative approximation of the exact range for all intermediate frequencies. For this purpose, a quadratic interpolation through the optimisation results in the frequency domain is proposed. Taking two consecutive frequencies $\omega_\iota < \omega_{\iota+1}$, the lower bound on the modal frequency response denominator function range of a positive mode for all $\omega^* \in [\omega_\iota, \omega_{\iota+1}]$ is approximated using:

$$\underline{\underline{\mathcal{D}(\omega^*)}} = \frac{\left(\omega_{\iota+1}^2 - \omega^{*2}\right) \underline{\Delta_\iota} + \left(\omega^{*2} - \omega_\iota^2\right) \underline{\Delta_{\iota+1}}}{\omega_{\iota+1}^2 - \omega_\iota^2} \tag{118}$$

The corresponding upper bound approximation yields:

$$\overline{\overline{\mathcal{D}(\omega^*)}} = \frac{\left(\omega_{\iota+1}^2 - \omega^{*2}\right) \overline{\Delta_\iota} + \left(\omega^{*2} - \omega_\iota^2\right) \overline{\Delta_{\iota+1}}}{\omega_{\iota+1}^2 - \omega_\iota^2} \tag{119}$$

The analysis in the third quadrant yields identical expressions for a negative mode. It can be proven that this quadratic interpolation preserves the guaranteed conservatism in the approach at all frequencies. The proof is given in Appendix 1.

Graphically, this procedure is equivalent to deriving the denominator range for frequencies between two discretely optimised frequencies $\omega_\iota$ and $\omega_{\iota+1}$ by using the cross point between the lines representing the optimisation results at these two discrete frequencies. From the cross point taken at both the lower and upper boundaries of the polygon, two lines with slope $\omega^{*2}$ are constructed. The interval bounded by the intersections of these lines

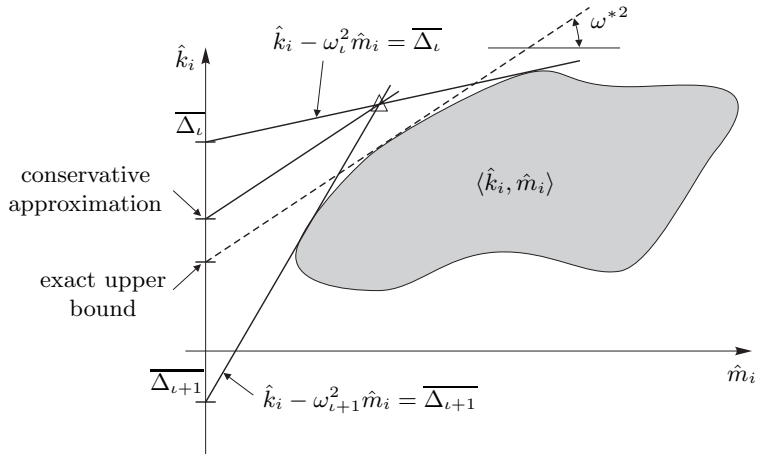


**Figure 28.** Conservative approximation of the upper bound of the modal frequency response denominator function range at frequencies $\omega^* \in [\omega_\iota, \omega_{\iota+1}]$

with the $\hat{k}_i$-axis yields the approximated modal frequency response denominator function range. Figure 28 illustrates the procedure for the upper bound and shows that the resulting approximation is conservative.

By repeating this procedure for all cross points obtained in the polygonal $\langle \hat{k}_i, \hat{m}_i \rangle$-domain approximation, the total frequency response function is assembled for the complete continuous frequency domain between $\omega_1$ and $\omega_\nu$. It is clear that after inverting the modal frequency response denominator function range, the extra delimiter lines reduce the conservatism in the modal envelope frequency response function. The effect of such an extra optimisation step is not unpredictable. It will be most efficient when applied at frequencies for which the $\langle \hat{k}_i, \hat{m}_i \rangle$-domain approximation of the MR method is the worst. This could be observed by comparing the MR $\langle \hat{k}_i, \hat{m}_i \rangle$-domain approximation with a sampled approximation of the exact $\langle \hat{k}_i, \hat{m}_i \rangle$-domain. Furthermore, the OMR procedure does not require that the optimisation for the lower and upper bound are performed at the same discrete frequencies. Therefore, the procedure is easily generalised in order to enable a more efficient approach when the $\langle \hat{k}_i, \hat{m}_i \rangle$-domain approximation needs optimisation for different slopes at the lower and upper side of the approximate MR rectangle.

When the complete frequency domain is analysed, $\omega_1$ equals zero and $\omega_\nu$ equals infinity. It is easily shown that the optimisation stated in Eq. (117) at zero and infinity is equivalent with the optimisation of the modal parameters and graphically represents the horizontal respectively vertical boundaries of the polygonal circumscription. The MR method is consequently a special case of the OMR method with only two discrete frequencies, one at zero and one at infinity. Similarly, the addition of the eigenvalue delimiters to the procedure as described in Section 5.2.3 is equivalent with introducing the eigenfrequency lower and upper bounds as discrete points for an optimisation of the lower respectively upper modal frequency response denominator function in the OMR procedure. This results in the OMRE procedure, which represents the combination of the MR method with the eigenvalue interval and locally optimisation enhancements.

### The OMR procedure for switch modes

For a switch mode, Figure 26 indicates that the modal frequency response denominator function range is not a continuous interval for frequencies outside the eigenfrequency interval. The modal envelope frequency response function on the other hand is. Therefore, if the

modal envelope frequency response function is to be improved using extra optimisations at discrete frequencies, these should be performed directly on the modal response value rather than on the modal frequency response denominator range value as for the positive and negative modes. Consequently, the direct optimisation for a switch mode yields:

$$\left\langle FRF^i_{jk} \right\rangle_{\{\mathbf{x}\}} = \left[ \min_{\{x\}\in\{\mathbf{x}\}} \left( \frac{1}{\hat{k}_i - \omega_\iota^2 \hat{m}_i} \right), \max_{\{x\}\in\{\mathbf{x}\}} \left( \frac{1}{\hat{k}_i - \omega_\iota^2 \hat{m}_i} \right) \right] \tag{120}$$

with the modal parameters depending on the input parameters through the eigenvalue analysis using their definitions of Eq. (77) and (78). The optimisation can be repeated for a number of discrete frequencies $\{\omega_1, \omega_2, \ldots \omega_\nu\}$ inside the considered frequency domain, but outside the eigenfrequency range of the considered mode. The optimisation results in a set of exact modal response ranges expressed as intervals at these frequencies, referred to as $\{\boldsymbol{\Psi_1}, \boldsymbol{\Psi_2}, \ldots \boldsymbol{\Psi_\nu}\}$. Again, this optimisation is equivalent to constructing extra delimiters to the $\langle \hat{k}_i, \hat{m}_i \rangle$-domain approximation similar to those for a positive mode in Figure 27.

The results of the optimisation yield a description of the modal envelope frequency response function in a continuous function domain using the inverse of the expressions obtained for the modal frequency response denominator function bounds in Eq. (118) and (119). Taking two consecutive frequencies $\omega_\iota < \omega_{\iota+1}$, the lower bound on the modal frequency response function range for all $\omega^* \in [\omega_\iota, \omega_{\iota+1}]$ is conservatively approximated using:

$$\underline{\underline{FRF^i_{jk}}} = \frac{\underline{\Psi_\iota}\,\underline{\Psi_{\iota+1}} \left(\omega^2_{\iota+1} - \omega^2_\iota\right)}{\underline{\Psi_\iota} \left(\omega^2_{\iota+1} - \omega^{*2}\right) + \underline{\Psi_{\iota+1}} \left(\omega^{*2} - \omega^2_\iota\right)} \tag{121}$$

The corresponding upper bound approximation yields:

$$\overline{\overline{FRF^i_{jk}}} = \frac{\overline{\Psi_\iota}\,\overline{\Psi_{\iota+1}} \left(\omega^2_{\iota+1} - \omega^2_\iota\right)}{\overline{\Psi_\iota} \left(\omega^2_{\iota+1} - \omega^{*2}\right) + \overline{\Psi_{\iota+1}} \left(\omega^{*2} - \omega^2_\iota\right)} \tag{122}$$

Again, by repetitively constructing these modal envelope frequency response function approximations for small continuous parts in the frequency domain, an improved modal envelope frequency response function is obtained which incorporates less conservatism as the corresponding MR modal envelope frequency response function.

#### *5.2.5 Extension of the hybrid algorithm to the analysis of damped structures*

Very often there is insufficient information to describe the damping properties of a structure exactly. Furthermore, it is extremely difficult to experimentally determine and quantify the exact sources of the energy dissipation. Usually there is more than one damping mechanism present. All of these contribute to some unknown extent to the total damping. Therefore, modelling the damping mechanisms numerically proves to be an extremely difficult task.

The lack of information to numerically describe the damping in a model exactly has given rise to a number of simplified damping models. These are inspired by mathematical considerations rather than by physical representation of the damping phenomena. One of the most popular mathematical concepts to model damping is the proportional or RAYLEIGH damping model. In this concept, the damping matrix is assumed to be a linear combination of the system mass and stiffness matrices:

$$[C] = \alpha_K\ [K]\ +\ \alpha_M\ [M] \tag{123}$$

with $\alpha_K$ and $\alpha_M$ proportional constants to be defined for each analysis. This is one of the most common models of damping. The assumption of proportional damping is purely

made for mathematical convenience as it simplifies the solution process. The proportional damping model has been proved to be reliable for structures with damping below 10% of critical [105].

This proportional damping model has been selected for the first development in the area of damped interval finite element frequency response function analysis. A constant damping model is considered, using constant values for $\alpha_K$ and $\alpha_M$ for the entire analysis. The proportional coupling propagates the interval uncertainties present on the stiffness and mass properties of the model to the damping properties. It is clear that any damping interval can be obtained through the appropriate choice of the proportional constants. The remainder of this section summarises the main implications of the addition of damping to the existing envelope frequency response function procedures. A more detailed description of this extension to damped structures can be found in [94].

The frequency response function between DOF $j$ and DOF $k$ of a damped finite element model is obtained taking the $j^{th}$ component of $X$ satisfying the dynamic equilibrium equation of the damped structure:

$$\left([K] + \jmath\omega\,[C] - \omega^2\,[M]\right)\{X\} = \left\{F^k\right\} \tag{124}$$

with $F^k$ as defined in Eq. (70) and $\jmath = \sqrt{-1}$. This means that in this case, the response is a complex value for each frequency. Consequently, there are a number of different possibilities for the definition of the required envelope frequency response function. Generally, most interest is paid to the amplitude of the response. The basic problem of the interval finite element frequency response function procedure is then the calculation of the range of the amplitude of the $j^{th}$ component of the response vector taking into account the interval ranges of the non-deterministic model properties in the interval vector $\{\mathbf{x}\}$:

$$\langle \|X_j\| \rangle_{\{\mathbf{x}\}} = \left\{ \|X_j\| \mid \Big(\{x\} \in \{\mathbf{x}\}\Big)\Big(\left([K] + \jmath\omega\,[C] - \omega^2\,[M]\right)\{X\} = \left\{F^k\right\}\Big)\right\} \tag{125}$$

with $[K]$, $[C]$ and $[M]$ incorporating implicitly the dependency of the system matrices to the input parameters. Similar, the range of the corresponding phase of the complex response result yields $\langle \varphi(X_j) \rangle_{\{\mathbf{x}\}}$. Other possibilities for the definition of the set are the range of the real or imaginary part of the response value, referred to respectively as $\langle \Re(X_j) \rangle_{\{\mathbf{x}\}}$ and $\langle \Im(X_j) \rangle_{\{\mathbf{x}\}}$.

For damped structures, there exists an alternative procedure for the frequency response function calculation similar to the modal superposition procedure described in Section 5.2.1, which yields:

$$FRF_{jk} = \sum_{i=1}^{n} \frac{1}{\left(\hat{k}_i - \omega^2 \hat{m}_i\right) + \jmath\left(\alpha_K \hat{k}_i + \alpha_M \hat{m}_i\right)\omega} \tag{126}$$

with $FRF^i_{jk}$ the $i^{th}$ modal frequency response function and $\hat{k}_i$ and $\hat{m}_i$ the normalised modal parameters as defined in Eq. (77) and (78). Equation 126 shows that the damped frequency response function calculation through the modal superposition principle is very similar to the undamped case. Compared to the undamped frequency response function modal superposition described in Section 5.2.1, the only difference caused by the addition of damping is that the modal frequency response function contributions $FRF^i_{jk}$ are complex functions. As for the undamped case, these modal frequency response function contributions depend only on the model input parameters through the modal stiffness and mass respectively $\hat{k}_i$ and $\hat{m}_i$. Therefore, the damped envelope frequency response function calculation procedure

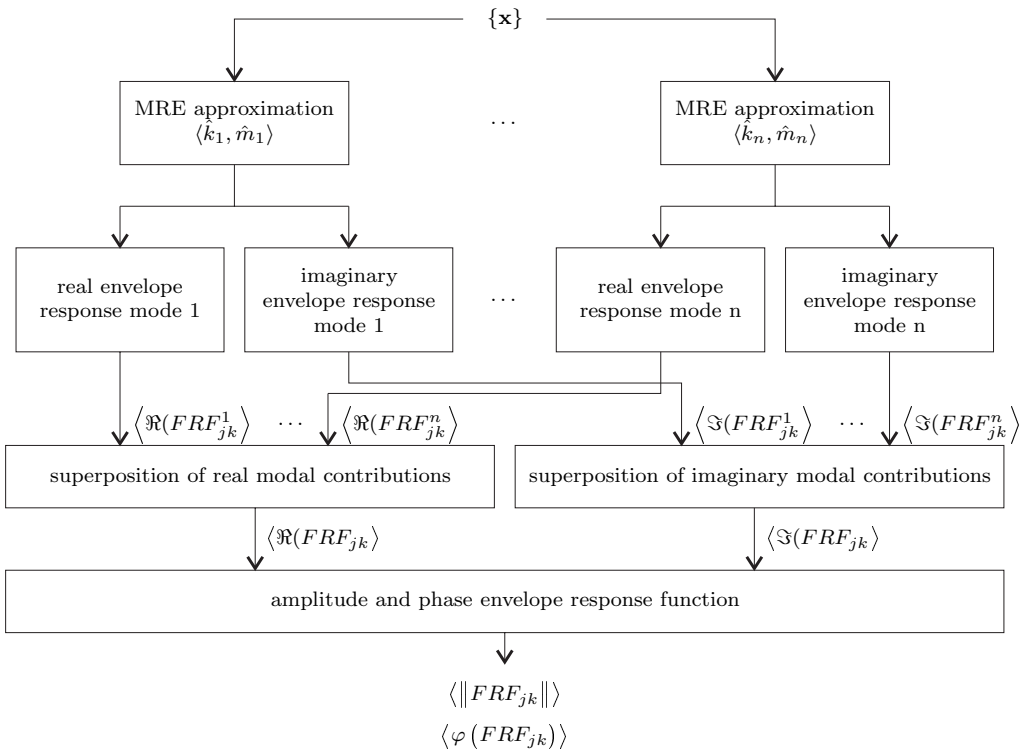


**Figure 29.** Scheme of the MRE interval procedure for damped structures

inherits the concept of the hybrid interval finite element procedure of the undamped case. Consequently, all the $\langle \hat{k}_i, \hat{m}_i \rangle$-domain approximations derived in the previous sections can be used to calculate conservative approximations of the damped modal envelope frequency response functions.

Compared to the undamped case, the main difference is in the fact that the modal frequency response function contributions now are complex functions. The procedure handles this by treating the real and the complex parts of the response separately. For both parts, the response range is calculated for each mode. The superposition then constructs the range of the real and imaginary parts of the total response by adding together all real respectively imaginary modal frequency response function contributions. Finally, based on these results, the amplitude and phase are directly derived from the total real and imaginary envelope frequency response functions. Figure 29 summarises this procedure for the MRE $\langle \hat{k}_i, \hat{m}_i \rangle$-domain approximation.

This algorithm requires the calculation of the range of the real and imaginary part of the modal frequency response function contributions taking into account that the variables are inside the used $\langle \hat{k}_i, \hat{m}_i \rangle$-domain approximation. For the MRE approximation, this is mathematically expressed as:

$$\left\langle \Re\left(FRF^i_{jk}\right)\right\rangle_{\langle\{\hat{q}_i\}\rangle} = \left\{ \frac{\hat{k}_i - \omega^2 \hat{m}_i}{(\hat{k}_i - \omega^2 \hat{m}_i)^2 + \omega^2(\alpha_K \hat{k}_i + \alpha_M \hat{m}_i)^2} \mid \left(\{\hat{q}_i\} \in \langle\{\hat{q}_i\}\rangle\right) \right\} \quad (127)$$

$$\left\langle \Im\left(FRF^i_{jk}\right)\right\rangle_{\langle\{\hat{q}_i\}\rangle} = \left\{ \frac{-\omega(\alpha_K \hat{k}_i + \alpha_M \hat{m}_i)}{(\hat{k}_i - \omega^2 \hat{m}_i)^2 + \omega^2(\alpha_K \hat{k}_i + \alpha_M \hat{m}_i)^2} \mid \left(\{\hat{q}_i\} \in \langle\{\hat{q}_i\}\rangle\right) \right\} \quad (128)$$

with $\langle\{\hat{q}_i\}\rangle$ defined as in Eq. (106). It has been shown that these envelopes can be de-

scribed analytically based on the MR or MRE $\langle \hat{k}_i, \hat{m}_i \rangle$-domain approximation. The reader is referred to [94] for a comprehensive description of this analytical derivation.

Finally, the total amplitude and phase envelope frequency response function are calculated using the total real and imaginary envelope frequency response functions. These result from the summation of the modal contributions derived in the previous section:

$$\langle \Re\left(FRF_{jk}\right) \rangle = \sum_{i=1}^{n} \left\langle \Re\left(FRF_{jk}^{i}\right) \right\rangle \tag{129}$$

$$\langle \Im\left(FRF_{jk}\right) \rangle = \sum_{i=1}^{n} \left\langle \Im\left(FRF_{jk}^{i}\right) \right\rangle \tag{130}$$

This summation is easily implemented because the modal response contributions all describe a finite interval both for the real and the imaginary part of the frequency response function. Consequently, the summation of all lower respectively upper bounds yields the bounds on the total frequency response function.

The result of the summation is an interval range for the real and imaginary part of the complex response for every frequency. This means that it defines a rectangle in the complex space in which the response vector is contained. Based on this rectangle, an approximation of the amplitude range of the complex response is easily obtained by taking the points on the rectangle which are respectively the nearest and most distant from the origin. The phase range is derived in a similar way. Figure 30 illustrates this procedure. This results in:

$$\langle \| FRF_{jk} \| \rangle_{\langle \{\mathcal{C}\} \rangle} \tag{131}$$

$$\langle \varphi\left(FRF_{jk}\right) \rangle_{\langle \{\mathcal{C}\} \rangle} \tag{132}$$

with

$$\langle \{\mathcal{C}\} \rangle = \left\{ \begin{array}{c} \langle \Re\left(FRF_{jk}\right) \rangle \\ \\ \langle \Im\left(FRF_{jk}\right) \rangle \end{array} \right\} \tag{133}$$

It should be noted that this final conversion to amplitude and phase envelope frequency response functions as shown in Figure 30 considers the imaginary and real part of the frequency response function independently. Although the situation in the figure is exaggerated in order to clarify this point, this introduces an additional source of conservatism. This source is due to the fact that not every combination of real and imaginary parts within the rectangle is feasible. This is equivalent to the decoupling of the modal mass and stiffness in the modal space as discussed for the MR method. However, while in the modal domain the conservatism was introduced in the analysis of each individual mode, in the amplitude and phase conversion, the conservatism is introduced only through a single operation on the final response. Therefore, the introduced conservatism is limited, as will be shown in the numerical test cases in Section 6 of this paper.

## 6 NUMERICAL EXAMPLE

### 6.1 Deterministic Reference Model

This section illustrates the presented methodology for frequency response analysis of structures with interval and fuzzy uncertainties. The mechanical structure under investigation is part of the satellite designed for the COROT space mission (COnvection ROtation and planetary Transits) conducted by the European Space Agency. This mission is scheduled

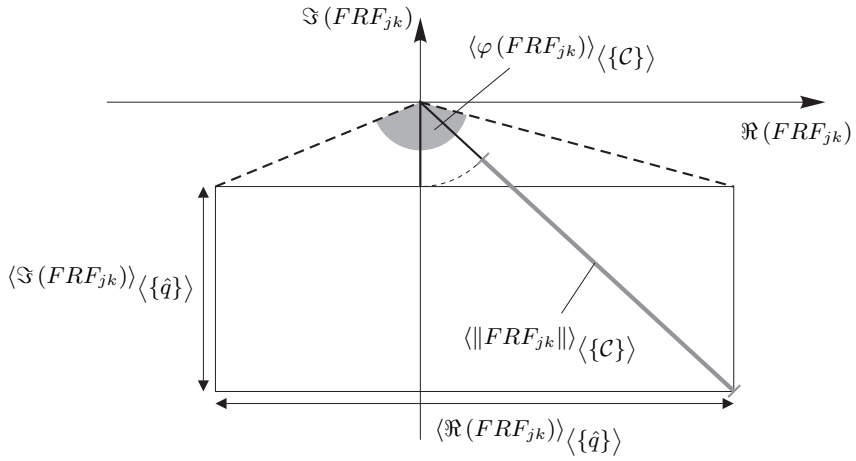


**Figure 30.** Conversion of the real and imaginary frequency response function range to the amplitude and phase frequency response function range

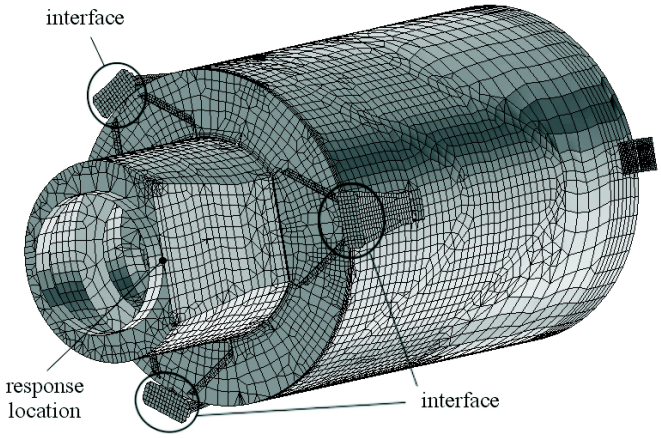


**Figure 31.** Nominal finite element model of the baffle of the COROT telescope, courtesy of Centre Spatiale de Liège (CSL), Belgium

for launch in June 2006, and its main objectives are to enable detailed stellar seismology, e.g. detection and measurement of stellar vibrations, and secondly, to search for small, rocky planets around stars other than the sun. The presented analysis focusses on the effect on the dynamic behaviour of uncertain parameters that actually occurred during the design phase of the telescope baffle. Figure 31 shows the nominal finite element model of the baffle used as the reference in the conducted analysis.

The nominal model contains 96210 degrees of freedom, and consists mainly of plate and beam elements. In its final launch configuration, the baffle is attached to the satellite structure at three interface zones indicated in Figure 31. Before launch, a satellite component of this size is typically tested for its dynamical behavior in a hardmounted vibration test with the component fixed to the shaker at its interfaces. The numerical analysis performed here corresponds to this base excitation test through the application of the large mass modelling concept. For this purpose, an additional large point mass is introduced in the model, rigidly connected to the structure at the interface degrees of freedom. The mass of the

added element equals $10^6$ times the mass of the original structure. A harmonic excitation force on the large mass serves as input for the dynamic analysis. The analysis focusses on the dynamic response at the lower interface point between the telescope and the flange on the smaller cylindrical part of the model (see also Figure 31). The response analysis takes the first ten modes into account. Rayleigh damping is applied, with proportional constants chosen such that the damping ratios of the considered modes are in the range between 0.5 and 1%.

Section 6.2 now first describes the procedure for envelope frequency response function analysis of the COROT baffle model with five uncertain parameters. The concept of the $\langle \hat{k}_i, \hat{m}_i \rangle$-domain and its approximation using respectively the MR, MRE and OMRE approach is illustrated. Section 6.3 then extends the procedure to a full fuzzy analysis using the $\alpha$-cut strategy.

### 6.2 Interval Analysis with Five Uncertainties

Five uncertain interval parameters are identified, as listed in Table 1. The first two uncertainties arise from a variability of 5% on the thickness of the aluminum sheets in the baffle. Typical production tolerances are considered on the thickness of the vanes and mounts.

| uncertain parameter | unit | nominal value | uncertainty interval |
|---|---|---|---|
| sheet thickness for tulip shape | mm | 0.8 | $[0.78, 0.82]$ |
| sheet thickness for thinner baffle part | mm | 0.4 | $[0.39, 0.41]$ |
| vane 1 thickness | mm | 0.8 | $[0.79, 0.81]$ |
| vane 1 bis thickness | mm | 1.2 | $[1.19, 1.21]$ |
| mounts thickness | mm | 1.8 | $[1.79, 1.81]$ |

**Table 1.** Uncertain parameters in the COROT baffle model

First, the $\langle \hat{k}_i, \hat{m}_i \rangle$-domain approximations resulting from the three different envelope frequency response function procedures are analysed. Since the exact $\langle \hat{k}_i, \hat{m}_i \rangle$-domain is unknown, the amount of conservatism in the approximations cannot be determined. Therefore, in order to assess the approximated $\langle \hat{k}_i, \hat{m}_i \rangle$-domains, they are compared to the cloud of modal parameter combinations resulting from a Monte Carlo simulation with 100 samples following a uniform distribution over the uncertain input intervals given in table 1. A comparison of the MR, MRE and OMRE $\langle \hat{k}_i, \hat{m}_i \rangle$-domain approximations with this cloud will give a clear indication of the quality of the approximations.

Figure 32 compares the cloud of 100 samples from a Monte Carlo simulation with the MR and MRE $\langle \hat{k}_i, \hat{m}_i \rangle$-domain approximation for the first mode of the structure. The dots represent the Monte Carlo samples, while the squares ($\square$) indicate the 32 modal parameter combinations resulting from a vertex analysis. This figure indicates that this mode substantially benefits from the addition of the eigenfrequency bounds since the conservatism of the MRE approximation is much lower than for the MR approximation. This is due to the fact that the exact $\langle \hat{k}_i, \hat{m}_i \rangle$-domain is diagonally oriented with respect to the modal rectangle. Furthermore, this figure indicates that for this mode, no explicit benefit is to be expected from the introduction of an extra local optimisation for any discrete frequency, because the MRE approach already results in a close approximation of the region indicated by the Monte Carlo samples.

The situation is different for the seventh mode. For this mode, the Monte Carlo samples clearly indicate that the MRE $\langle \hat{k}_i, \hat{m}_i \rangle$-domain approximation leaves room for improvement at both the upper and lower side of the sample cloud, as indicated in Figure 33(a). From this figure, one can easily derive the optimal discrete frequency to perform the extra op-

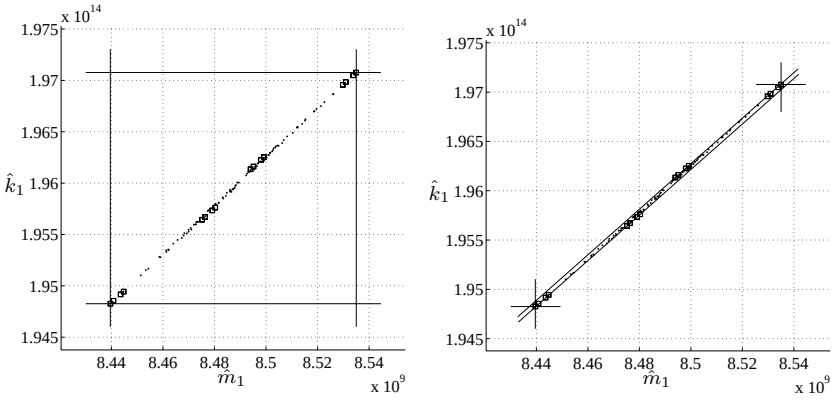


(a) MR approximation (b) MRE approximation

**Figure 32.** Comparison of MR and MRE $\langle \hat{k}_i, \hat{m}_i \rangle$-domain approximation of the first mode

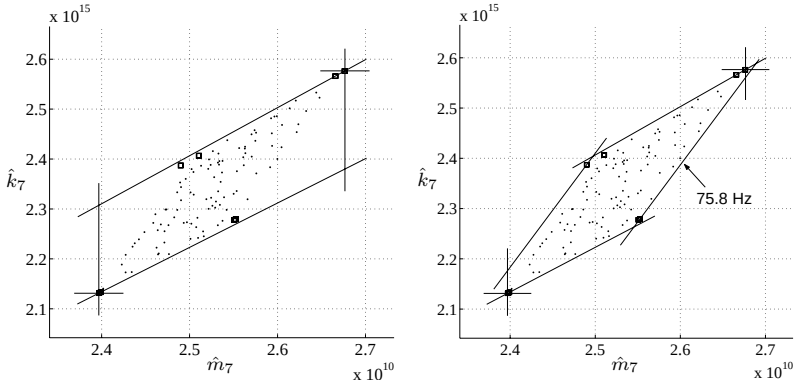


(a) MRE approximation (b) OMRE approximation

**Figure 33.** Comparison of MRE and OMRE $\langle \hat{k}_i, \hat{m}_i \rangle$-domain approximation of the seventh mode

timisation step in the OMRE procedure by taking the square root of the slope of the line which approximately describes the upper bound of the sample cloud. In this case, a frequency of 75.8 Hz is chosen for an extra modal frequency response denominator function range optimisation at both the upper and lower $\langle \hat{k}_i, \hat{m}_i \rangle$-domain approximation boundaries. Figure 33(b) gives the corresponding OMRE $\langle \hat{k}_i, \hat{m}_i \rangle$-domain approximation, which is a substantial improvement compared to the MRE approximation. For the OMRE calculation, a similar procedure is applied for modes 1, 2, 4, 8 and 10, resulting in a substantial reduction of the $\langle \hat{k}_i, \hat{m}_i \rangle$-domain approximations.

Figure 34 compares the real and imaginary parts of the MR and MRE envelope frequency response functions with the frequency response functions resulting from the Monte Carlo samples. This figure clearly shows the effect of the addition of the exact eigenfrequency intervals in the MRE procedure. The amount of conservatism in the MRE approach is clearly reduced compared to the MR approach. Figure 35 gives the corresponding calculated MRE bounds on the amplitude and phase of the frequency response function. Finally, Figure 36 illustrates the effect on the envelope of the amplitude of the frequency response function resulting from the additional OMRE local optimisations for the modes specified above. Since the improvement of the OMRE approach is hardly visible on the full envelope

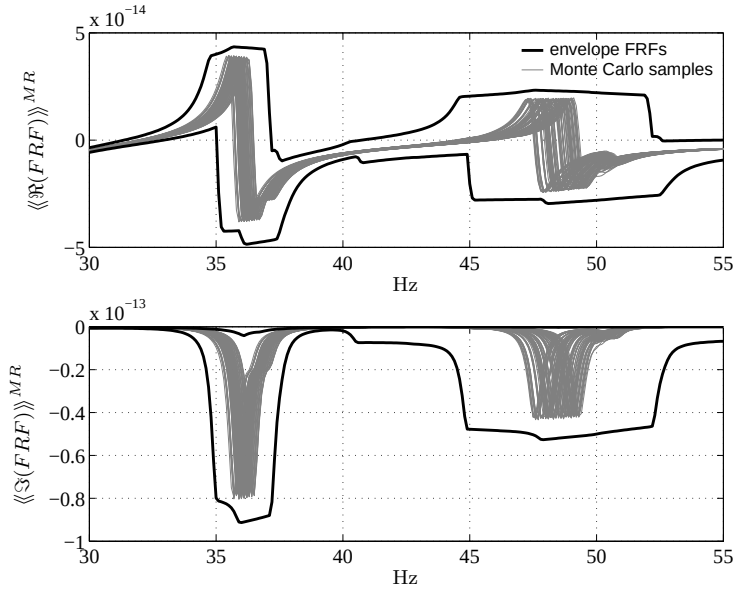


(a) MR envelope FRFs

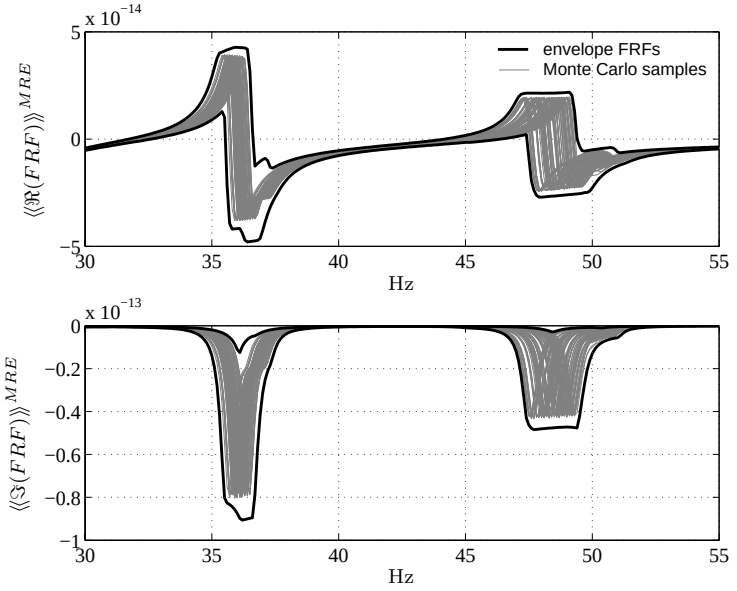


(b) MRE Envelope FRFs

**Figure 34.** Comparison of the MR and MRE envelope frequency response functions

frequency response function plot, this figure gives the proportional reduction of the response interval at every frequency. The response interval indeed is reduced over the complete observed frequency domain.

### 6.3 Fuzzy Analysis with Five Uncertainties

A fuzzy analysis is performed with symmetrical triangular membership functions. These are defined such that the intervals as specified in Table 1 appear exactly in the center of the membership range (at $\alpha = 0.5$). A total of 5 $\alpha$-levels are examined. The resulting envelope response functions are assembled to a fuzzy frequency response function in Figure 37. Only

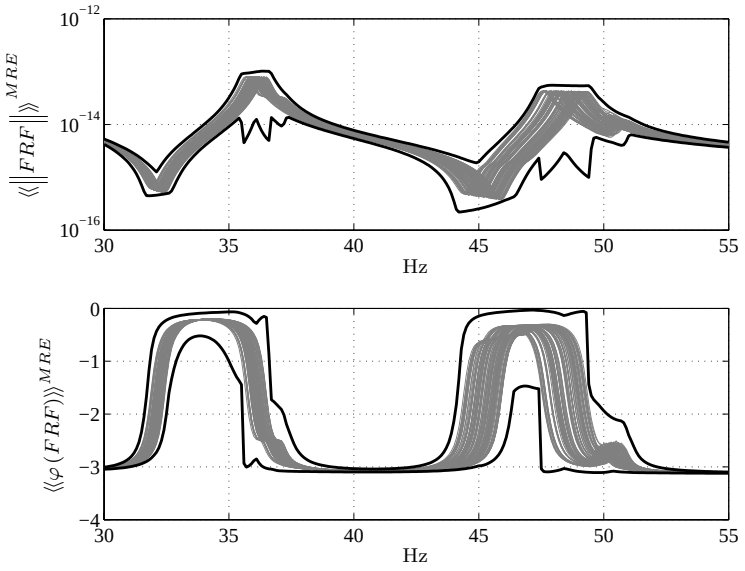


**Figure 35.** Envelope on the amplitude and phase of the frequency response function

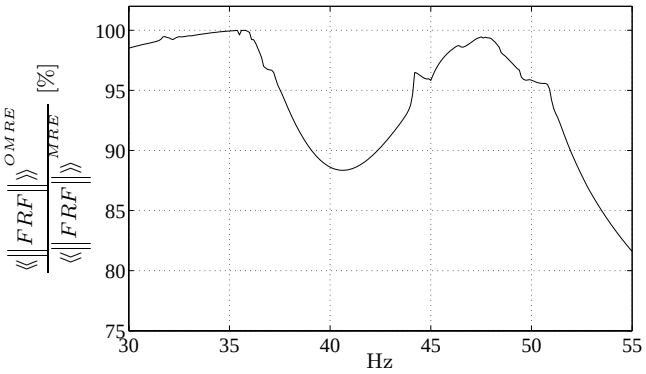


**Figure 36.** Proportional reduction of the OMRE response interval compared to the MRE response interval

the evolution on the upper bound of the response curves is shown, as this is the most interesting result from a designer point of view.

This figure shows that the deviation of the obtained upper response bound at a specific $\alpha$-level from the nominal case is not constant over the frequency domain. This indicates that the sensitivity of the structural response at the output location is varying over different regions in the frequency domain. In this case, the amplitude sensitivity to the introduced uncertainties increases with increasing frequency. This can be very valuable information in a design validation process. For instance, when a design criterion is placed on the amplitude, it can be seen that the first mode at about 36 Hz is the most important one in the deterministic case. However, in the fuzzy analysis, the maximum response level at this first eigenfrequency proves to be little sensitive to the present uncertainties. The response amplitude in the neighbourhood of the eigenmode at 47 Hz is much more sensitive, and therefore could play an important role in the dynamic assessment of the design subject to uncertainty.

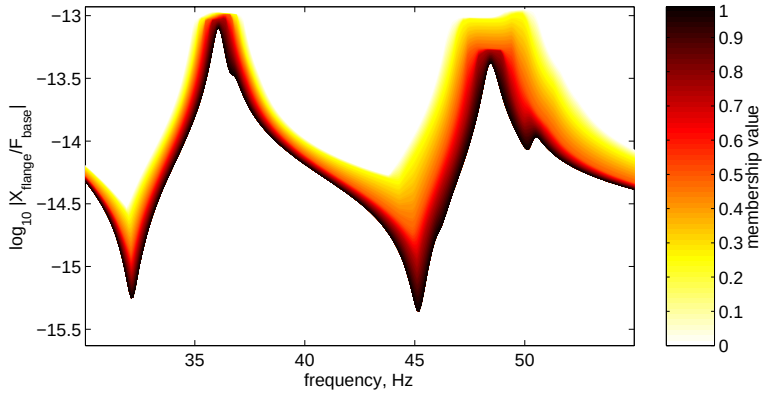


**Figure 37.** Fuzzy evolution of the upper bound on the frequency response function of the baffle between a large base mass and flange displacement

## 7 CONCLUSION

In this paper, the different available concepts for the analysis of parametric model uncertainty in the finite element framework are discussed. A survey of non-deterministic numerical models indicates two valid alternatives for the probabilistic concept: the interval and the fuzzy model. The main advantage of the interval model compared to the probabilistic model is that it requires less information and, therefore, is less vulnerable to the influence of subjective data. The result of a numerical interval analysis defines a crisp borderline between possible and impossible analysis outcomes, without attaching probability values to the occurrence of the analysis results within their range. The fuzzy uncertainty model requires more information than the interval model. This information is put in an explicitly subjective form, which prohibits the translation of the outcome to objective reliability measures. Furthermore, it is shown that through the extension principle, the fuzzy analysis can be regarded as a large-scale sensitivity analysis of the interval analysis result to the bounds on the interval properties.

It is than discussed how these alternative concepts for numerical uncertainty representation can be put to use in a design process. In this context, distinction between two fundamentally different kinds of non-deterministic properties is made. Variabilities represent model properties which will actually vary in the final product. Uncertainties on the other hand represent model properties that cannot be described exactly with the available information. It is shown how the alternative models for uncertainty representation in numerical analysis could be of great value in an engineering design process. Especially in an early design stage, the information necessary to construct a representative probabilistic analysis is mostly missing. Furthermore, the probabilistic analysis in this case produces probabilistic information which is often not requested in this stage of the design process. The crisp distinction between possible and impossible analysis results produced by the interval analysis enables a worst-case analysis which could be of great value for a design engineer. Furthermore, the extension to an iterative procedure using the fuzzy approach enables a worst-case oriented design optimisation.

From a numerical viewpoint, the application of the interval uncertainty model requires an interval finite element methodology which is able to propagate intervals defined on input parameters to a range of possible analysis outcomes. This interval analysis forms also the core of the implementation of the fuzzy finite element method. The exact solution of the interval finite element problem can be formulated as a global optimisation problem.

However, the limited practical applicability of the optimisation strategy has lead to the development of an alternative interval arithmetic approach. This approach, however, is extremely vulnerable to conservatism especially during the interval system matrices assembly phase. This conservatism causes the interval finite element result to be a severe overestimation of the exact range of the finite element analysis with respect to the input intervals. It is concluded that, due to the problem of conservatism implicitly incorporated in the interval arithmetic approach, the vertex and global optimisation strategies are the only viable alternatives for interval finite element procedure developments that envisage application to realistically sized and industrially relevant finite element models.

The paper then focusses on the specific application of the interval or fuzzy finite element analysis to frequency response function analysis. In order to cope with the excessive conservatism, a hybrid solution strategy is introduced which consists of an optimisation step followed by an interval arithmetic procedure. This hybrid approach cancels all sources of conservatism captured in the optimisation step. In order to reduce the impact of the remaining sources of conservatism in the interval arithmetic part of the algorithm, the results of an eigenvalue optimisation are introduced in the procedure. The resulting method proves to be a very good trade-off between computation time and exactness of the result. If there is special interest in the response at specific frequencies, the method can be further enhanced using the results of an exact modal response optimisation at discrete frequencies. The method is first developed for undamped structures and later generalised to proportionally damped structures. The effectiveness of the interval finite element frequency response function methodology is demonstrated by comparing the resulting envelope frequency response function functions with compatible Monte Carlo simulations.

## ACKNOWLEDGMENTS

The research of D. Moens is funded by a post-doctoral fellowship from the Institute for the promotion of Innovation by Science and Technology in Flanders (IWT - Vlaanderen), Brussel. The test case of the COROT baffle was made available by the Centre Spatial de Liège (B).

## Appendix 1

This appendix shows that using the results of the maximisation and minimisation of the undamped modal frequency response denominator function at discrete frequencies, conservative bounds on the modal frequency response function can be derived for the complete frequency domain. Only the proof for the upper bound is given here. The proof for the lower bound is completely similar.

Consider that $\mathcal{D}(\omega)$ represents the modal frequency response denominator function:

$$\mathcal{D}(\omega) = \hat{k}_i - \omega^2 \hat{m}_i \tag{134}$$

Given the exact optimized values of the goal function $\mathcal{D}(\omega)$ for two distinct values of $\omega$:

$$\max_{\{x\}\in\{\mathbf{x}\}} \mathcal{D}(\omega_\iota) = \overline{\Delta_\iota} \tag{135}$$

$$\max_{\{x\}\in\{\mathbf{x}\}} \mathcal{D}(\omega_{\iota+1}) = \overline{\Delta_{\iota+1}} \tag{136}$$

with $\omega_\iota < \omega_{\iota+1}$, it can be shown that for all $\omega^* \in [\omega_\iota, \omega_{\iota+1}]$:

$$\overline{\mathcal{D}}(\omega^*) \leq \frac{\left(\omega_{\iota+1}^2 - \omega^{*2}\right)\overline{\Delta_\iota} + \left(\omega^{*2} - \omega_\iota^2\right)\overline{\Delta_{\iota+1}}}{\omega_{\iota+1}^2 - \omega_\iota^2} \tag{137}$$

**Proof**

If this theorem would be false, there exists a $\omega^* \in [\omega_\iota, \omega_{\iota+1}]$ for which:

$$\overline{\mathcal{D}}(\omega^*) > \frac{\left(\omega_{\iota+1}^2 - \omega^{*2}\right)\overline{\Delta_\iota} + \left(\omega^{*2} - \omega_\iota^2\right)\overline{\Delta_{\iota+1}}}{\omega_{\iota+1}^2 - \omega_\iota^2} \tag{138}$$

Stating that $\overline{\mathcal{D}}(\omega^*)$ is achieved for $\{x\} = \{x^*\}$ and using the definition of $\mathcal{D}(\omega)$, this is equivalent to stating that there exist values for the modal parameters $\hat{k}_i^* = \hat{k}_i(\{x^*\})$ and $\hat{m}_i^* = \hat{m}_i(\{x^*\})$ for which:

$$\hat{k}_i^* - \omega^{*2}\hat{m}_i^* > \frac{\left(\omega_{\iota+1}^2 - \omega^{*2}\right)\overline{\Delta_\iota} + \left(\omega^{*2} - \omega_\iota^2\right)\overline{\Delta_{\iota+1}}}{\omega_{\iota+1}^2 - \omega_\iota^2} \tag{139}$$

Since $\overline{\Delta_\iota}$ and $\overline{\Delta_{\iota+1}}$ are the results of the maximisation of $\mathcal{D}(\omega)$ at respectively $\omega = \omega_\iota$ and $\omega = \omega_{\iota+1}$, they satisfy:

$$\hat{k}_i^* - \omega_\iota^2\hat{m}_i^* \leq \overline{\Delta_\iota} \tag{140}$$

$$\hat{k}_i^* - \omega_{\iota+1}^2\hat{m}_i^* \leq \overline{\Delta_{\iota+1}} \tag{141}$$

Therefore, equation 139 is equivalent to:

$$\begin{aligned}
\hat{k}_i^* - \omega^{*2}\hat{m}_i^* &> \frac{\left(\omega_{\iota+1}^2 - \omega^{*2}\right)\left(\hat{k}_i^* - \omega_\iota^2\hat{m}_i^*\right)}{\omega_{\iota+1}^2 - \omega_\iota^2} \ldots \\
&\quad + \frac{\left(\omega^{*2} - \omega_\iota^2\right)\left(\hat{k}_i^* - \omega_{\iota+1}^2\hat{m}_i^*\right)}{\omega_{\iota+1}^2 - \omega_\iota^2} \\
&> \frac{\hat{k}_i^*\left(\omega_{\iota+1}^2 - {\omega_\iota}^2\right) - \hat{m}_i^*\left({\omega_{\iota+1}}^2\omega^{*2} - \omega_\iota^2\omega^{*2}\right)}{\omega_{\iota+1}^2 - \omega_\iota^2} \\
&> \hat{k}_i^* - \omega^{*2}\hat{m}_i^*
\end{aligned} \tag{142}$$

The assumption in equation 138 must thus be invalid. This proves the theorem ad absurdum. ⊠

## REFERENCES


1 Guyader, J. and Parizet, E. (1997). Uncertainty of Vibroacoustic Behaviour of Industrially Identical Structures. A new Challenge for Structural Acoustic People. *Proceedings of the Fifth International Congress on Sound and Vibration*, pp. 2347–2358.

2 Elishakoff, I. (1990). An Idea of the Uncertainty Triangle. *Shock and Vibration Digest*, **22**, No. 10, pp. 1.

3 Klir, G. (1999). Uncertainty and Information Measures for Imprecise Probabilities: An Overview. *Proceedings of the* $1^{st}$ *International Symposium on Imprecise Probabilities and Their Applications*.

4 Miller, I. and Freund, J. (1985). *Probability and Statistics for Engineers*. Prentice Hall, Englewood Cliffs.

5 Haldar, A. and Mahadevan, S. (2000). *Reliability Assessment Using Stochastic Finite Element Analysis*. John Wiley & Sons, New York.

6 Soize, C. (2000). A nonparametric model of random uncertainties for reduced matrix models in structural dynamics, *Probabilistic Engineering Mechanics*, **15**, No. 3, 277–294.

7 Ibrahim, R. (1987). Structural Dynamics with Parameter Uncertainties. *ASME Applied Mechanics Reviews*, **40**, No. 3, 309–328.

8 Manohar, C. and Ibrahim, R. (1999). Progress in structural dynamics with stochastic parameter variations: 1987-1998. *ASME Applied Mechanics Reviews*, **52**, No. 5, 177–197.

9 Binder, K. (1984). *Application of the Monte Carlo Method in Statistical Physics*. Springer-Verlag, Berlin.

10 Rubenstein, R. (1981). *Simulation and the Monte Carlo Method*. John Wiley & Sons, New York.

11 Annis, C. (2004). Probabilistic Life Prediction Isn't as Easy as It Looks. *Journal of ASTM International*, **1**, No. 2.

12 Schuëller, G. and Stix, R. (1987). A Critical Appraisal of Methods to Determine Failure Probabilities. *Structural Safety*, **4**, 293–309.

13 Bucher, C. (1988). Adaptive Sampling - An Iterative Fast Monte Carlo Procedure. *Structural Safety*, **5**, No. 2, 119–126.

14 Ditlevsen, O., Bjerager, P., Olesen, R. and Hasofer, A. (1988). Directional Simulation in Gaussian Processes. *Probabilistic Engineering Mechanics*, **3**, No. 4, 207–217.

15 Kijawatworawet, W., Pradlwarter, H. and Schuëller, G. (1997). Structural Reliability Estimation by Adaptive Importance Directional Sampling. *Proceedings of the* $7^{th}$ *International Conference on Structural Safety and Reliability, ICOSSAR '97*, pp. 891–897.

16 Mckay, M., Beckman, R. and Conover, W. (1979). Comparison of 3 Methods for Selecting Values of Input Variables in the Analysis of Output from A Computer Code. *Technometrics*, **21**, No. 2, 239–245.

17 Schuëller, G. (2001). Computational Stochastic Mechanics - Recent Advances. *Computers & Structures*, **79**, 2225–2234.

18 Pradlwarter, H. and Schuëller, G. (1999). Assessment of Low Probability Events of Dynamical Systems by Controlled Monte Carlo Simulation. *Probabilistic Engineering Mechanics*, **14**, 213–227.

19 Vanmarcke, E. (1993). *Random fields: analysis and synthesis*. MIT Press, Cambridge.

20 Ghanem, R. and Spanos, P. (1991). *Stochastic finite elements: a spectral approach*. Springer-Verlag, New-York.

21 Moore, R. (1966). *Interval Analysis*. Prentice Hall, Englewood Cliffs.

22 Ben Haim, Y. and Elishakoff, I. (1990). *Convex Models of Uncertainty in Applied Mechanics*. Elsevier Science, Amsterdam.

23 Ben Haim, Y., Chen, G. and Soong, T. (1996). Maximum Structural Response Using Convex Models. *Journal of Engineering Mechanics*, **122**, No. 4, 325–333.

24 Niki, M., Yoshikawa, N. and Nakagiri, S. (2000). Worst Case Estimation of Time-history Response Subject to Uncertain Excitation Bounded in Convex Set. *Proceedings of the 5th International Conference on Probabilistic Safety Assessment and Management*, 1071–1076.

25 Elseifi, M., Gürdal, Z. and Nikolaidis, E. (1999). Convex/Probabilistic Models of Uncertainties in Geometric Imperfections of Stiffened Composite Panels. *AIAA Journal*, **37**, No. 4, 468–474.

26 Givoli, D. and Elishakoff, I. (1992). Stress Concentration at a Nearly Circular Hole with Uncertain Irregularities. *Journal of Applied Mechanics, ASME Paper 91-WA/APM-22*, **59**, 65–71.

27 Elishakoff, I. and Colombi, P. (1993). Combination of Probabilistic and Convex Models of Uncertainty when Scarce Knowledge is Present on Acoustic Excitation Parameters. *Computer Methods in Applied Mechanics and Engineering*, **104**, 187–209.

28 Zadeh, L. (1965). Fuzzy sets. *Information and Control*, **8**, 338–353.

29 Dubois, D. and Prade, H. (1980). *Fuzzy Sets and Systems: Theory and Applications*. Academic Press, Orlando.

30 Dubois, D. and Prade, H. (1986). Fuzzy Sets and Statistical Data. *European Journal of Operational Research*, **25**, 345–356.

31 Dubois, D. and Prade, H. (1988). *Possibility Theory. An Approach to Computerized Processing of Uncertainty*. Plenum Press, New York.

32 Driankov, D., Hellendoorn, H. and Reinfrank, M. (1996). *An Introduction to Fuzzy Control*. Springer-Verlag, Berlin.

33 Zadeh, L. (1978). Fuzzy Sets as a Basis for a Theory of Possibility. *Fuzzy Sets and Systems*, **1**, 3–28.

34 Wasfy, T. and Noor, A. (1998). Finite Element Analysis of Flexible Multibody Systems with Fuzzy Parameters. *Computer Methods in Applied Mechanics and Engineering*, **160**, 223–243.

35 Schulz, K., Huwe, B. and Peiffer, S. (1999). Parameter uncertainty in chemical equilibrium calculations using fuzzy set theory. *Journal of Hydrology*, **217**, No. 1-2, 119–134.

36 Barpi, F. (2004). Fuzzy modelling of powder snow avalanches. *Cold Regions Science and Technology*, **40**, 213–227.

37 Valliappan, S. and Pham, T. (1993). Fuzzy Finite Element Analysis of a Foundation on an Elastic Soil Medium. *International Journal for Numerical and Analytical Methods in Geomechanics*, **17**, 771–789.

38 Rao, S. and Sawyer, P. (1995). Fuzzy Finite Element Approach for the Analysis of Imprecisely Defined Systems. *AIAA Journal*, **33**, No. 12, 2364–2370.

39 Ross, T., Booker, J. and Parkinson, W. (2002). *Fuzzy Logic and Probability Applications: Bridging the Gap*. SIAM, Philadelphia, ASA, Alexandria, VA.

40 Zadeh, L. (1975). Concept of A Linguistic Variable and Its Application to Approximate Reasoning .1. *Information Sciences*, **8**, No. 3, 199–249.

41 Moens, D. and Vandepitte, D. (2005). A Survey of Non-Probabilistic Uncertainty Treatment in Finite Element Analysis. *Computer Methods in Applied Mechanics and Engineering*, **194**, No. 14-16, 1527–1555.

42 Mullen, R. and Muhanna, R. (1999). Bounds of Structural Response for All Possible Loading Combinations. *Journal of Structural Engineering*, **125**, No. 1, 98–106.

43 Cherki, A., Plessis, G., Lallemand, B., Tison, T. and Level, P. (2000). Fuzzy Behavior of Mechanical Systems with Uncertain Boundary Conditions. *Computer Methods in Applied Mechanics and Engineering*, **189**, 863–873.

44 Chen, L. and Rao, S. (1997). Fuzzy Finite-Element Approach for the Vibration Analysis of Imprecisely-Defined Systems. *Finite Elements in Analysis and Design*, **27**, 69–83.

45 Wasfy, T. and Noor, A. (1998). Application of Fuzzy Sets to Transient Analysis of Space Structures. *Finite Elements in Analysis and Design*, **29**, 153–171.

46 Valliappan, S. and Pham, T. (1995). Elasto-Plastic Finite Element Analysis with Fuzzy Parameters. *International Journal for Numerical Methods in Engineering*, **38**, 531–548.

47 Fetz, T., Jäger, J., Köll, D., Krenn, G., Lessmann, H., Oberguggenberger, M. and Stark, R. (1999). Fuzzy Models in Geotechnical Engineering and Construction Management. *Computer-Aided Civil and Infrastructure Engineering*, **14**, 93–106.

48 Muhanna, R. and Mullen, R. (1999). Formulation of Fuzzy Finite-Element Methods for Solid Mechanics Problems. *Computer-Aided Civil and Infrastructure Engineering*, **14**, No. 2, 107–117.

49 Akpan, U., Koko, T., Orisamolu, I., and Gallant, B. (2001). Fuzzy Finite Element Analysis of Smart Structures. *Smart Materials and Structures*, **10**, 273–284.

50 Muc, A. (2002). A fuzzy set approach to interlaminar cracks simulation problems. *International Journal of Fatigue*, **24**, No. 2-4, 419–427.

51 McNeill, D. (1993). *Fuzzy Logic*. Simon and Schuster, New York.

52 Oberkampf, W., DeLand, S., Rutherford, B., Diegert, K. and Alvin, K. (1999). A New Methodology for the Estimation of Total Uncertainty in Computational Simulation. *Proceedings of the* $40^{th}$ *AIAA/ASME/ASCE/AHS/ASC Structures, Structural Dynamics and Materials Conference, AIAA-99-1612*, 3061–3083.

53 Klir, G. and Folger, T. (1988). *Fuzzy Sets, Uncertainty and Information*. Prentice Hall, Englewood Cliffs.

54 Freudenthal, A. (1961). Fatigue Sensitivity and Reliability of Mechanical Systems, especially Aircraft Structures. *WADD Technical Report 61-53*.

55 Civanlar, M. and Trussell, H. (1986). Constructing Membership Functions Using Statistical Data. *Fuzzy Sets and Systems*, **18**, 1–13.

56 Dubois, D. and Prade, H. (1991). Random Sets and Fuzzy Interval Analysis. *Fuzzy Sets and Systems*, **42**, 87–101.

57 Shafer, G. (1976). *A Mathematical Theory of Evidence*. Princeton University Press, Princeton.

58 Zang, T.A., Hemsch, M.J., Hilburger, M.W., Kenny, S.P., Luckring, J.M., Maghami, P. and Padula, S.L. (2002). Needs and Opportunities for Uncertainty-Based Multidisciplinary Design Methods for Aerospace Vehicles. Tech. Rep. NASA/TM-2002-211462, Langley Research Center, Hampton, Virginia.

59 Ross, T., Sellers, K. and Booker, J. (2002). Considerations for using fuzzy set theory and probability theory. *Fuzzy Logic and Probability Applications: Bridging the Gap*, Chap. 5, SIAM, Philadelphia, ASA, Alexandria, VA, pp. 87–104.

60 Casciati, F. and Roberts, J. (1996). *Mathematical Models for Structural Reliability Analysis*. CRC Press, New York.

61 Haldar, A. and Mahadevan, S. (1993). First-order/second-order reliability methods (FORM/SORM). *Probabilistic Structural Mechanics Handbook*, 27–52.

62 Schuëller, G., Pradlwarter, H. and Koutsourelakis, P. (2004). A critical appraisal of reliability estimation procedures for high dimensions. *Probabilistic Engineering Mechanics*, **19**, No. 4, 463–474.

63 Salita, M. (2004). Shuttle disasters: a common cause? *Aerospace America*, **4**, 41–43.

64 Ben Haim, Y. (1995). A Non-Probabilistic Measure of Reliability of Linear Systems based on Expansion of Convex Models. *Structural Safety*, **17**, 91–109.

65 Zingales, M. and Elishakoff, I. (2000). Anti-Optimization Versus Probability in an Applied Mechanics Problem: Vector Uncertainty. *Transactions of the ASME, Journal of Applied Mechanics*, **67**, 472–483.

66 Sawyer, J. and Rao, S. (1999). Strength-based reliability and fracture assessment of fuzzy mechanical and structural systems. *AIAA Journal*, **37**, No. 1, 84–92.

67 Biondini, F., Bontempi, F. and Malerba, P. (2004). Fuzzy reliability analysis of concrete structures 4. *Computers & Structures*, **82**, No. 13-14, 1033–1052.

68 Catallo, L. (2004). Genetic anti-optimization for reliability structural assessment of precast concrete structures 1. *Computers & Structures*, **82**, No. 13-14, 1053–1065.

69 Ferrari, P. and Savoia, M. (1998). Fuzzy Number Theory to Obtain Conservative Results with respect to Probability. *Computer Methods in Applied Mechanics and Engineering*, **160**, 205–222.

70 Youn, B. and Choi, K. (2004). Selecting probabilistic approaches for reliability-based design optimization. *AIAA Journal*, **42**, No. 1, 124–131.

71 Ross, T., Sellers, K. and Booker, J. (2002). Introduction. *Fuzzy Logic and Probability Applications: Bridging the Gap*, Chap. 1, SIAM, Philadelphia, ASA, Alexandria, VA, 3–27.

72 Choi, K., Du, L. and Youn, B. (2004). Vertex-Domain Fuzzy Analysis Method for Possibility-Based Design Optimization. *10th AIAA/ISSMO Multidisciplinary Analysis and Optimization Conference*.

73 Elishakoff, I. (1998). Three Versions of the Finite Element Method Based on Concepts of either Stochasticity, Fuzziness, or Anti-Optimization. *ASME Applied Mechanics Reviews*, **51**, No. 3, 209–218.

74 Lima, B. and Ebecken, N. (2000). A Comparison of Models for Uncertainty Analysis by the Finite Element Method. *Finite Elements in Analysis and Design*, **34**, 211–232.

75 Maglaras, G., Nikolaidis, E., Haftka, T. and Cudney, H. (1997). Analytical-Experimental Comparison of Probabilistic Methods and Fuzzy Set Based Methods for Designing under Uncertainty. *Structural Optimization*, **13**, 69–80.

76 Nikolaidis, E., Cudney, H. and Chen, Q. (1999). Bayesian and Fuzzy Set Methods for Design Under Uncertainty. *Proceedings of the 13th ASCE Engineering Mechanics Division Specialty Conference (CDROM)*.

77 Langley, R. (2000). Unified Approach to Probabilistic and Possibilistic Analysis of Uncertain Systems. *Journal of Engineering Mechanics*, **126**, No. 11, 1163–1172.

78 Rao, S., Chen, L. and Mulkay, E. (1998). Unified Finite Element Method for Engineering Systems with Hybrid Uncertainties. *AIAA Journal*, **36**, No. 7, 1291–1299.

79 Köylüoğlu, U., Çakmak, A. and Nielsen, S. (1995). Interval Algebra to Deal with Pattern Loading and Structural Uncertainties. *Journal of Engineering Mehanics*, **121**, No. 11, 1149–1157.

80 Möller, B., Graf, W. and Beer, M. (2000). Fuzzy Structural Analysis Using $\alpha$-level Optimization. *Computational Mechanics*, **26**, 547–565.

81 Dong, W. and Shah, H. (1987). Vertex Method for Computing Functions of Fuzzy Variables. *Fuzzy Sets and Systems*, **24**, 65–78.

82 Hanss, M. and Willner, K. (2000). A Fuzzy Arithmetical Approach to the Solution of Finite Element Problems with Uncertain Parameters. *Mechanics Research Communications*, **27**, No. 3, 257–272.

83 Hanss, M. (2003). The extended transformation method for the simulation and analysis of fuzzy-parameterized models. *International Journal of Uncertainty Fuzziness and Knowledge-Based Systems*, **11**, No. 6, 711–727.

84 Shary, S. (1997). Algebraic Approach in the 'Outer Problem' for Interval Linear Equations. *Reliable Computing*, **3**, 103–135.

85 Oettli, W. and Prager, W. (1964). Compatibility of Approximate Solution of Linear Equations with given Error Bounds for Coefficients and Right-hand Sides. *Numerische Mathematik*, **6**, 405–409.

86 Neumaier, A. (1990). *Interval Methods for Systems of Equations*. Cambridge University Press, Cambridge.

87 Alefeld, G. and Herzberger, J. (1983). *Introduction to Interval Computations*. Academic Press, Inc., New York.

88 Shary, S. (1995). On Optimal Solution of Interval Linear Equations. *SIAM Journal on Numerical Analysis*, **32**, No. 2, 610–630.

89 Rao, S. and Berke, L. (1997). Analysis of Uncertain Structural Systems Using Interval Analysis. *AIAA Journal*, **34**, No. 4, 727–735.

90 Rao, S. and Chen, L. (1998). Numerical Solution of Fuzzy Linear Equations in Engineering Analysis. *International Journal for Numerical Methods in Engineering*, **43**, 391–408.

91 Dessombz, O., Thouverez, F., Laîné, J.-P. and Jézéquel, L. (2001). Analysis of Mechanical Systems Using Interval Computations Applied to Finite Element Methods. *Journal of Sound and Vibration*, **239**, No. 5, 949–968.

92 Qiu, Z. and Elishakoff, I. (1998). Antioptimization of Structures with Large Uncertain-but-non-random Parameters via Interval Analysis. *Computer Methods in Applied Mechanics and Engineering*, **152**, 361–372.

93 McWilliam, S. (2001). Anti-Optimization of Uncertain Structures Using Interval Analysis. *Computers & Structures*, **79**, 421–430.

94 Moens, D. (2002). *A Non-Probabilistic Finite Element Approach for Structural Dynamic Analysis with Uncertain Parameters, PhD thesis*. K.U.Leuven, Leuven.

95 Chen, S., Qiu, Z. and Song, D. (1995). A New Method for Computing the Upper and Lower Bounds on Frequencies of Structures with Interval Parameters. *Mechanics Research Communications*, **22**, No. 5, 431–439.

96 El Gebeily, M., Abu-Baker, Y. and Elgindi, M. (1999). The Generalized Eigenvalue Problem for Tridiagonal Symmetric Interval Matrices. *International Journal on Control*, **72**, No. 6, 531–535.

97 Chen, S., Lian, H. and Yang, X. (2003). Interval eigenvalue analysis for structures with interval parameters 1. *Finite Elements in Analysis and Design*, **39**, No. 5-6, 419–431.

98 Qiu, Z., Wang, X. and Friswell, M. (2005). Eigenvalue bounds of structures with uncertain-but-bounded parameters 2. *Journal of Sound and Vibration*, **282**, No. 1-2, 297–312.

99 Fox, R. and Kapoor, M. (1968). Rates of Change of Eigenvalues and Eigenvectors. *AIAA Journal*, **6**, No. 12, 2426–2429.

100 Balmès, E. (1998). Predicted Variability and Differences between Tests of a Single Structure. *Proceedings of the 16th International Modal Analysis Conference, IMAC XVI*, 558–564.

101 Hasselman, T. and Chrostowski, J. (1997). Effects of Product and Experimental Variability on Model Verification of Automobile Structures. *Proceedings of the 15th International Modal Analysis Conference, IMAC XV*, 612–620.

102 Worden, K. (1998). Confidence Bounds for Frequency Response Functions from Time Series Models. *Mechanical Systems and Signal Processing*, **12**, No. 4, 559–569.

103 Enling, L. (1997). A New Solution to Structural Fuzzy Finite Element Equilibrium Equations (SFFEEE). *Applied Mathematics and Mechanics*, **18**, No. 4, 385–391.

104 Laveuve, S. (1975). Definition einer Kahan-Arithmetik und ihre Implementierung. *Interval Methematics 1975, Lecture Notes in Computer Science,29*, 236–245.

105 Hitchings, D. (1992). A Finite Element Dynamics Primer. *A Finite Element Dynamics Primer*, 170–196.

Please address your comments or questions on this paper to:
International Center for Numerical Methods in Engineering
Edificio C-1, Campus Norte UPC
Grand Capitán s/n
08034 Barcelona, Spain
Phone: 34-93-4016035; Fax: 34-93-4016517
E-mail: onate@cimne.upc.edu